Disclaimer

This Report, including the data and information contained in this Report, is provided to you on an "as is" and "as available" basis at the sole discretion of the Government of Alberta and subject to the terms and conditions of use below (the "Terms and Conditions"). The Government of Alberta has not verified this Report for accuracy and does not warrant the accuracy of, or make any other warranties or representations regarding, this Report. Furthermore, updates to this Report may not be made available. Your use of any of this Report is at your sole and absolute risk.

This Report is provided to the Government of Alberta, and the Government of Alberta has obtained a license or other authorization for use of the Reports, from:

> Shell Canada Energy, Chevron Canada Limited. and Marathon Oil Canada Corporation, for the Quest Project
>
> (collectively the "Project")

Each member of the Project expressly disclaims any representation or warranty, express or implied, as to the accuracy or completeness of the material and information contained herein, and none of them shall have any liability, regardless of any negligence or fault, for any statements contained in, or for any omissions from, this Report. Under no circumstances shall the Government of Alberta or the Project be liable for any damages, claims, causes of action, losses, legal fees or expenses, or any other cost whatsoever arising out of the use of this Report or any part thereof or the use of any other data or information on this website.

Terms and Conditions of Use

Except as indicated in these Terms and Conditions, this Report and any part thereof shall not be copied, reproduced, distributed, republished, downloaded, displayed, posted or transmitted in any form or by any means, without the prior written consent of the Government of Alberta and the Project.

The Government of Alberta's intent in posting this Report is to make them available to the public for personal and non-commercial (educational) use. You may not use this Report for any other purpose. You may reproduce data and information in this Report subject to the following conditions:

- any disclaimers that appear in this Report shall be retained in their original form and applied to the data and information reproduced from this Report
- the data and information shall not be modified from its original form
- the Project shall be identified as the original source of the data and information, while this website shall be identified as the reference source, and
- the reproduction shall not be represented as an official version of the materials reproduced, nor as having been made in affiliation with or with the endorsement of the Government of Alberta or the Project

By accessing and using this Report, you agree to indemnify and hold the Government of Alberta and the Project, and their respective employees and agents, harmless from and against any and all claims, demands, actions and costs (including legal costs on a solicitor-client basis) arising out of any breach by you of these Terms and Conditions or otherwise arising out of your use or reproduction of the data and information in this Report.

Your access to and use of this Report is subject exclusively to these Terms and Conditions and any terms and conditions contained within the Report itself, all of which you shall comply with. You will not use this Report for any purpose that is unlawful or prohibited by these Terms and Conditions. You agree that any other use of this Report means you agree to be bound by these Terms and Conditions. These Terms and Conditions are subject to modification, and you agree to review them periodically for changes. If you do not accept these Terms and Conditions you agree to immediately stop accessing this Report and destroy all copies in your possession or control.

These Terms and Conditions may change at any time, and your continued use and reproduction of this Report following any changes shall be deemed to be your acceptance of such change.

If any of these Terms and Conditions should be determined to be invalid, illegal or unenforceable for any reason by any court of competent jurisdiction then the applicable provision shall be severed and the remaining provisions of these Terms and Conditions shall survive and remain in full force and effect and continue to be binding and enforceable.

These Terms and Conditions shall: (i) be governed by and construed in accordance with the laws of the province of Alberta and you hereby submit to the exclusive jurisdiction of the Alberta courts, and (ii) ensure to the benefit of, and be binding upon, the Government of Alberta and your respective successors and assigns.

Figure 3.1-2: Landsat 5 Land Cover Classification

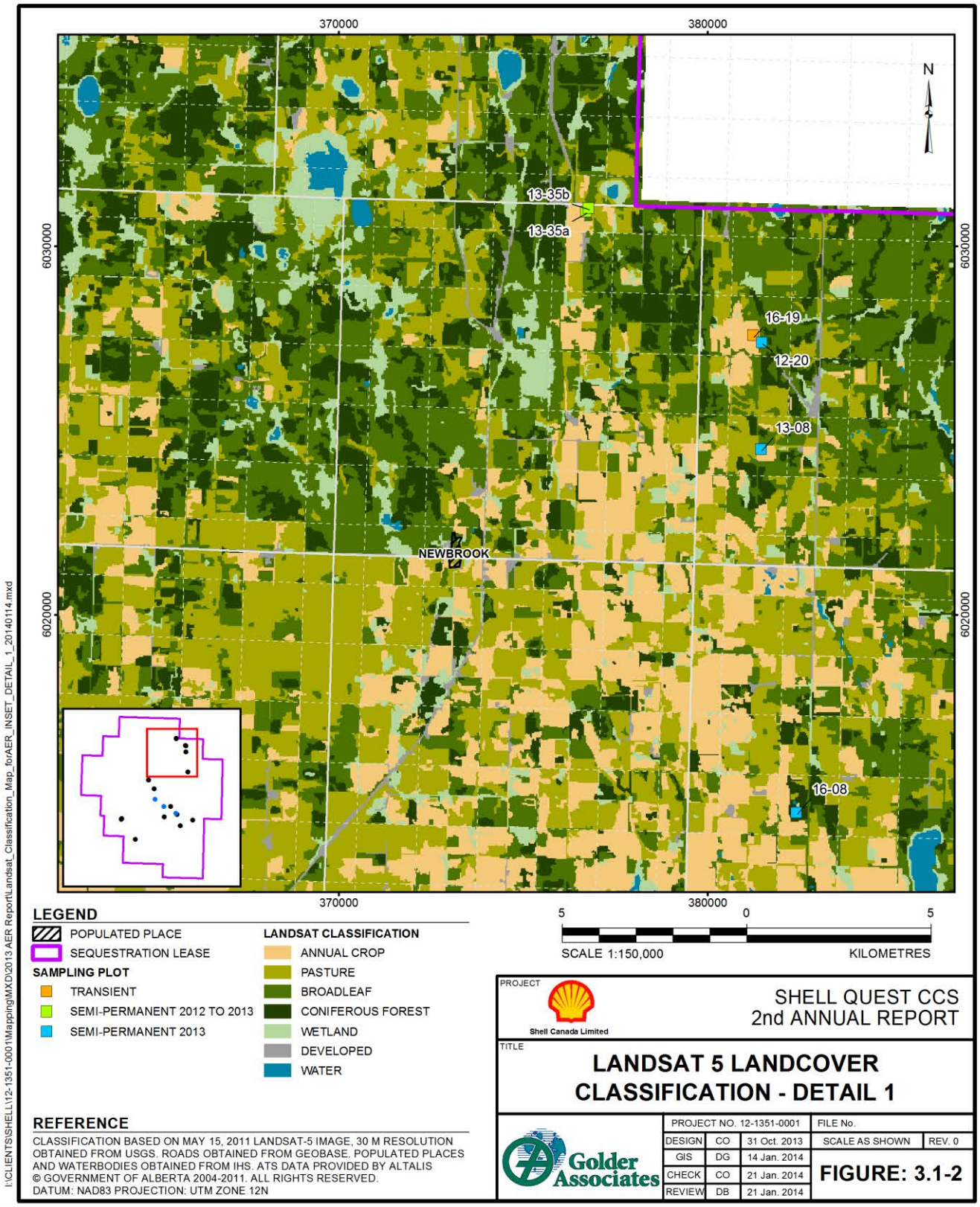

Figure 3.1-3: Landsat 5 Land Cover Classification: Detail 1 (Northeastern Sampling Plots)

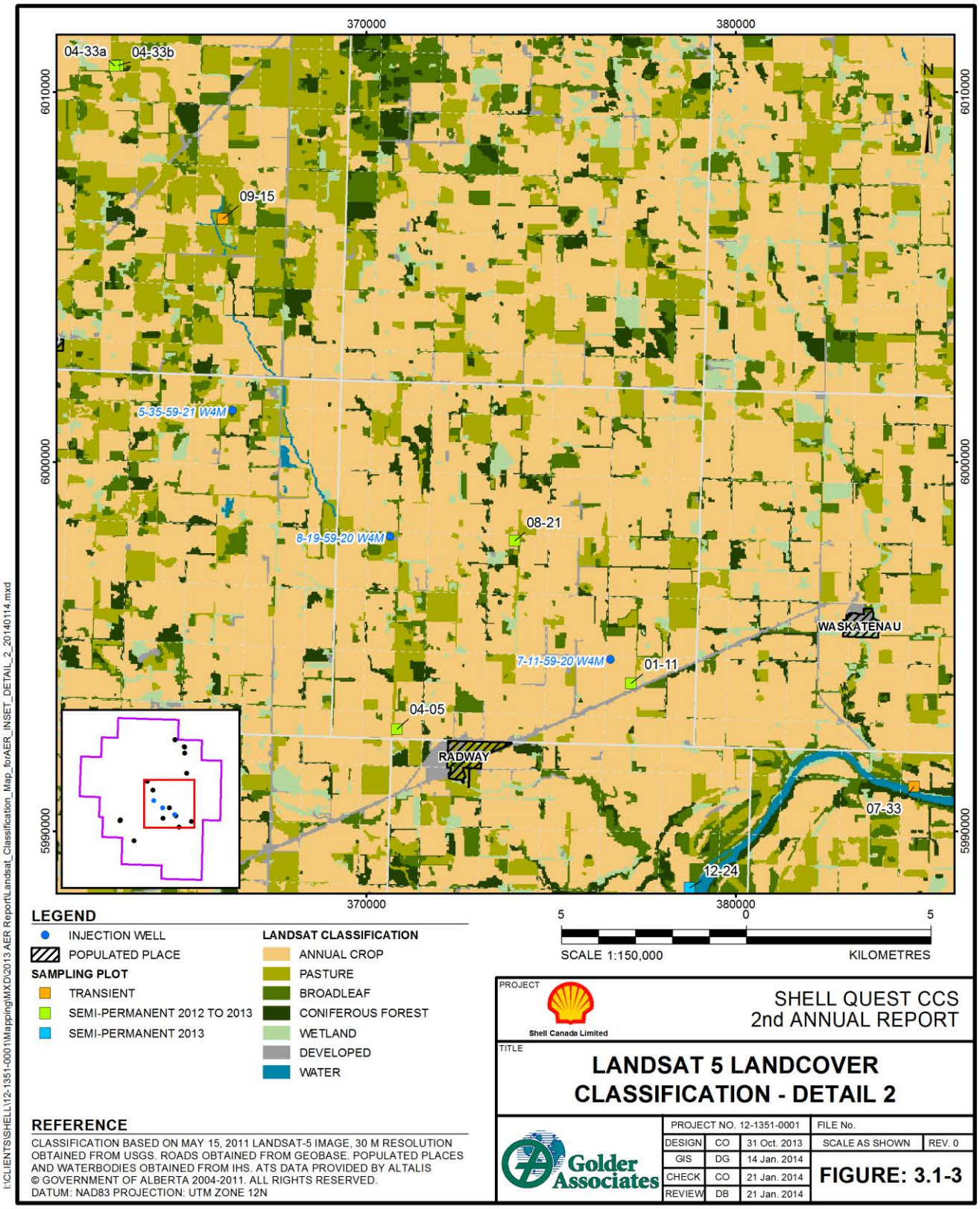

Figure 3.1-4: Landsat 5 Land Cover Classification: Detail 2 (Central Sampling Plots)

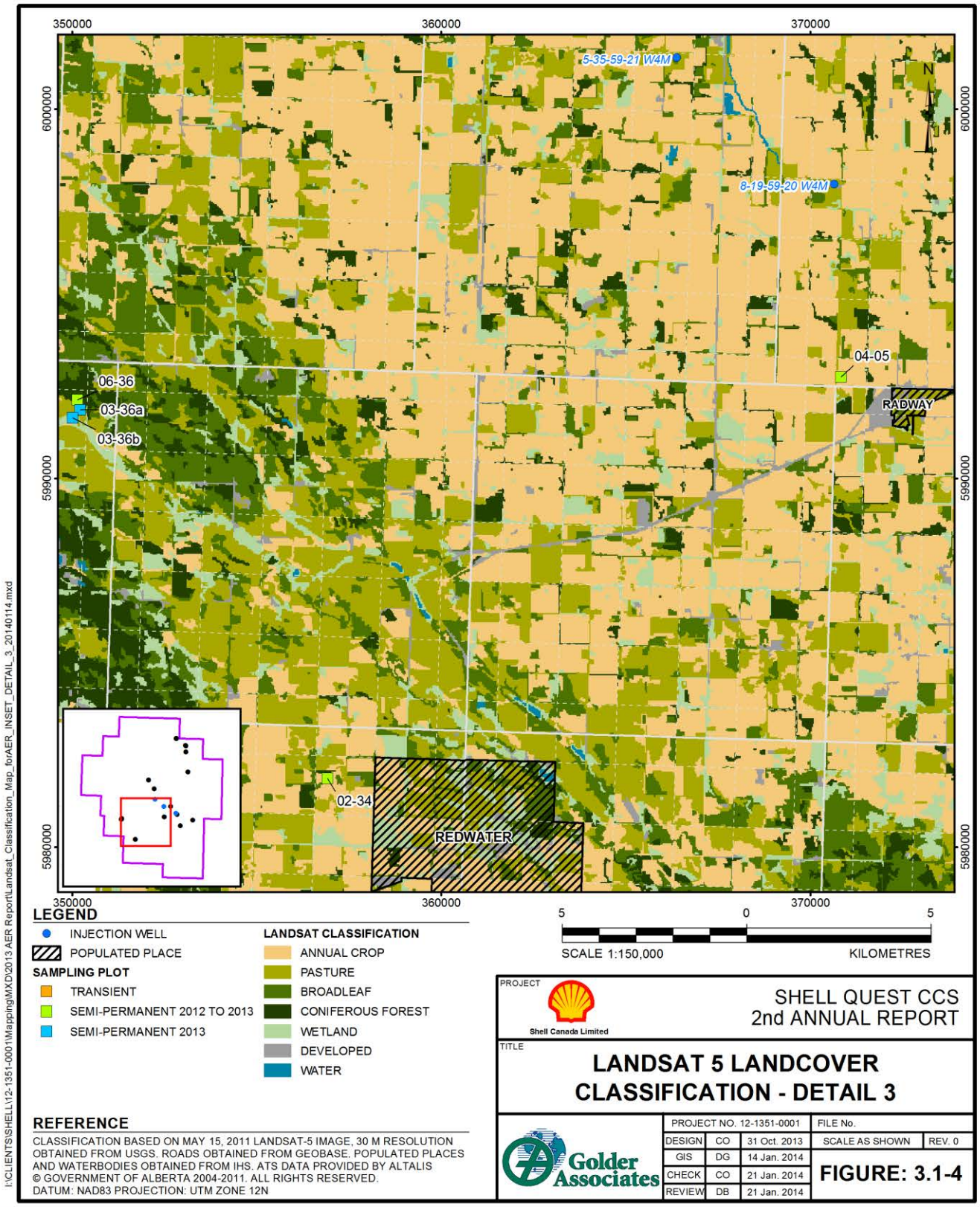

3.2 Plot Selection

Plot selection was designed around the vegetation land classification to represent the major vegetation classes within the Project area. The plot design has gone through two iterations as the Project has evolved from lessons learned in the first field season. Three plot structures were used for the Project:

- Transient plots: A series of plots that may or may not be required during the injection phase and are likely a one-time evaluation. These plots may be established to assess a potential anomaly seen on a previous satellite image or another monitoring technology.
- Semi-permanent plots: Sample plots that occupy the same location from season to season and year-to-year to calibrate the remote sensing images both temporally and spatially and may or may not be used for long-term monitoring.
- Permanent Plots: Plots that will remain as references for the duration of the Project, or until such time that it is agreed that the risks to the biosphere are so low such that these plots are no longer necessary. No permanent plots have been established at this time.

The first surveys in September 2012 used ten 1-hectare (ha; 100 by 100 metre [m]) plots. These locations were established before the vegetation land classification was developed, and in areas that were assumed to represent the majority of vegetation and land use for the Project area. Developed areas, other than for agricultural use, were omitted from the Project due to a lack of consistency in the use and potential cover types (i.e., lawns, parks, urban landscapes).

For the 2013 sampling season, the plot design was updated to use a smaller and more efficient sampling methodology. By using a 50 m by 50 m (2,500 square metres [m^2]) plot, rather than the 1 ha plot, the biosphere components have sufficient area to gather the information needed, with the advantage of less heterogeneity in the vegetation cover types. Having more than one vegetation community within a plot caused confusion when trying to identify representative pixels for a vegetation class on the satellite imagery. In addition, once the vegetation classification was completed (early spring 2013), plot locations were revaluated and some plots were relocated while others were removed in an effort to make the plots more representative of the dominant vegetation classes. Fifteen (15) plots were used in 2013 representing the five dominant land vegetation classes (Table 3.2-1). Since these plots will be sampled for more than one year (2012 to 2014), they have been designated as semi-permanent plots. The plot structure of transient plots surveyed in 2012 and the semi-permanent plots surveyed in 2012 and 2013 is shown in Table 3.2-1.

Table 3.2-1: Names and Locations of the 2012 Transient Plots and 2012/2013 Semi-Permanent Plots

Plot Name	LSD[a]	Plot Type	Year Surveyed	Vegetation type
04-33[b]	04-33-60-21	Transient	2012	Pasture/ Coniferous Forest
07-33	07-33-58-19	Transient	2012	Water/Riparian/Broadleaf Forest/Annual Crop
06-36[c]	06-36-58-23	Transient	2012	Coniferous Forest/Pasture/Broadleaf Forest
13-35[d]	13-35-62-20	Transient	2012	Broadleaf Forest/Pasture
16-19	16-19-62-19	Transient	2012	Annual Crop/Wetland
09-15	09-15-60-21	Transient	2012	Annual Crop
01-11	01-11-59-20	Semi-Permanent	2012/2013	Annual Crop
02-34	02-34-57-22	Semi-Permanent	2012/2013	Annual Crop
04-05	04-05-59-20	Semi-Permanent	2012/2013	Annual Crop
08-21	08-21-59-20	Semi-Permanent	2012/2013	Annual Crop

Plot Name	LSD[(a)]	Plot Type	Year Surveyed	Vegetation type
13-08	13-08-62-19	Semi-Permanent	2013	Annual Crop
12-20	12-20-62-19	Semi-Permanent	2013	Broadleaf Forest
12-24	12-24-58-20	Semi-Permanent	2013	Broadleaf Forest
13-35a	13-35-62-20	Semi-Permanent	2013	Broadleaf Forest
04-33b	04-33-60-21	Semi-Permanent	2013	Coniferous Forest
06-36	06-36-58-23	Semi-Permanent	2013	Coniferous Forest
03-36a	03-36-58-23	Semi-Permanent	2013	Pasture
04-33a	04-33-60-21	Semi-Permanent	2013	Pasture
13-35b	13-35-62-20	Semi-Permanent	2013	Pasture
03-36b	03-36-58-23	Semi-Permanent	2013	Wetlands
16-08	16-08-61-19	Semi-Permanent	2013	Wetlands

(a) Legal subdivisions
(b) In 2012, this plot consisted of two vegetation classes (i.e., Pasture/ Coniferous Forest) and was reduced to two 50 x 50 m plots in 2013 to include only one vegetation class in each plot.
(c) In 2012, this plot consisted of three vegetation classes (i.e., Coniferous Forest/Pasture/Broadleaf Forest) and was reduced to a 50 x 50 m plot in 2013 to include only one vegetation class (Coniferous Forest).
(d) In 2012, this plot consisted of two vegetation classes (i.e., Broadleaf Forest/Pasture) and was reduced to two 50 x 50 m plots in 2013 to include only one vegetation class in each plot.

Plot names use the first two numbers in the Legal Subdivision (LSD). To distinguish between the season and year a plot is sampled, the year and month the satellite image is taken is added to the end of the name. However, the date is only added when distinguishing between specific measurement dates. If more than one plot is in the same LSD, then an alphabetic letter is used to designate different plots. For example, there are two plots located at 03-36-58-23 and the satellite flyover was April 29, 2013; these plots would be named 03-36a-0413 and 06-36b-0413.

For the 2013 survey program, a second change was implemented to plots within annual crops. The original 1 ha plot for annual crops was sampled and, to reduce trampling effect on the spectral signature of annual vegetation, only one quarter section was sampled in each season. The sampled quarter changed each season and no quarter was sampled twice in the same year. The farmers will continue to farm the plot as per the practice in the area. A 1-ha plot broken down into four quarter sections, with the season of sampling labelled, and a 50 m by 50 m plot for a perennial vegetation plot (i.e., broadleaf, conifer, pasture, and wetlands), is shown on Figure 3.2-1. Perennial vegetation plots do not need a rotating quarter design, since these vegetation types can withstand a greater amount of disturbance and the impact of survey will not affect the spectral characteristics.

Figure 3.2-1: Plot Design for Annual Crops and Perennial Vegetation Plots (Non-Annual Croplands)

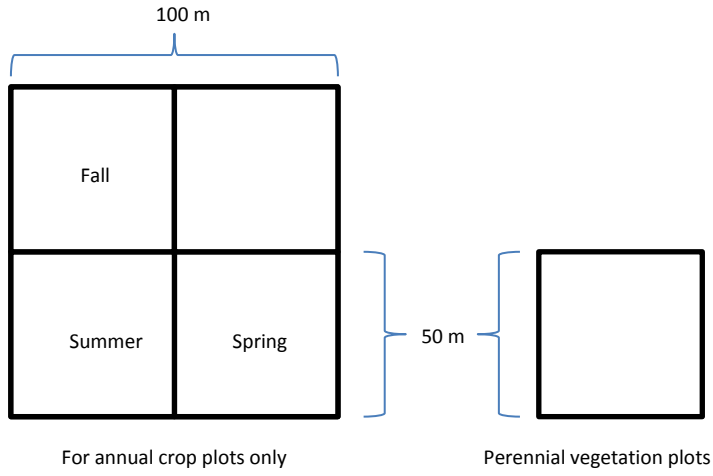

The following sections present data collected in 2012 and 2013. Since plot design and the use of the vegetation land classification have evolved from the initial data collection in September 2012, all data are grouped by land classification. For 2012 transient plots with multiple vegetation classes present within a plot, data collected from a vegetation type is grouped by the land classification. For example, transient plot 13-35 in 2012 had pasture and conifer land classes. These data are separated and presented in the respective land classification.

3.3 Vegetation

3.3.1 Methodology

The purpose of the vegetation field program was to gather baseline information for each vegetation land cover class within the 15 plots for the Project. Remote sensing technologies are used to monitor vegetation (species, health/vigour, and percentage of cover) over the life of the Project. At each subplot, an Ocean Optics Jaz™ Spectrometer was used to capture the spectral signature of the vegetation. This information was correlated with satellite imagery to create a spectral library for remotely sensing vegetation.

Sampling Protocol

A desktop assessment of each site was performed before the field programs to pre-assess vegetation communities. Each vegetation plot was mapped using high-resolution aerial photography and developed into a Geographic Information System (GIS) polygon layer. In addition, the locations of any land features (i.e., wetlands, ponds, roads) were identified to ensure that they were excluded from plot locations. In the field, plot corners were determined using a Garmin 76CSx with less than 10 m Global Positioning System (GPS) accuracy. Plots were classified into five broad vegetation classes: Annual Crops, Pastures, Broadleaf Forests, Coniferous Forests and Wetlands.

Vegetation Subplots

Vegetation subplots were chosen within each 50 m × 50 m sample plot to characterize the vegetation community represented by the sample plot. A nested plot design was used in establishing monitoring subplots, which

includes two levels: tree canopy and shrub/ground cover (i.e., graminoid/forb layer). Subplots represent the primary sampling unit for the monitoring program.

Site characteristics, including vegetation (i.e., species and percent cover), topography and other comments were recorded for each subplot. Key administrative information documented for each subplot included Project name and number, subplot number, Universal Transverse Mercator (UTM) coordinates using North American Datum 83 (NAD 83), time of day, weather, date, surveyor initials, and photo numbers.

Plant health was estimated on a species level. General health of vegetation depends on species, phenology, climate, and environmental site characteristics (soils, disturbances, anthropogenic land use). The vigour of each species was assessed based on a five-value quantitative scale ranging from excellent health (4) with no evidence of stress or necrosis (death of cells or plant parts), to dead with 100% necrosis (0) (Table 3.3-1). Those species undergoing natural senescence (biological aging resulting in death or loss of leaves) due to age and seasonal changes, compared to death due to anthropogenic stresses, were identified.

Plant species identification followed the keys described by Moss (1983) and the naming conventions of Alberta Conservation Information Management System (ACIMS 2013). At each subplot, photographs were taken in the centre of the subplot facing in the same sequential order each time (i.e., north, east, south, west, ground, and canopy/sky).

Table 3.3-1: Plant Vigour Descriptions

Code	Plant Vigour Descriptions
0	Dead; leaves, twigs or vegetative parts 100% necrotic
1	Poor; leaves dead, but some growth on stems; 70% to 90% necrotic or stress symptoms
2	Fair (average); necrotic spots on leaves twigs, stems, or vegetative parts, 30% to 69% necrotic or stress symptoms
3	Good; few necrotic spots present; may have curled margins or insect damage; 10% to 29% necrotic or stress symptoms
4	Very good to excellent; no evidence of stress or necrosis; 0% to 9% necrotic or stress symptoms

At each subplot without a canopy, an Ocean Optics Jaz™ Spectrometer was used to characterize the spectral signature of the vegetation. Due to the potential heterogeneity of the vegetation and composition, multiple signatures were captured to maximize signature details. All spectral signature files and data were provided to the remote sensing team at the end of each field program.

Post-Field Analyses

Vegetation data were analyzed and presented using percent cover by strata, species richness and a general health assessment within each broad vegetation class. A Quality Control (QC) program was implemented to verify that data collection, data entry, and data analysis were conducted with a high level of confidence.

Percent Cover Results

Within all plots, percent cover was estimated for each plant species identified (i.e., the percent of the plot occupied by each species). The total summed percent cover of each species may be greater than 100% due to

multiple structural layers. Living and senesced and/or non-living species percent covers were estimated to give a representation of vegetation cover. Living vegetation refers to vegetation with living tissues and includes vigour rankings from 2 to 4. Senesced and/or non-living vegetation includes plants that have undergone cell death due to age and/or seasonal changes and/or vegetation that may be left over from the previous growing season or died of unknown causes (i.e., winter kill). Senesced and/or non-living vegetation have vigour rankings of 0 to 1.

Species Richness Results

Species richness refers to the number of different species occupying a given area (i.e., the 5 m by 5 m subplot sampled within each plot). For each field program, average species richness was estimated for each broad vegetation class. Maximum and minimum species richness was also calculated.

Health Assessment Results

The health assessment of vegetation was completed qualitatively for each broad vegetation class, and was based on species vigour rankings and observations made during field surveys.

3.3.2 Results

The following sections present the results from the vegetation transient and semi-permanent plots for September 2012, May 2013, July 2013 and September 2013. For each vegetation class, the following data are presented: a qualitative description of the vegetation class, a summary of plots and survey periods, graphs depicting percent cover of living and senesced and/or non-living plant species by strata and survey period, an analysis of species richness, and a qualitative report of plant health (vigour).

3.3.2.1 Annual Crops

The Annual Crop vegetation class refers to cultivated lands with plant species that are seeded, survive one growing season and are harvested. Annual Crops make up the largest portion (1,324 square kilometres [km^2], 34.8%) of the Project area and are made up of crops such as barley, wheat, pea, annual hay and canola. Due to crop rotation, dominant vegetation can vary by year within the same plot location depending on which crop is seeded. The number of Annual Crop plots assessed in each sample period was as follows: seven in September 2012, four in May 2013, five in July 2013, and five in September 2013. The Annual Crop plots were generally situated on flat topography which had little to no slope; the average slope was less than 1%.

Percent Cover Results

The average percent cover by strata for all plots in each field program for the Annual Crops vegetation class is shown on Figure 3.3-1. Living and senesced and/or non-living species percent covers were estimated to give a representation of vegetation cover.

Annual crops planted with wheat and barley had high percent covers of graminoids, while plots planted with canola and pea had high covers of forbs. Average percent covers of senesced and/or non-living forbs and graminoids were highest in the shoulder seasons (i.e., September 2012, May 2013 and September 2013); while during the July 2013 survey only living species were observed. This result is expected because July is in the middle of the growing season. Tree, shrub, bryophyte, terrestrial lichen and epiphyte layers did not exist in the Annual Crop vegetation class because these landscapes have been modified and cleared for the purpose of producing crops. An example of the Annual Crop vegetation class in each season is provided on Figure 3.3-2

Figure 3.3-1: Average Percent Cover by Strata for Each Vegetation Survey Period in the Annual Crop Vegetation Class: Living and Senesced and/or Non-Living

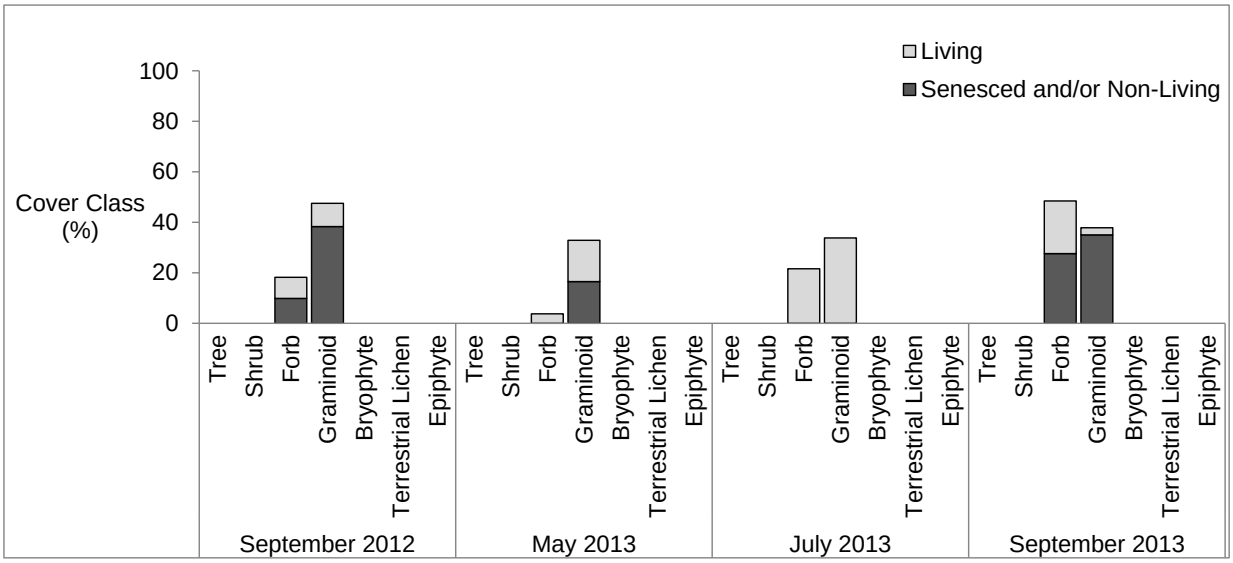

Note: Species with a vigour class of 2 to 4 are considered to be living. Species with vigour class rankings of 0 to 1 are considered to be senesced and/or non-living. The cause of senesced and/or non-living species may be due to seasonal causes or unknown causes (i.e., winter kill).

Figure 3.3-2: Example of the Annual Crop Vegetation Class (Plot 08-21)

September 2012
(senesced wheat - harvested)

May 2013
(pre-planting for canola; wheat – harvested in previous year)

July 2013
(canola – growing)

September 2013
(senesced canola)

Species Richness Results

Species richness data for each sample season within the Annual Crop vegetation class is presented in Table 3.3-2. In general, species richness within the Annual Crop vegetation class was low relative to other vegetation classes within the Project area with one planted crop species and a few weed species per plot. Plot 02-34 had the highest species richness because this plot was left fallow in 2013; therefore, weed species were more prevalent than other plots which were likely sprayed with herbicide before seeding. The species richness average across all field programs was six species per plot. The maximum number of species recorded at one plot was 17 and the minimum was one. Average species richness was highest in the spring (8) and lowest in the summer (5).

Table 3.3-2: Species Richness Values Within Annual Crops

Parameter	Survey Period			
	Spring (May 2013)	Summer (Summer 2013)	Fall (September 2012 and 2013)	Across All Field Programs
Average Species Richness	8	5	6	6
Maximum Species Richness	11	11	17	17
Minimum Species Richness	3	2	1	1
Number of Surveys[(a)]	3	5	17	25
Number of Plots[(b)]	3	5	8	8

(a) Refers to the number of survey visits. A single vegetation plot may have had multiple vegetation surveys completed over various seasons.
(b) Refers to the numbers of physical plot locations.

Health Assessment Results

Overall, the assessment of species vigour indicates that plants within Annual Crops were healthy. The only signs of stress were due to natural senescence (fall) or vegetation left over from the previous growing season that died of unknown causes (i.e., winter kill) (spring). Vigour class rankings were good to excellent during the summer (i.e., July 2013) with an average of 3.8 for graminoids and 4.0 for forbs. These results are expected, because July is the middle of the growing season when conditions are optimal for plant growth.

During the fall season (i.e., September 2012 and September 2013) vigour classes were more variable because some species were undergoing or had undergone natural senescence due to age and/or seasonal changes. Additionally, in the September 2012 and 2013 survey periods, crops had generally been cut or harvested which were recorded as lower vigour ranks (i.e., 0 or 1).

Minor amount of fungi were found growing on some plant species (i.e., *Potentilla norvegica* at plot 02-34-0913), but plants were not stressed. Other stresses such as grazing, herbivory, disease, over-fertilization or other anthropogenic disturbances aside from harvesting were not observed in substantial amounts during vegetation surveys. The use of herbicides is common practice for some crop species, but actual herbicide application was not witnessed by field crews.

3.3.2.2 Pasture

The Pasture vegetation class refers to lands with native or non-native species that are used for grazing by domestic livestock. Pastures have been cleared and planted with tame forages (Moisey et al. 2012) and cover 853 km^2 (22.5%) of the Project area. The number of Pasture plots assessed in each sample period was as follows: three plots in each of September 2012, May 2013, July 2013 and September 2013. The Pastures sampled in 2012 and 2013 had an average slope of 1%.

Percent Cover Results

The average percent cover by strata for each vegetation survey period within the Pasture vegetation class is shown on Figure 3.3-3. In all survey plots and periods, graminoids had the highest percent cover. This result is expected because tame pastures are dominated by grasses with varying amounts of weeds and small amounts of shrub species depending on the amount of grazing pressure. Heavy grazing leads to grazing resistant species and higher amounts of weedy species, while light grazing may result in more native species and shrub species (Moisey et al. 2012). Natural senescence (i.e., seasonal cell death) due to seasonal weather changes is not as evident in pastures because these plots are dominated by cool season grasses that grow well in lower temperatures. Weedy species are also more tolerant of cold conditions resulting in early spring growth and late senescence in the fall. An example of the Pasture vegetation class in each survey season is provided on Figure 3.3-4.

Figure 3.3-3: Average Percent Cover by Strata for Each Vegetation Survey Period in the Pasture Vegetation Class: Living and Senesced and/or Non-Living

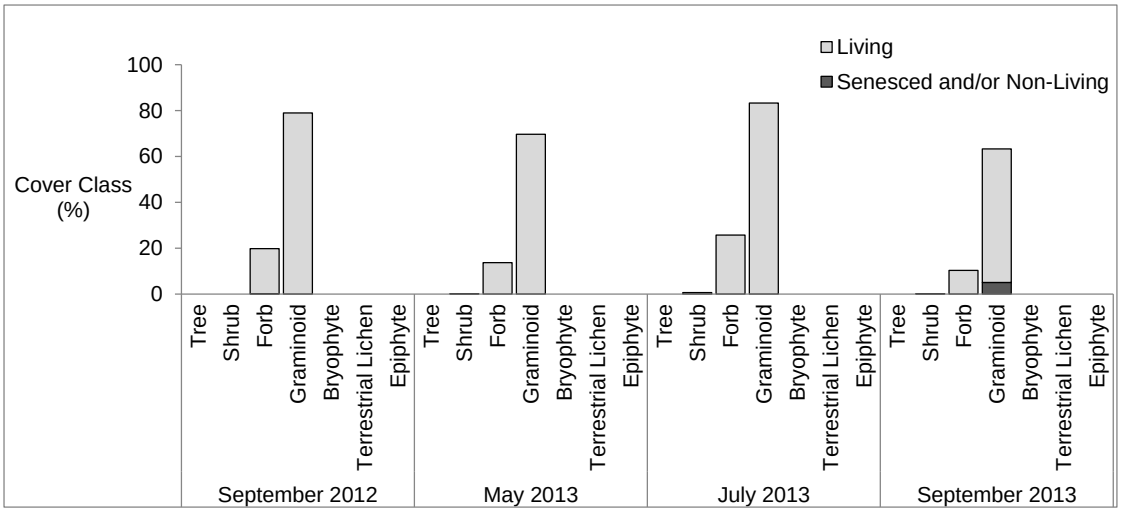

Note: Species with a vigour class of 2 to 4 are considered to be living. Species with vigour class rankings of 0 to 1 are considered to be senesced and/or non-living. The cause of senesced and/or non-living species may be due to seasonal causes or unknown causes (i.e., winter kill).

Figure 3.3-4: Example of the Pasture Vegetation Class (Plot 13-35b)

September 2012

May 2013

July 2013

September 2013

Species Richness Results

Species richness data for each sample season within the Pasture vegetation class are presented in Table 3.3-3. In general, species richness within the Pasture vegetation class was low to medium relative to other vegetation classes within the Project area with one to two dominant perennial grasses (i.e., Kentucky blue grass [*Poa pratensis*] and smooth brome [*Bromus inermis*]), and a few native forbs and weeds (i.e., downy chess [*Bromus tectorum*] and creeping thistle [*Cirsium arvense*]). The average species richness across all field programs was eight species per plot. The maximum number of species recorded at one plot was 11 and the minimum was five. Average species richness was highest in the summer (10).

Table 3.3-3: Species Richness Values Within Pastures Table

Parameter	Survey Period			
	Spring (May 2013)	Summer (Summer 2013)	Fall (September 2012 and 2013)	Across All Field Programs
Average Species Richness	7	10	7	8
Maximum Species Richness	9	10	11	11
Minimum Species Richness	5	9	5	5
Number of Surveys[(a)]	3	3	8	14
Number of Plots[(b)]	3	3	4	4

(a) Refers to the number of survey visits. A single vegetation plot may have had multiple vegetation surveys completed over various seasons.
(b) Refers to the numbers of physical plot locations.

Health Assessment Results

Overall, the assessment of species vigour indicates that plants within Pastures were healthy with the only signs of stress due to natural senescence (fall). Vigour class rankings were good to excellent during the summer (i.e., July 2013) with an average of 4.0 for graminoids and 3.9 for forbs. These results are expected because July is the middle of the growing season when conditions are optimal for plant growth. During the spring and fall seasons (i.e., September 2012, May 2013 and September 2013) vigour class averages ranged from 2.9 to 4.0. Species with vigour rankings of 4.0 in the May and September primarily included cool season species such as weeds (i.e. common dandelion [*Taraxacum officinale*]).

Minor stresses from domestic animal grazing also resulted in lower vigour class rankings; however, pastures had generally not been over-grazed and plants were adapted to these stresses. Other stresses, such as disease or over-fertilization, were not observed in substantial amounts during vegetation surveys.

3.3.2.3 Broadleaf Forests

The Broadleaf Forests vegetation class refers to forested land dominated by broadleaf deciduous trees. Broadleaf forest stands may contain coniferous tree components, but they are not the dominant tree species. This vegetation class occupies 867 km^2 (22.8%) of the Project area. The number of Broadleaf Forest plots assessed in each sample period was as follows: three in September 2012, two in May 2013, three in July 2013 and three in September 2013. The Broadleaf Forests sampled in 2012 and 2013 had an average slope of 2%.

Percent Cover Results

The average percent cover by strata for each vegetation survey period within the Broadleaf Forest vegetation class is shown on Figure 3.3-5. Broadleaf forests observed in the Project area contain a diversity of structural layers including: trees, shrubs, forbs, graminoids, bryophytes (mosses, liverworts and hornworts) and epiphytic lichens (lichens that grow on other plants). Fully senesced species were uncommon in Broadleaf Forests; however, dead leaf litter on the ground was prevalent in the September 2012, May 2013, and September 2013 surveys. While species were not fully senesced, some species were undergoing natural seasonal senesce (i.e., leaves changing from green to yellow) in the September 2012 and 2013 survey periods. Tree and shrub species percent cover were highest in the July 2013 plots, because this is when fully developed leaves are found in the largest quantities. An example of the Broadleaf Forest vegetation class in each survey season is provided on Figure 3.3-6.

Figure 3.3-5: Average Percent Cover by Strata for Each Vegetation Survey Period in the Broadleaf Vegetation Class: Living and Senesced and/or Non-Living

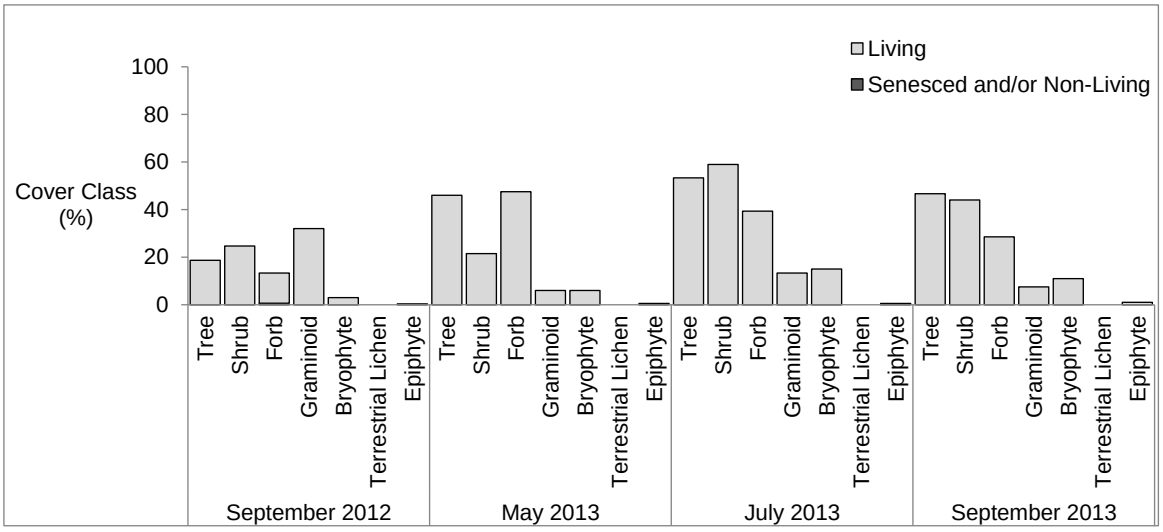

Note: Species with a vigour class of 2 to 4 are considered to be living. Species with vigour class rankings of 0 to 1 are considered to be senesced and/or non-living. The cause of senesced and/or non-living species may be due to seasonal causes or unknown causes (i.e., winter kill).

Figure 3.3-6: Example of the Broadleaf Forest Vegetation Class (Plot 13-35a)

September 2012

May 2013

July 2013

September 2013

Species Richness Results

Species richness data for each sample season within the Broadleaf Forest vegetation class is presented in Table 3.3-4. In general, species richness within the Broadleaf Forest vegetation class was high relative to other vegetation classes within the Project area with multiple structural layers of species (i.e., tree, shrub, forb). Common dominant tree species included trembling aspen (*Populus tremuloides*) and balsam poplar (*Populus balsamifera*). Shrub layers varied by plot with common dominant species including beaked hazelnut (*Corylus cornuta*) and red-osier dogwood (*Cornus stolonifera*). Plot ground layers included small shrubs, forbs and grasses as well as smaller amounts of bryophytes and lichens. The average species richness across all field programs was 22 species per plot. The maximum number of species recorded at one plot was 29 and the minimum was 11. Average species richness was highest in the summer (26) and lowest in the fall (21).

Table 3.3-4: Species Richness Values within Broadleaf Forests

Parameter	Survey Period			
	Spring (May 2013)	Summer (Summer 2013)	Fall (September 2012 and 2013)	Across All Field Programs
Average Species Richness	22	26	21	22
Maximum Species Richness	22	27	29	29
Minimum Species Richness	21	25	11	11
Number of Surveys[(a)]	2	3	6	11
Number of Plots[(b)]	2	3	5	5

(a) Refers to the number of survey visits. A single vegetation plot may have had multiple vegetation surveys completed over various seasons.
(b) Refers to the numbers of physical plot locations.

Health Assessment Results

Overall, the assessment of species vigour indicates that plants within Broadleaf Forests were healthy. Vigour class rankings were good to excellent during the summer (i.e., July 2013) with an average of 3.9 for trees, 3.8 for shrubs, 3.9 for forbs, 4.0 for graminoids, 4.0 for bryophytes and 4.0 for epiphytic lichens (i.e., lichens that grow on other plants). These results are expected because July is the middle of the growing season when conditions are optimal for plant growth. During the spring and fall seasons (i.e., September 2012, May 2013 and September 2013), vigour classes averages ranged from 2.4 to 4.0.

Minor stresses from fungal disease and herbivory also resulted in lower vigour class rankings; however, these were only present in minor amounts and plants did not appear stressed. For example, insect galls were observed on pin cherry (*Prunus pensylvanica*) within plot 12-24-0713. Other stresses such as anthropogenic disturbances were not observed in substantial amounts during vegetation surveys.

3.3.2.4 Coniferous Forests

The Coniferous Forests vegetation class refers to forested land dominated by coniferous (evergreen) and/or larch trees. Coniferous forest stands may contain less abundant components of deciduous broadleaf trees. This vegetation class occupies 374 km^2 (9.8%) of the Project area. The number of Coniferous Forest plots assessed in each sample period was as follows: two plots in each of September 2012, May 2013, July 2013 and September 2013. The Coniferous Forests sampled in 2012 and 2013 had an average slope of 0%.

Percent Cover Results

The average percent cover by strata for each vegetation survey period within the Coniferous Forest vegetation class is shown on Figure 3.3-7. Coniferous forests observed in the Project area contain a diversity of structural layers including: trees, shrubs, forbs, graminoids, bryophytes (mosses, liverworts and hornworts), terrestrial lichens (lichens that grow on the ground) and epiphytic lichens (lichens that grow on other plants). Similar to Broadleaf forests, fully senesced species were uncommon in Coniferous Forests; however, dead leaf litter on the ground was prevalent in the September 2012, May 2013, and September 2013 surveys. In addition, while species were not fully senesced, species were undergoing natural seasonal senescence (i.e., leaves changing from green to yellow) in the September 2012 and 2013 survey periods. Average bryophyte percent cover was high in all of the 2013 field survey periods; however, it was less in September 2012 due to a change in plots between years. Within a plot, bryophyte cover does not change much between seasons and percent cover is higher in areas with higher moisture regimes, making up the majority of the forest floor. An example of the Coniferous Forest vegetation class in each survey season is provided on Figure 3.3-8.

Figure 3.3-7: Average Percent Cover by Strata for Each Vegetation Survey Period in the Coniferous Forests Vegetation Class: Living and Senesced and/or Non-Living

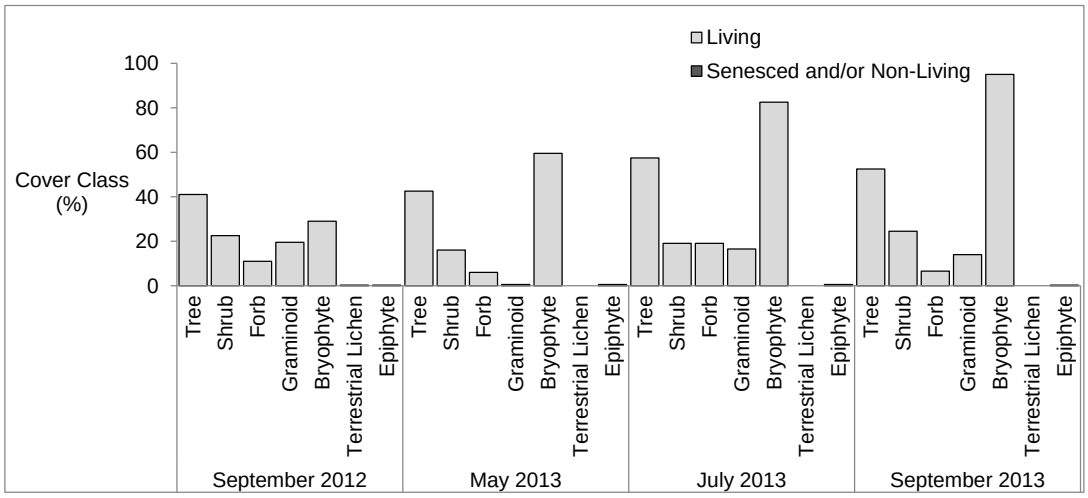

Note: Species with a vigour class of 2 to 4 are considered to be living. Species with vigour class rankings of 0 to 1 are considered to be senesced and/or non-living. The cause of senesced and/or non-living species may be due to seasonal causes or unknown causes (i.e., winter kill).

Figure 3.3-8: Example of the Coniferous Forest Vegetation Class (Plot 04-33b)

September 2012

May 2013

July 2013

September 2013

Species Richness Results

Species richness data for each sample season within the Coniferous Forest vegetation class is presented in Table 3.3-5. In general, species richness within the Coniferous Forest vegetation class was high relative to other vegetation classes within the Project area due to multiple structural layers of species (i.e., tree, shrub, forb). Common dominant tree species included black spruce (*Picea mariana*) and white spruce (*Picea glauca*). Shrub layers varied by plot with common dominant species including wild red raspberry (*Rubus idaeus*) and northern gooseberry (*Ribes oxyacanthoides*). Plot ground layers included mainly bryophytes and grasses with lesser amounts of small shrubs, forbs and lichens. The species richness average across all field programs was 17 species per plot. The maximum number of species recorded at one plot was 29 and the minimum was ten. Average species richness was highest in the fall (20) and lowest in the spring (13).

Table 3.3-5: Species Richness Values Within Coniferous Forests

Parameter	Survey Period			
	Spring (May 2013)	Summer (Summer 2013)	Fall (September 2012 and 2013)	Across All Field Programs
Average Species Richness	13	14	20	17
Maximum Species Richness	16	18	29	29
Minimum Species Richness	10	10	10	10
Number of Surveys[(a)]	2	2	4	8
Number of Plots[(b)]	2	2	2	2

(a) Refers to the number of survey visits. A single vegetation plot may have had multiple vegetation surveys completed over various seasons.
(b) Refers to the numbers of physical plot locations.

Health Assessment Results

Overall, the assessment of species vigour indicates that plants within Coniferous Forests were healthy. Vigour class rankings were good to excellent during the summer (i.e., July 2013) with an average of 3.6 for trees, 4.0 for shrubs, 4.0 for forbs, 4.0 for graminoids, 4.0 for bryophytes and 4.0 for epiphytic lichens (i.e., lichens that grow on other plants). These results are expected because July is the middle of the growing season when conditions are optimal for plant growth. During the spring and fall seasons (i.e., September 2012, May 2013 and September 2013) vigour class averages ranged from 3.0 to 4.0.

Minor stresses from fungal herbivory also resulted in lower vigour class rankings; however, generally these were only present in minor amounts and plants did not appear stressed. For example, evidence of minor insect herbivory was observed on shrubs within plot 04-33b-0913. Dead trees were noted in some plots; however, this is common as forests age and species are outcompeted. Other stresses such as anthropogenic disturbances were not observed in substantial amounts during vegetation surveys.

3.3.2.5 Wetlands

The Wetlands vegetation class refers to areas where the water table is at, near or above the surface or that is saturated for a long enough period to promote such features as wet-altered soils and water-tolerant vegetation. Wetlands include organic wetlands or peatlands, and mineral wetlands or mineral soil areas that are influenced by excess water, but produce little or no peat. The Wetlands vegetation class occupies 270 km^2 (7.1%) of the Project Area. The number of Wetland plots assessed in each sample period was as follows: one in September

2012, two in each of May 2013, July 2013 and September 2013. The Wetlands sampled in 2012 and 2013 had an average slope of 0%.

Percent Cover Results

The average percent cover by strata for each vegetation survey period within the Wetlands vegetation class is shown on Figure 3.3-9. Within the Wetlands vegetation class, the graminoid stratum was highest in all survey seasons due to the abundance of sedges and hydrophytic (plants adapted to growing in wet areas or water) grass species commonly found in wetlands. Plots were primarily in open wetland types aside from one plot in a treed wetland that was surveyed as a transient plot in September 2012. Forbs were generally present, in low amounts, in each survey period, and included weed species and species adapted to wet-altered soils. Senesced species were observed in the May 2013 program only. This was primarily observed in the semi-permanent plot 16-08 where reed canary grass (*Phalaris arundinacea*) was senesced from the previous growing season without any early season growth. In contrast, beaked sedge (*Carex atherodes*) had already started to begin growing and this species makes up the living graminoid percent cover from May 2013 at plot 16-08. In the September 2013 survey period, reed canary grass and beaked sedge had started to senesce; however these species were not fully senesced at the time of the survey and were, therefore, included in the living percent cover average. An example of the Wetlands vegetation class in each survey season is provided on Figure 3.3-10.

Figure 3.3-9: Average Percent Cover by Strata for Each Vegetation Survey Period in the Wetland Vegetation Class: Living and Senesced and/or Non-Living

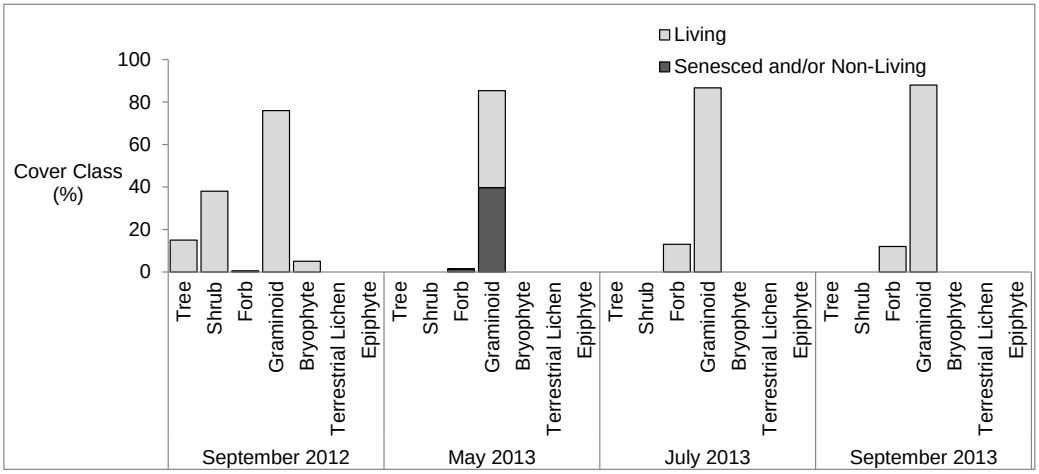

Note: Species with a vigour class of 2 to 4 are considered to be living. Species with vigour class rankings of 0 to 1 are considered to be senesced and/or non-living. The cause of senesced and/or non-living species may be due to seasonal causes or unknown causes (i.e., winter kill).

Figure 3.3-10: Example of the Wetlands Vegetation Class (Plot 16-08)

Plot 16-08 was not surveyed as it was added in 2013

May 2013

September 2012

July 2013

September 2013

Species Richness Results

Species richness data for each sample period within Wetlands is presented in Table 3.3-6. In general, species richness within the Wetlands vegetation class was low relative to other vegetation classes within the Project area. Most wetlands were open areas dominated by one or two grass such as reed canary grass (*Phalaris arundinacea*) and smooth brome (*Bromus inermis*) or sedge species such as awned sedge (*Carex atherodes*) and water sedge (*Carex aquatilis*) with minor amounts of forbs. The species richness average across all field programs was seven species per plot. The maximum number of species recorded at one plot was 11 and the minimum was one. Average species richness was highest in the fall and summer (8) and lowest in the spring (3).

Table 3.3-6: Species Richness Values Within Wetlands

Parameter	Survey Period			
	Spring (May 2013)	Summer (Summer 2013)	Fall (September 2012 and 2013)	Across All Field Programs
Average Species Richness	3	8	8	7
Maximum Species Richness	5	10	11	11
Minimum Species Richness	1	5	3	1
Number of Surveys[(a)]	3	3	4	10[(a)]
Number of Plots[(b)]	2	2	3	3

(a) Refers to the number of survey visits. A single vegetation plot may have had multiple vegetation surveys completed over various seasons.
(b) Refers to the numbers of physical plot locations.

Health Assessment Results

Overall, the assessment of species vigour indicates that plants within Wetlands were healthy. The only signs of stress were due to natural senescence (fall), or left over from the previous growing season that died of unknown causes (i.e., winter kill) (spring). Vigour class rankings were good to excellent during the summer (i.e., July 2013) with an average of 4.0 forbs and 3.8 for graminoids. These results are expected because July is the middle of the growing season when conditions are optimal for plant growth. During the spring and fall seasons (i.e., September 2012, May 2013 and September 2013) vigour class averages ranged from 2.0 to 3.1. Grazing pressures from cattle lead to lower vigour rankings during the May 2013 surveys at plot 03-36b-0513. Some forbs species such as Canada thistle (*Cirsium* arvense) in plot 16-08 showed signs of senescence in the September 2013 field program and were given vigour rankings of 2. Other stresses such as disease were not observed in substantial amounts during vegetation surveys.

3.3.3 Summary of Key Findings

Percent Cover Results

Percent cover results were consistent with the growing season. For example, in the spring non-living tissue was more evident because species were not yet beginning to grow for the season. Similarly in the fall, species were undergoing natural senescence as the days start to become shorter and the temperature decreases. Plots with human disturbance (i.e., Annual Crops and Pasture) generally contained only the graminoid and forb layers, while forested plots contained multiple structural layers.

Species Richness

- The largest species richness averages were found in the Broadleaf Forest (22) and Coniferous Forest (17) vegetation classes, which is likely due to the multiple structural layers and also because these areas are largely undisturbed (Table 3.3-7).
- The lowest average species richness was found in Annual Crops (6). This result is expected because these lands have been modified to produce monocultures of one crop type and usually contain only a few weed species due to herbicide application.

Table 3.3-7: Species Richness Averages Within Each Vegetation Class

Parameter	Vegetation Class				
	Annual Crop	Pasture	Broadleaf Forest	Coniferous Forest	Wetlands
Average Species Richness	6	8	22	17	7
Maximum Species Richness	17	11	29	29	11
Minimum Species Richness	1	5	11	10	1
Number of Surveys[(a)]	25	14	11	8	10
Number of Plots[(b)]	8	4	5	2	3

(a) Refers to the number of survey visits. A single vegetation plot may have had multiple vegetation surveys completed over various seasons.
(b) Refers to the numbers of physical plot locations.

Health Assessment Results

- Overall, the assessment of species vigour indicates that plants within all plots were healthy.
- Vigour class rankings were good to excellent during the summer (i.e., July 2013).
- During the fall season (i.e., September 2012 September 2013) vigour classes were more variable because some species were undergoing or had undergone natural senescence (i.e., seasonal cell death) due to age and/or seasonal changes.
- During the spring (i.e., May 2013), some plots had left over vegetation from the previous growing season that died of unknown causes (i.e., winter kill).
- In some pasture plots, grazing was evident; however, plants were still healthy and not over-grazed in most cases.
- Minor amounts of parasitic fungi and insect herbivory were found on some plant species, which did not result in plants being greatly stressed.

3.4 Soils

The focus of the soil program was to gather baseline soil data from dominant soil types within the Area of Review (AOR). A soil characterization program (See Section 3.4.1) was carried in 2012 and 2013 by collecting soil profile data from the monitoring plots within each correlation area (i.e., Soil Correlation Areas [SCA]) contained in the AOR. Soil chemistry data was also collected from the soil profiles for future use as reference data to be used for future monitoring of the AOR.

In addition, the soils program was intended to characterize soil properties that could influence vegetation and satellite spectral signatures over time. The soil properties targeted as potential indicators for spectral signature changes included soil moisture content and soil chemistry (i.e., salinity). A shallow surface soil assessment was conducted in 2012 and 2013 (See Section 3.4.2) to determine soil moisture and soil salinity levels during satellite and spectral data collection.

3.4.1 Soil Profile Characterization Program

The objective of the detailed soil profile characterization was to classify soils within each vegetation land classification across the three SCA encompassed by the AOR; these include SCA 10, SCA 12, and SCA 21. Soil chemical and physical characteristics were collected from each soil profile to establish baseline conditions within

each plot. In addition, the baseline chemical and physical data provided pertinent parameters for soil classification such as organic carbon content and salinity. This baseline information provides a data set that can be used to correlate soil properties within the plots to soil types present within the AOR.

3.4.1.1 Field Methods

Soil profile characterization required collecting sufficient soil profile information to classify the soils to the sub-group level within the Canadian System of Soil Classification. Fieldwork was completed on all of the plots in October 2012, May 2013 and October 2013. Soil field programs were offset by one week from other disciplines and the satellite flyovers to minimize disturbance during spectral signature collecting. Offsetting the soils programs acted as a precaution to eliminate disturbances such as trampling vegetation and soil rutting.

Soil inspections were completed by digging soil pits with a shovel on each of the monitoring plots. Soil horizon information collected from each of the detailed inspection sites includes:

- horizon type;
- horizon thickness;
- texture;
- mottling;
- structure;
- colour;
- stoniness;
- root abundance; and
- parent material.

Detailed inspection points were classified to the sub-group level of the Canadian System of Soil Classification (SCWG 1998). Once the sub-group was determined, the soils were assigned an Alberta soil series name based on the applicable SCA, soil sub-group, and parent material. The Project is located within SCA 10, 12 and 21 which are referred to as the Thick Black/Dark Gray – Gray Soil Zone of Central and East-Central Alberta, the Dark Gray – Gray Soil Zone of Northeast-Central Alberta, and the Central Mixedwood Area of East-Central Alberta, respectively (Brierley et al. 2006) Figure 3.4-1.

After each plot survey, the soil survey equipment, including shovels, augers and footwear, were disinfected with a 2% bleach water solution, as prescribed by the *Alberta Clubroot Management Plan* developed by Alberta Clubroot Management Committee, revised May 2010 (ACMC 2010). Additionally, the crew also followed, where applicable, the Best Management Practices outlined by the Canadian Association of Petroleum Producers *Best Management Practices, Clubroot Disease Management* (CAPP 2008).

Figure 3.4-1: Map of Area of Review Boundary Showing Soil Correlation Areas and Monitoring Plot Locations.

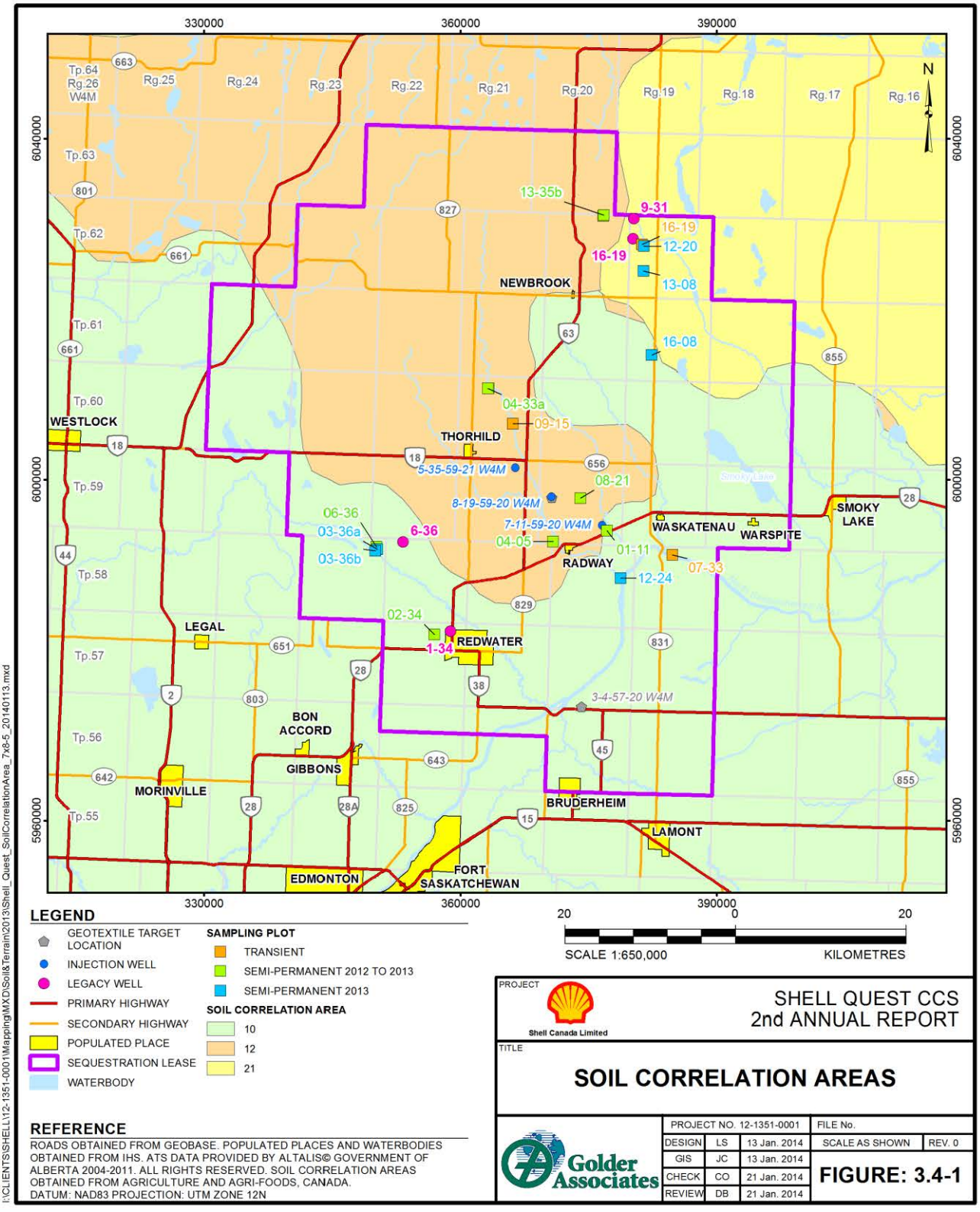

3.4.1.2 Soil Sampling

Soil samples were gathered from the detailed soil inspection sites to determine chemical and physical properties of each soil profile. The soil sampling program was carried out in conjunction with the soil profile characterization in October 2012, May 2013, and October 2013. Soil samples were not collected in July 2013 because land access had not been granted for the remaining plots requiring soil characterization; these plots were completed during the October 2013 program.

A soil sample was collected with a hand trowel from each of the horizons in the soil profile (i.e., one sample from Litter, Fibric, Humic (LFH), Ah or Ap, Bm, BC, Ck). All samples were packed in either sealable plastic sample bags or glass sample jars and stored temporarily before delivery to Exova Laboratories.

3.4.1.3 Laboratory Analytical Methods

Each soil sample was analyzed for the following characteristics:

- cation exchange capacity;
- available nutrients;
- percent organic matter;
- soil texture; and
- salinity.

The methods implemented by Exova Laboratories to analyze the soil samples for each soil horizon are listed in Table 3.4-1.

Table 3.4-1: Exova Soil Analytical Methods

Analysis	Reference	Method
Cation exchange capacity (CEC)	McKeague, 1978	CEC and exchangeable cations by NH4Ac at pH 7, 3.32
Percent organic matter (%OM)	Bartels, 1996	total carbon, organic carbon, and organic matter, Ch 34
Particle size distribution	Carter, 2008	hydrometer method, 55.3
Total moisture	Carter, 2008	gravimetric method with oven drying, 51.2
Percent saturation (% saturation)	Carter, 2008	gravimetic method with oven drying, 51.2
Salinity	Carter, 2008	saturated paste method
Bulk density	Klute, 1986	core method, 13-2

3.4.2 Results

Soil sub-groups for each vegetation type and plot location are summarized in Table 3.4-2. Soil series names corresponding to the SCA that the plots were located within were also determined for each of the soils identified. Some plots had more than one soil sub-group identified within the same vegetation type. Plot 01-11 contained two different soil sub-groups both developed on Glacial Till on an Annual Crop plot. This difference can be

explained by variations in topography, its effects on soil water, and their combined influence on native vegetation within the plot. These factors affect development at a scale resulting in observable changes in soil type within the 100 x 100 m monitoring plots.

Table 3.4-2: Soil Characteristics Within Monitoring Plots Sorted by Soil Correlation Area and Vegetation Type

Plot	Vegetation Type	SCA	Parent Material	Soil Sub-Group	Soil Series Name
02-34	Annual Crop	10	Glacial Till	Black Solodized Solonetz	Dnister
01-11	Annual Crop	10	Glacial Till	Dark Gray Luvisol	Uncas
01-11	Annual Crop	10	Glacial Till	Orthic Black Chernozem	Peace Hills
12-24	Annual Crop	10	Glaciofluvial	Orthic Regosol	Lindbrook
03-36b	Wetland	10	Glaciofluvial	Orthic Dark Grey Chernozem	Redwater
12-24	Broadleaf	10	Glaciofluvial	Orthic Regosol	Lindbrook
06-36	Broadleaf	10	Glaciofluvial	Eluviated Eutric Brunisol	Primula
06-36	Conifer	10	Glaciofluvial	Eluviated Eutric Brunisol	Primula
03-36a	Pasture	10	Glaciolacustirine	Orthic Humic Gleysol	Haight
08-21	Annual Crop	12	Glacial Till	Dark Gray Luvisol	Spedden
09-15	Annual Crop	12	Peat overlying Glacial Till	Terric Mesisol	Manatokan
07-33	Annual crop	12	Glacial Till	Orthic Dark Gray Chernozem	Rolley View
04-05	Annual crop	12	Glaciofluvial	Orthic Dark Gray Chernozem	Kehiwin
13-08	Annual Crop	12	Glacial Till	Orthic Gray Luvisol	La Corey
16-08	Wetland	12	Fen Peat	Terric Mesisol	Manatokan
07-33	Broadleaf	12	Glacial Till	Orthic Dark Gray Chernozem	Rolley View
13-35a	Broadleaf	12	Glacial Till	Orthic Gray Luvisol	La Corey
04-33b	Conifer	12	Peat overlying Glacial Till	Terric Mesisol	Manatokan
04-33a	Pasture	12	Peat overlying Glacial Till	Terric Mesisol	Manatokan
13-35b	Pasture	12	Peat overlying Glacial Till	Terric Mesisol	Manatokan
16-19	Annual Crop	21	Glacial Till	Orthic Gray Luvisol	La Corey
12-20	Broadleaf	21	Glacial Till	Humic Luvic Gleysol	Mapova

Soil sub-groups and parent materials were identified within the plots across the three SCAs located in the AOR. Soil sub-groups identified in the SCA 10 plots included: Eluviated Eutric Brunisol, Black Solodized Solonetz, Dark Gray Luvisol, Orthic Black Chernozem, Orthic Humic Gleysol, Orthic Dark Grey Chernozem, Regosolic Humic Gleysol, and Orthic Regosol. Soil correlation area 12 plots were found to include the following soil sub-groups: Dark Gray Luvisol, Orthic Dark Gray Chernozem, Orthic Gray Luvisol, Eluviated Eutric Brunisol and Terric Mesisol. Soil sub-groups found on plots in SCA 21 included Orthic Gray Luvisol and Humic Luvic Gleysol.

Parent materials within the SCA 10 plots include glacial till, glaciofluvial and glaciolacustrine deposits. Soils within SCA 12 plots were found to have formed on a number of parent materials, including: glacial till, glaciofluvial, fen peat, and fen peat overlying glacial till. Plots in SCA 21 contained soils formed on glacial till.

3.4.3 Summary of Key Findings

Soil classification results on monitoring plots within SCA 10 do not indicate a correlation between vegetation type and soil sub-group. However, the data do indicate that parent material types could influence vegetation cover among the plots; this supposition cannot be extrapolated to other areas within the AOR because the study lacks the comprehensive data to support this conclusion. The results show that the conifer vegetation plot was associated with glaciofluvial parent material. Glacial till parent material was found on all annual crop plots. The broadleaf plot and both pasture vegetation types were found to contain glaciofluvial parent material. Wetland vegetation types were associated with glaciolacustrine and organic parent materials.

Soil type within the plots located within SCA 12 was generally influenced by location within the SCA. Specifically, climatic factors moving northward through the SCA account for changing vegetation and soil type (Pedocan, 1993). Further north within SCA 12, the climate is cooler, with a lower rate of evapotranspiration (Pedocan, 1993). As a result, SCA 12 transitions from parkland vegetation cover in the south to a forested vegetation cover in the north (Pedocan, 1993). Monitoring plots found in the southern portion of SCA 12 were predominantly Chernozemic soils, characteristic of grassland and parkland ecosystems. These soils were identified on plots with annual crop vegetation cover. Plots located further north in SCA 12 contained soils associated with a forested ecosystem, such as Luvisols and Mesisols, and were identified on wetlands, annual crops, pasture, conifer, and broadleaf vegetation types. The annual crop and pasture plots in the northern part of SCA 12 appeared to be located on cleared forests, since Luvisolic soils are formed under forest vegetation.

Soils on the plots within SCA 21 were found on annual cropland and broadleaf vegetation types. Both plots contained soils expected for the forested vegetation cover (Orthic Grey Luvisol, and Humic Luvic Gleysol).

3.4.4 Shallow Surface Soil Sampling Program

The objective of the shallow surface soil sampling program was to collect soil moisture data from the 0 to 15 cm soil depth during satellite data collection. The October 2012, May 2013, and July 2013 sampling programs collected samples for moisture data alone. The October 2013 shallow sampling program was modified to include soil salinity and percent saturation data along with the soil moisture data. Further, the sampling intensity was increased with the objective of correlating remote sensing data with soil moisture and salinity by image pixel collected by the satellite. Ultimately, these data may be used to calibrate satellite data with surface soil data that can be referred to beyond the baseline phase of the Project.

3.4.4.1 Field Methods

During the 2012 and 2013 field programs, shallow surface soil samples were collected in conjunction with the vegetation assessments. Surface soil samples were collected in a random pattern to a depth of 0 to 15 cm below the soil surface and then mixed to create a composite sample. The 0 to 15 cm sampling depth was selected due to the effective depth of the remote sensing technology for analyzing soil salinity, which does not penetrate below 15 cm. The soils were placed in sealable sample bags for transport to the Golder Associates Ltd. Geotechnical Lab in Edmonton for soil moisture content analysis.

The October 2013 shallow surface sampling program was designed to collect soil moisture, soil salinity (electrical conductivity), and percent saturation data to allow correlations with remote sensing spectral signatures and RadarSat2 data. A sampling pattern was established to capture 10 soil samples (0-15 cm) per 50 x 50 m plot to represent individual RadarSat2 image pixels (5 m by 5 m). A consistent sampling pattern was applied to all plots. Prior to collecting the field data, the sampling pattern was geo-referenced for each plot. The sampling points were located in the field using sub-metre accurate GPS. The samples were packed into 1 L glass jars and delivered to Exova Laboratories for moisture, percent saturation, and salinity analysis.

3.4.4.2 Laboratory Analytical Methods

The analytical methods implemented by Exova Laboratories and the Golder Edmonton materials testing lab are listed in Table 3.4-3.

Table 3.4-3: Exova and Golder Edmonton Material Testing Laboratory Soil Analytical Methods

Analysis	Reference	Method
Total moisture	Carter, 2008	gravimetric method with oven drying, 51.2
Percent saturation (% saturation)	Carter, 2008	saturated paste with gravimetric method and oven drying, 51.2
Salinity	Carter, 2008	saturated paste method

3.4.4.3 Results

The soil data analyzed for the October 2012, May 2013, July 2013, and October 2013 shallow surface sampling programs are summarized in Figure 3.4-1 and Figure 3.4-2 to Figure 3.4-6. The data are grouped by vegetation type for the monitoring plots visited during each field program. Values are displayed as number of samples taken (n), maximum value (Max), minimum value (Min), mean, and standard deviation (SD).

Table 3.4-4: Soil Moisture Contents by Vegetation Type – October 2012

Vegetation Type	Field Program	n	Max [%]	Min [%]	Mean [%]	SD
Annual Crop	October 2012	36	129.0	9.3	42.3	36.2
Pasture/Conifer	October 2012	9	151.0	10.9	76.6	56.2
Broadleaf/Pasture	October 2012	9	256.1	39.1	154.3	90.3
Water/Riparian/ Conifer/Annual Crop	October 2012	12	22.0	5.9	13.0	4.5
Conifer/Pasture/ Broadleaf	October 2012	9	84.8	2.0	23.2	30.9

Figure 3.4-2: Mean Soil Moisture content by Plot Vegetation Type for Spring 2013 Sampling Period

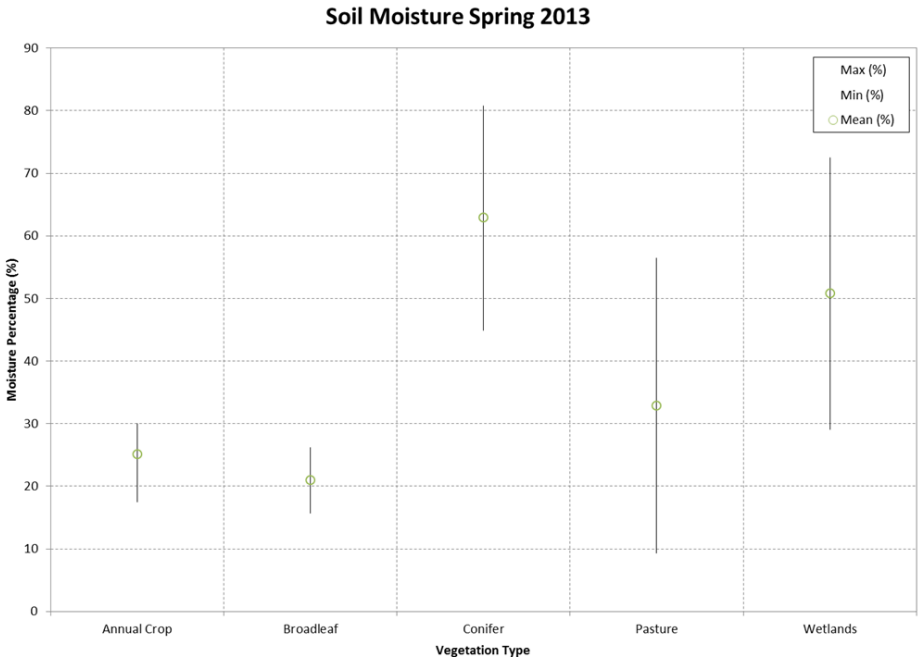

Note: Points equal the percent mean, while bars represent the maximum and minimum values.

Figure 3.4-3: Mean Soil Moisture Content by Plot Vegetation Type for Summer 2013 Sampling Period

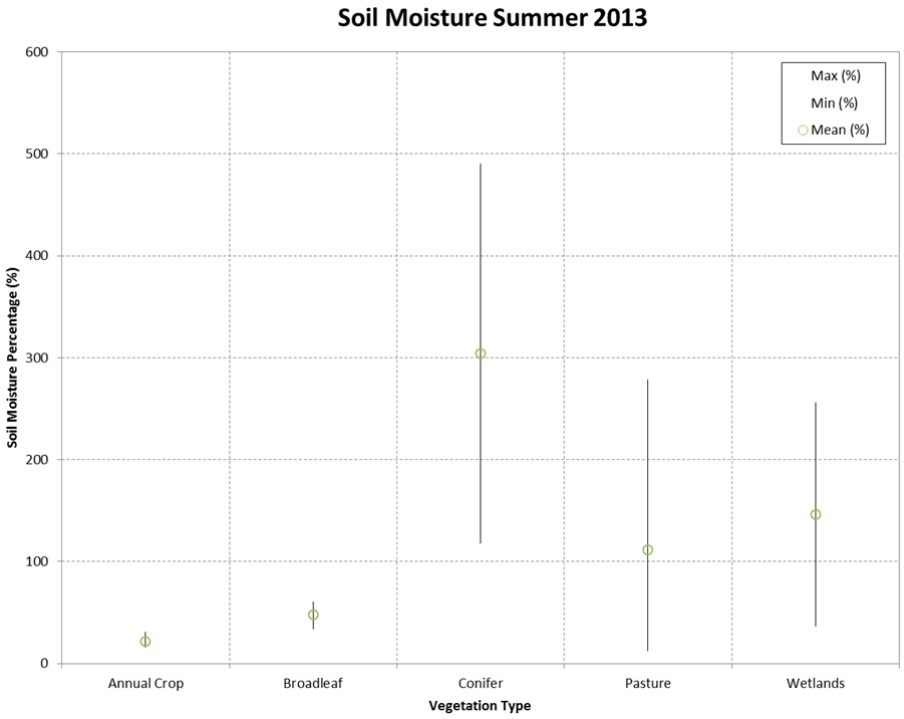

Note: Points equal the percent mean, while bars represent the maximum and minimum values.

Figure 3.4-4: Mean Soil Moisture Content by Plot Vegetation Type for Fall (October) 2013 Sampling Period

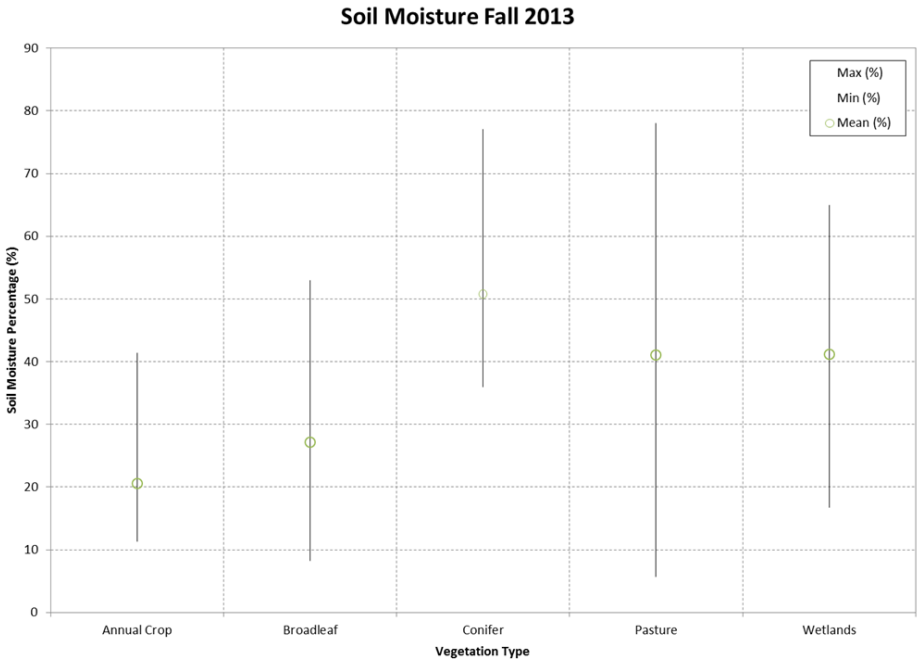

Note: Points equal the percent mean, while bars represent the maximum and minimum values.

Figure 3.4-5: Mean Soil Percent Saturation by Vegetation Type for Fall (October) 2013 Sampling Period

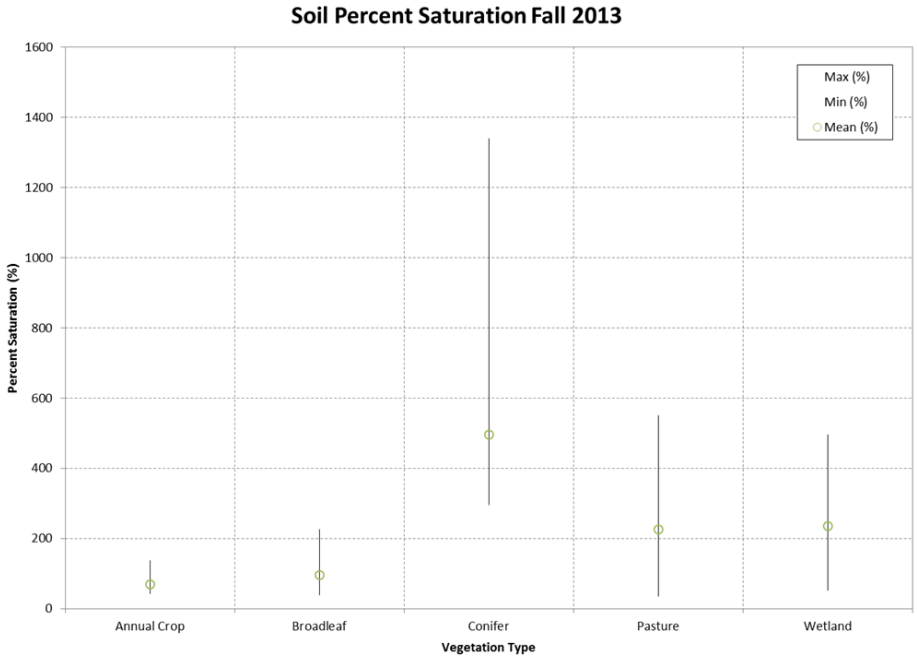

Note: Points equal the percent mean, while bars represent the maximum and minimum values.

Figure 3.4-6: Mean Soil Electrical Conductivity by Vegetation Type for Fall (October) 2013 Sampling Period

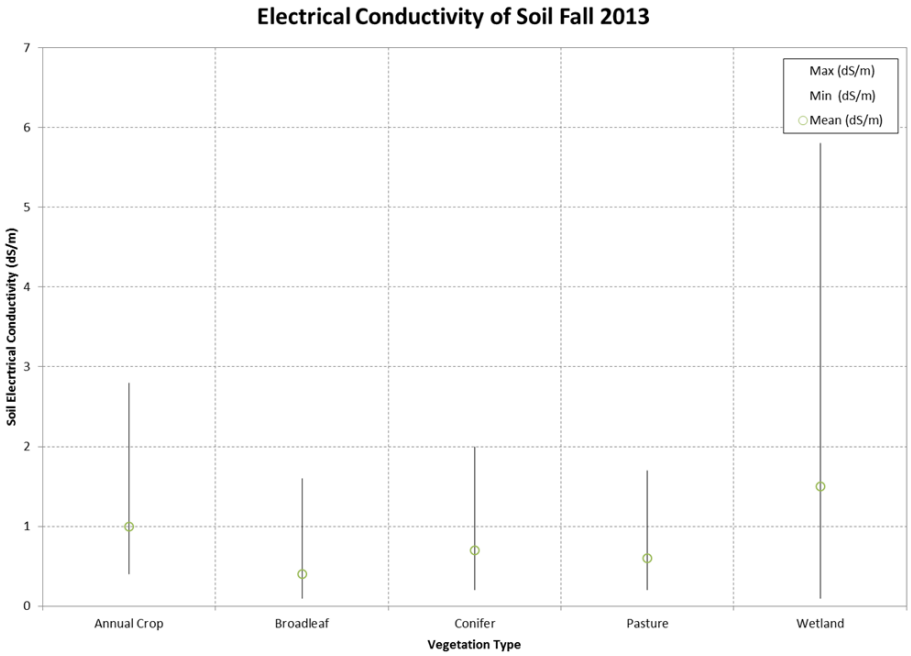

Note: Points equal the percent mean, while bars represent the maximum and minimum values.

The results indicate that the vegetation types with organic surface soil horizons contain very high soil moisture contents. In several samples, the moisture percentage exceeded 100%. Organic material has very high water holding capacity and hence soils possessing an organic surface layer exhibit high moisture contents. Since the shallow samples were taken from a depth of 0 to 15 cm, quite often the surface soil samples consisted completely of organic soil or had a significant percentage of organic matter in them (i.e., peat), resulting in high surface soil moisture contents on these sites.

3.4.4.4 Summary of Key Findings

Soil Moisture

The conifer, wetlands and pasture vegetation types consistently showed the highest mean soil moisture contents among the three sampling programs. This can be attributed to the soil type (Organic and Gleysolic soils) and landscape position (level areas) predominantly found within these cover types. Organic and Gleysolic soils have a high organic matter content which increases moisture holding capacity. Both Gleysolic and Organic soils are typically saturated throughout much of the year, since they are located in lower slope positions where water accumulates. In addition, both soil types are typically poorly drained, which indicates that water does not leave the profile readily. Broadleaf and annual crop cover types showed the lowest soil moisture contents throughout the three sampling programs. Plots from both of these cover types were dominated by upland soils such as Luvisols and Chernozems, which generally have lower organic matter contents (lower moisture holding capacity) and are better drained than Organic and Gleysolic soils. The October 2013 mean percent saturation data show that soils from conifer, pasture, and wetland plots have saturation percent values of 496.7%, 225.9%, and 235.6%, respectively, compared with annual crop cover plots at 69.2% and broadleaf plots at 95.0%, leading to the conclusion that some soil types have higher soil moisture retention capacity than others, largely as a result of an organic surface layer.

The variability in soil moisture content among the sampling programs can also be affected by factors such as seasonal drainage, rainfall, and evapotranspiration rates at the time of sample collection. The July 2013 data showed the highest overall soil moisture contents among the sampling programs. This is most likely a result of rainfall accumulation throughout the spring and early summer. The May 2013 and October 2013 data showed similar mean soil moisture patterns between sampling programs. Rapid snowmelt and low rainfall leading up to the May 2013 sampling program likely resulted in the lower soil moistures found during that time. Evapotranspiration and lower rainfall throughout the late summer and early fall are likely factors resulting in lower soil moisture content recorded during the October 2013 sampling program. The conifer, wetlands, and pasture vegetation types showed the greatest variation in soil moisture contents among the sampling programs, likely a result of the poor drainage and high water retention capability of the soils on these plots. The mean soil moisture contents on broadleaf and annual crop plots were more consistent among the sampling programs, which is likely attributed to the well-drained soils on these plots.

Mean soil salinity levels on the monitoring plots ranged from 0.4 d S/m to 1.5 d S/m. According to the Canada Soil information System, soils are considered slightly saline when conductivity measures between 4.0 to 8.0 dS/m (CanSIS, 1983). Therefore, the surface soils (0-15 cm) within the plots would not be considered to be non-saline with very low levels of soluble salts in the surface horizon.

3.5 EM38

Geophysical ground conductivity surveys were carried out at several transient and semi-permanent plots using the electromagnetic (EM) method. The purpose of this investigation is to assess soil salinity on individual plots to help calibrate RapidEye Satellite data.

3.5.1 Methodology and Quality Assurance/Quality Control

The EM38-MK2 (EM38) Terrain Conductivity Meter measures soil conductivity by considering the inductive response of the ground (Figure 3.5-1). An alternating current is supplied to a wire transmitter coil, producing time-varying magnetic field that penetrates the ground and induces electrical eddy currents within the subsurface materials. The eddy currents give rise to a secondary magnetic field that is measured, together with the primary field, by the receiver coil. The strength of the quadrature component of the secondary field (i.e., that which is 90º out of phase with the primary field), is measured in millisiemens per metre (mS/m) and is approximately equivalent to ground conductivity.

Soil conductivity is controlled principally by porosity, relative pore saturation, pore water ion concentrations (i.e., Total Dissolved Solids [TDS]), temperature and ice content. Clays and silts are typically more conductive than sands and gravels. Ground conductivity increases with elevated TDS (i.e., soil salinity) and with the proportion of clay within the soil. In addition, ground conductivity changes with ground temperature at a rate of approximately 2.2% per degree centigrade.

Both surface and subsurface metal (ferrous and non-ferrous), including fences, steel frame structures, vehicles, underground utilities and storage tanks, affect measured conductivity.

The EM38 instrument contains one transmitting coil and two receiving coils. The coils are oriented in the vertical dipole mode, with the receiver coils spaced 0.5 m and 1.0 m from the transmitter coil; measurements for each receiver coil are recorded simultaneously. The vertical dipole response should be interpreted as a weighted average (apparent) conductivity for hemispherical subsurface volumes that have a radius approximately equivalent to 0.75 and 1.5 m for coil separations of 0.5 m and 1.0 m, respectively. However, peak sensitivity occurs at a depth of 0.35 m and 0.70 m below the instrument, respectively.

Figure 3.5-1: EM38-MK2 Instrument

The EM38 is typically operated in continuous mode while coupled to a data recorder and an integrated GPS receiver. Survey data are typically collected and digitally recorded at a rate of 5 measurements per second as the instrument is carried at ground level by the operator. The GPS receiver utilizes real-time differential corrections provided by the Wide Area Augmentation System which typically enables sub-metre precision in the horizontal. All data are presented in UTM coordinates referenced to the 1983 North American Datum (NAD83), zone 12N.

Quality Assurance/Quality Control (QA/QC) is maintained by calibrating the EM38 through a nulling procedure prior to data collection at each site. The calibration is automatic and software-based, requiring only minimal input from the operator.

During data collection, QA/QC is maintained by monitoring the real-time numerical and graphical readout of conductivity and in-phase values for anomalous responses. Upon completion of data collection, data are uploaded to a laptop computer and graphically plotted to ensure that conductivity and in-phase values are within the expected ranges for the soil type surveyed and that GPS positioning is correct. Additionally, the positions of surface features such as fences, electrical lines, and bodies of water which may affect the data are recorded with a GPS device.

3.5.2 Results

Ground conductivity was measured at transient plots and semi-permanent plots during the fall of 2012 and the spring, summer and fall of 2013. Variations in ground conductivity are evident both between and within the individual plots as a result of variable soil types, ground temperature, pore water ion concentrations, and relative pore saturation. In general, ground conductivity increases with pore saturation, pore water ion concentrations and ground temperature. Fine-grained soils, such as clay and till, are typically more conductive than coarse-grained soils such as sand and gravel.

Results of the EM38 surveys are most commonly presented as colour conductivity maps that illustrate lateral variations in measured ground conductivity as illustrated in the examples on Figure 3.5-2a and Figure 3.5-3b Separate maps are prepared for the 0.5 m and 1 m receiver coil spacings and are labelled as “0.75 Metre Depth” (i.e., Figure 3.5-2a) and “1.5 Metre Depth” (i.e. Figure 3.5-3b), with the depth number denoting the maximum depth of investigation. Increasing ground conductivity is indicated by a gradation from cool colours (blues and greens) to warm colours (yellows and reds). Positions are presented in UTM coordinates referenced to NAD83, zone 12N.

The results of the EM38 survey data are summarized below for each of the five vegetation types.

Figure 3.5-2a: Example Colour Conductivity Map 0.75 m Depth

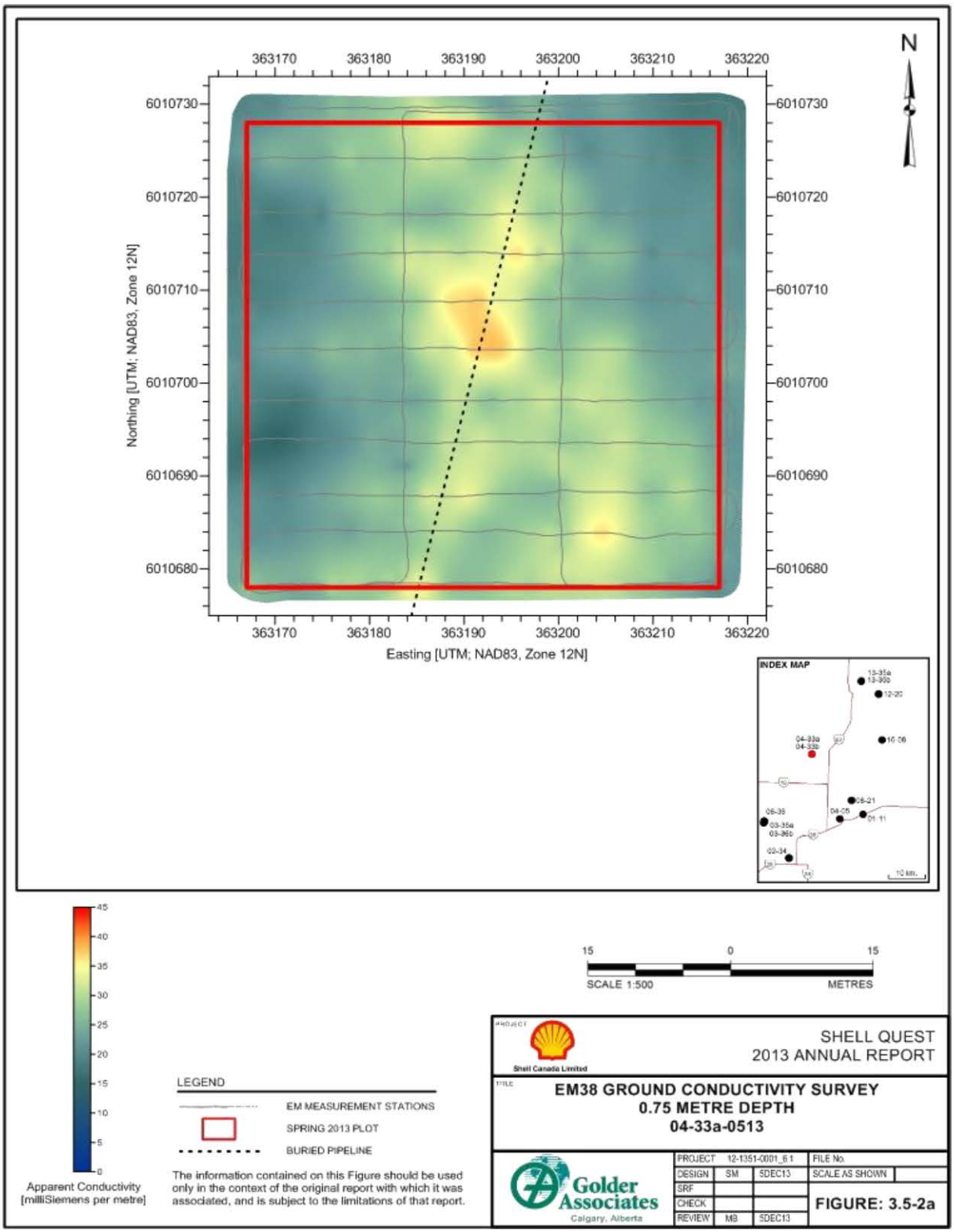

Figure 3.5-3b: Example Colour Conductivity Map 1.5 m Depth

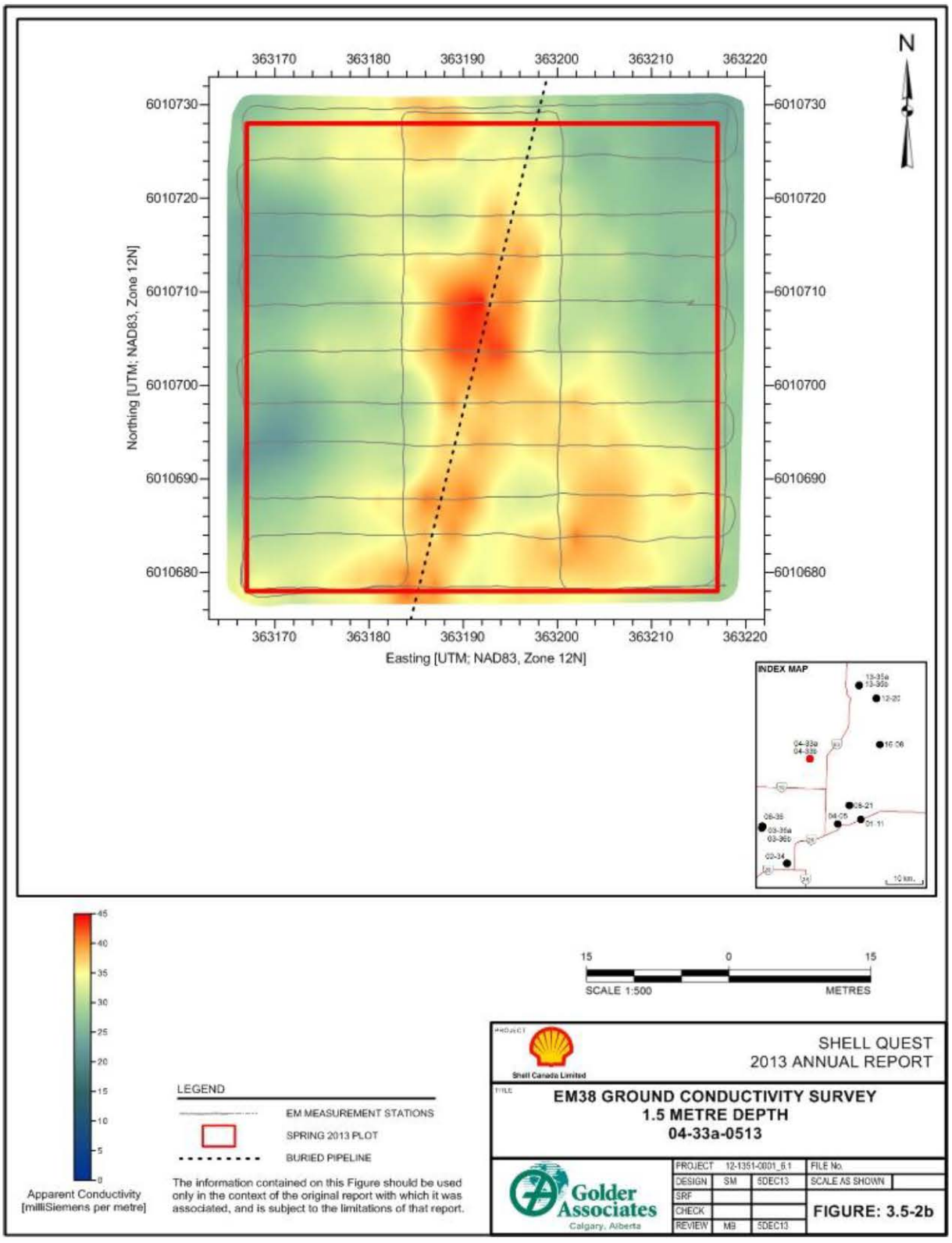

3.5.2.1 Annual Crops

Mean and median ground conductivity at the annual crop plots range from 20 mS/m to 55 mS/m, which is typical of sandy to clayey glacial till. Ground conductivity for the annual crop plot types is relatively high in comparison to the pasture and forest plot types within the Project area.

Measured conductivity for the 1.5 m depth data is generally greater than for the 0.75 m depth data.

Conductivity measured within the annual crop plots is highest during the spring and summer surveys. This may be a result of an increase in moisture content resulting from seasonal variations in precipitation and/or the seasonal addition of soil nutrients for agricultural purposes.

Localized conductivity variations within the individual annual crop plots may be attributed to variations in soil type and/or pore water ion (i.e., TDS) concentrations. Variations in TDS may be, in part, attributable to the distribution of soil nutrients.

Localized high lateral variations in measured conductivity suggest the presence of buried metal within plots 01-11 and 04-05. The presence of buried metal has influenced the minimum and maximum conductivity values, and to some extent the mean and median conductivity values, within these plots.

3.5.2.2 Pastures

The mean and median ground conductivity at the pastures plots range from less than 10 mS/m to approximately 35 mS/m, which is typical of sandy to clayey glacial till.

At plots 04-33 and 04-33a, measured conductivity for the 1.5 m depth is greater than for the 0.75 m depth data. This may indicate higher moisture content and/or higher clay content with soil depth. At the other plots within the pastures vegetation type, there is little variation evident between the two survey depths which may indicate a higher consistency in soil type and/or less variation in soil moisture content with depth.

Conductivity is only slightly higher during the summer surveys. This may be attributed to an increase in moisture content resulting from seasonal variations in precipitation. The generally lower ground conductivity measured in the spring may also be a result of lower ground temperature.

Localized conductivity variations are evident in the immediate vicinity of the existing pipeline at transient plot 04-33 and semi-permanent plot 04-33a. The metal pipeline has resulted in a localized increase in ground conductivity.

Localized elevated ground conductivity is evident adjacent to, and northwest of, the cattle feeder located at the eastern boundary of semi-permanent plot 03-36a. This anomaly may be due, at least in part, to the effects of metal.

3.5.2.3 Broadleaf Forest

Mean and median ground conductivity at the broadleaf plots range between 10 and 20 mS/m. The relatively low conductivities are typical of mostly coarse-grained glaciofluvial and glacial till soils. In addition, uncompacted organic material in the near subsurface also tends to reduce ground conductivity.

In general, little variation is evident between ground conductivity measurements made during the successive seasons. In addition, there are only slight conductivity variations between the 0.75 m and 1.5 m depths.

Localized elevated conductivity is apparent within the northeast quadrant of the 13-35a plot both in the 0.75 m and 1.5 m data. It is possible that this response is a result of a localized increase in pore water ion concentrations (increase in TDS).

Localized variations in ground conductivity are apparent predominantly within the summer and fall survey data at plot 12-20. These anomalies are more evident in the 0.75 m depth data set and may be the result of an increase in TDS at, or close to, ground surface.

Buried metal, as identified by the localized high lateral variations in measured conductivity, is apparent at the transient 06-36 plot. These anomalies may be due, at least in part, to the effects of metal.

3.5.2.4 Coniferous Forests

Little variation in mean and median ground conductivity is evident between the coniferous forests plots, with conductivity generally less than 10 mS/m. The relatively low conductivities are typical of mostly coarse-grained glaciofluvial, peat and glacial till soils (Table 3.4-2). In addition, uncompacted organic material in the near subsurface also tends to reduce ground conductivity.

Little conductivity variation is evident between the 0.75 m and 1.5 m depths. In addition, there is only a very minor variation in ground conductivity between seasons, with just a slight increase in the fall measurements at plot 04-33b.

Localized elevated conductivity is apparent within the southeast quadrant of the 04-33b plot both in the 0.75 m and 1.5 m data. It is possible that this response is a result of a localized increase in pore water ion concentrations (increase in TDS). This anomaly may also be due, at least in part, to the effects of buried metal.

3.5.2.5 Wetlands

Mean and median ground conductivity at the wetlands plots are relatively high in comparison to the pasture and forest plot types within the Project area, with values ranging between 25 and 38 mS/m. The higher conductivity is attributed to the higher moisture content and poor drainage of the relatively low lying plots.

Measured ground conductivity is slightly higher in the 1.5 m depth data than in the 0.75 m depth data at the 16-08 plot. At the 03-36b plot, little difference in ground conductivity is evident between the two depths.

Ground conductivity is at a minimum during the spring and fall surveys and highest during the summer surveys at both of the plots. This is most likely a result of rainfall accumulation throughout the early summer, poor drainage and high water retention capability of the soils (Fen Peat and Glaciofluvial) on these plots.

Variations in ground conductivity are evident within the 16-08 and 03-36b plots and may be attributed to variations in soil type, water saturation and/or TDS. At the 16-08 site, anomalously high conductivity is most evident within the northeast corner of the plot during the summer 2013 sampling period.

3.5.3 Summary of Key Findings

The EM38 surveys have measured ground conductivity at transient and semi-permanent sites at plots within five different vegetation types. Temporal and lateral conductivity variations have been identified at each plot and conductivity variations between plots in each of the vegetation types are also evident.

Temporal variations are mostly attributed to variable soil types, ground temperature, pore water ion concentrations, and relative pore saturation within the near-surface soils. Lateral changes in ground conductivity within each plot and between plots in each of the five vegetation types may be due to differences in porosity, relative pore saturation and/or TDS.

Average ground conductivity was higher for the annual crop and wetland plot types in comparison to the pasture, broadleaf and conifer plot types.

At several sites, ground conductivity has been affected by pipelines and what has been interpreted to be buried metal objects. Any conductivity variations due to differences in soil type and/or TDS concentrations that may occur immediately adjacent to metallic anomalies would likely be masked by the effects of metallic influence.

3.6 Soil Gas and Surface Flux

3.6.1 Fluxnet Literature Review

3.6.1.1 Background

The Fluxnet-Canada Research Network (FCRN) of eddy covariance[2] flux towers and carbon cycle research stations were established across Canada in 2002. The primary objective of the FCRN is to study how management practices (harvesting), natural disturbance (fire), and climate variability influence carbon-cycling in forest and peatland ecosystems in Canada (Margolis et al. 2006).

The FCRN is part of a larger international consortium of regional measurement networks including: Ameriflux, Fluxnet-Canada, AsiaFlux, and CARBOEUROPE. These long-term, ecosystem-level measurement programs contribute to the following scientific objectives (Margolis et al. 2006):

- to collect long-term empirical information necessary for the development, assessment and improvement of mechanistic models of ecosystem physiology that can be used to predict responses to future environmental changes;
- to perform long-term measurements at specific locations that are relevant to larger areas with similar vegetation and climate in order to monitor, and potentially document, environmental changes as they occur within specific ecosystems or geographic regions; and
- to enable coordinated, multi-site comparisons of ecosystem processes and physiological properties across a range of ecosystem types.

The locations of the FCRN measurement sites across Canada are illustrated in Figure 3.6-1. These sites often contain multiple eddy covariance measurements in close local proximity and are not individual eddy covariance measurement locations. For example, data collected at the Saskatchewan BERMS site included measurements in areas disturbed by fire and logging at various dates, as well as measurements in two types of old growth forest (aspen and black spruce). Three FCRN stations were identified as most similar to the environment and climate of the Shell Quest HBMP area near Fort Saskatchewan, Alberta. These sites include the Grassland (AB) site; the Western Peatland (AB) site; and the Saskatchewan (BERMS) site (Table 3.6-1).

[2] A technique used to measure vertical turbulent fluxes of mass and energy within atmospheric boundary layers.

The FCRN data were reviewed, including geographic location, environmental setting, and the length of the available data records. Based on this information, a qualitative indicator of the applicability of the FCRN data to the Shell Quest study area was assigned (i.e., Low, Medium, and High relevance). The station information and quality assessment is summarized in Table 3.6-1.

The FCRN database also includes a well-documented bibliography of peer-reviewed literature produced from FCRN data. These references were evaluated to assess whether they concisely summarized CO_2 fluxes and factors controlling the spatial and temporal variability of CO_2 flux in a format that was directly applicable to the goals of the HBMP. These scientific publications are often focused on detailed ecosystem processes that, in general, are not relevant to the goals of the HBMP. However, early data summaries provide key insights and some of the FCRN results relevant to the HBMP are summarized by ecosystem type in the following sections. The primary advantage of these key publications (i.e., Flanagan et al. 2002) is that they provide an excellent framework for constructing a robust approach for analyzing the FCRN data in the context of the goals of the Shell Quest HBMP.

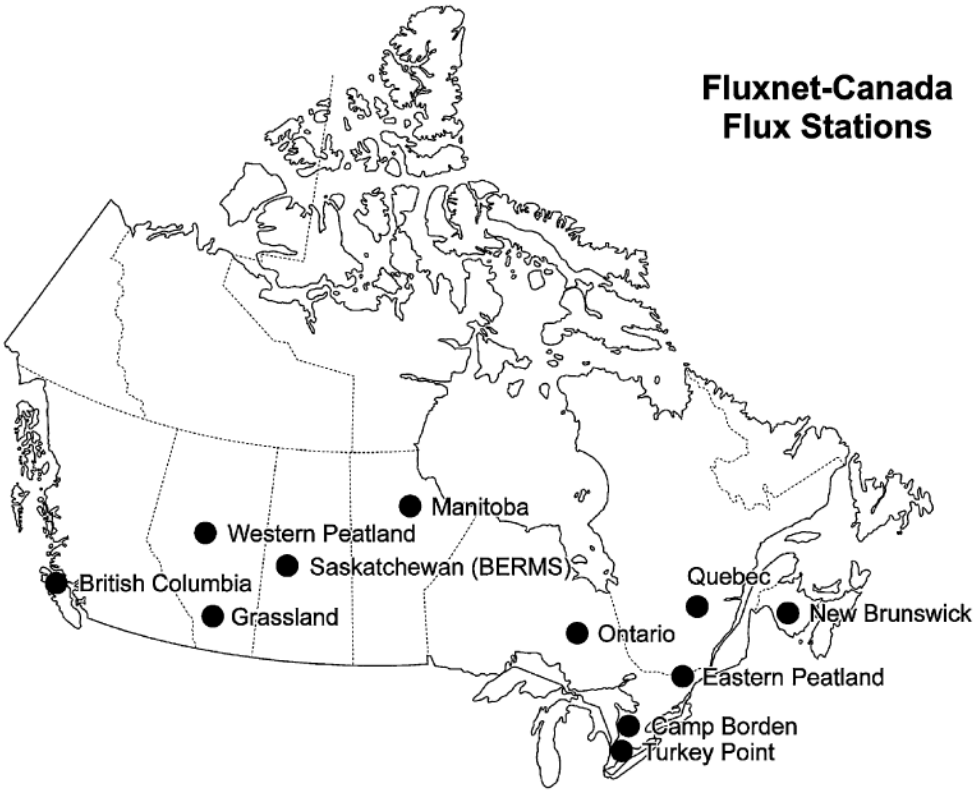

Figure 3.6-1: Fluxnet-Canada Research Network Measurement Locations (Source: Margolis et al. 2006.)

Table 3.6-1: Fluxnet Canada Research Network Data Availability

Site Location (see Figure 3.5-1)	Site Name	North Latitude (deg)	West Longitude (deg)	Site Elevation (masl)	Tower Height (m)	Surface Type	Start Date	End Date	Relevance to Shell Quest
Grassland	AB - Grassland	49.43	112.56	951	6	Mixed Grass Prairie	June-1998	April-2008	High
Western Peatland	AB - Poor Fen	55.54	112.33	626	3	Poor Fen dominated by Sphagnum moss	May-2004 May-2005 May-2006	Oct-2004 Oct-2005 Oct-2006	Low
Western Peatland	AB - Rich Fen	54.47	113.32	626	3	Rich fen dominated by *Carex* (sedges)	May-2004 May-2005 May-2006	Oct-2004 Oct-2005 Oct-2006	Low
Western Peatland	AB - Treed Fen	54.95	112.47	626	9	Peatland dominated by *Larix* (Larch) and *Picea* (Spruce)	Aug-2003	Sept-2009	Medium
Saskatchewan (BERMS)	SK - Fen	53.80	104.62	525	16	n/a - Meteorology Only - No CO_2 Flux			
Saskatchewan (BERMS)	SK - 1977 Fire	54.48	105.82	590	12	Regenerating mixed forest burned in 1977	Jan-2003	Dec-2006	Medium
Saskatchewan (BERMS)	SK - 1989 Fire	54.25	105.88	520	9	Regenerating mixed forest burned in 1989	Jan-2001	Dec-2005	Medium
Saskatchewan (BERMS)	SK - 1998 Fire	53.92	106.08	540	18	Regenerating mixed forest burned in 1998	Jan-2001	Dec-2006	Medium
Saskatchewan (BERMS)	SK - 1975 Harvest	53.88	104.65	534	16	Regenerating Jack Pine forest harvested in 1975	Jan-2004	Dec-2006	Low
Saskatchewan (BERMS)	SK - 1994 Harvest	50.90	104.65	580	5	Regenerating Jack Pine forest harvested in 1994	March-2001	Dec-2002	Low
Saskatchewan (BERMS)	SK - 2002 Harvest	53.94	104.65	517	2	Regenerating Jack Pine forest harvested in 2002	Jan-2003	Dec-2008	Low
Saskatchewan (BERMS)	SK - Old Aspen	53.63	106.20	601	39	Aspen with hazelnut understorey naturally regenerated from 1919 fire	Jan-1996	Dec-2009	High
Saskatchewan (BERMS)	SK - Old Black Spruce	53.99	105.12	629	28	90% *Picea*; 10% *Larix* occasional pine and aspen	Jan-1999	Dec-2009	High

3.6.1.2 Boreal Forests

According to Margolis, Flanagan and Amiro (2006):

> "*Younger forests (<20 years old) tend to be a net source of [carbon] to the atmosphere, while intermediate-aged forests (>20 years old and up to approximately 60 years old or more) have high net [carbon] sequestration. Mature forests, on the other hand, are often nearly neutral in terms of net [carbon] exchange with the atmosphere (Amiro et al., 2006; Coursolle et al., 2006), although they can also remain sinks under certain environmental conditions (Dunn et al., 2006).*"

Net Ecosystem Productivity (NEP; also called Net Ecosystem Exchange [NEE]) determines the net exchange of carbon between the land surface (vegetated or non-vegetated) and the atmosphere. Some results from a modelling study of boreal forests in Canada (Chen et al. 2003), constrained with the FCRN eddy covariance measurements (hollow squares), are included in Figure 3.6-2. Post disturbance (1927 in the old aspen stand), and in the early years of growth, ecosystem respiration (i.e., carbon emission) is predicted to exceed primary productivity (i.e., carbon uptake). This negative NEP (i.e., carbon loss by the ecosystem) results in a net annual flux of CO_2 from the ecosystem to the atmosphere. As the trees mature, primary productivity increases, NEP becomes positive (i.e., carbon gain by the ecosystem), reaches a maximum, and then decreases with age, potentially reaching dynamic equilibrium at some point in the future.

Note the interannual or longer periodic variability in NEP. This is the result of other controlling environmental factors, especially amount and timing of annual precipitation (Kljun et al. 2007), as well as annual nutrient deposition and/or availability (Migliavacca et al. 2011).

Figure 3.6-2: Modelling Simulation of Net Ecosystem Productivity for (left) a 73-year-old Aspen Stand, and (right) a 121-year-old Black Spruce Stand (Source: Chen et al. 2003.)

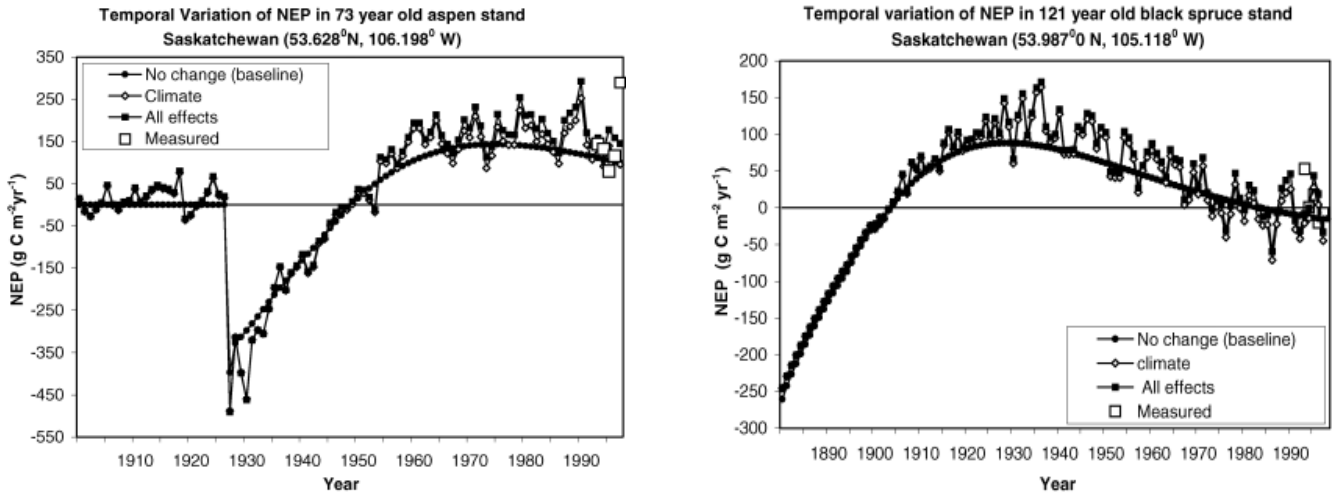

The Shell Quest HBMP employs chamber-based measurements of surface CO_2 flux, compared to net ecosystem CO_2 flux, the term measured by FCRN eddy covariance towers. On September 24, 2012, Golder collected surface CO_2 flux measurements in a young black spruce forest with a pine needle forest floor, and in a mature black spruce stand with a well-developed moss floor. The surface CO_2 flux values for the young stand were 4.04 +/- 0.14 micromoles per metre squared per second ($\mu mol\ m^{-2}\ s^{-1}$; mean and standard deviation),

whereas the moss surface values were 2.41 +/- 0.48 μmol m^{-2} s^{-1}. These HBMP results can be compared to Goulden and Crill (1997) who compared chamber-based measurements of surface CO_2 flux on feather and sphagnum mosses in a mature Saskatchewan black spruce forest to eddy covariance measurements. The Goulden and Crill results show positive surface fluxes of only 0 to 2 μmol m^{-2} s^{-1}, but whole forest fluxes of -7 to +5 μmol m^{-2} s^{-1} in late September of 1995 (days 260 to 274; Figure 3.6-3) the HBMP results illustrate the variability introduced by different surface types (needle-leaf versus mossy forest floor), while the FCRN data illustrate the daily cycles of CO_2 flux and the large numerical difference between fluxes measured by chambers at the surface compared to whole forest fluxes (i.e., NEP), which require eddy covariance measurements.

Figure 3.6-3: Simultaneous Measurements of Moss-Surface Net Exchange (solid lines) and Whole-Forest Net Exchange (dashed lines) in a Black Spruce Forest in Saskatchewan (Source: Goulden and Crill 1997).

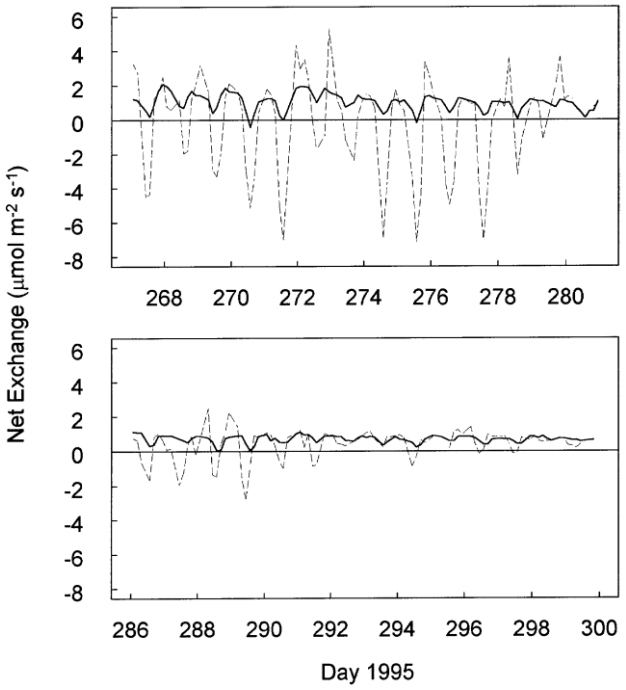

3.6.1.3 Western Canadian Wetlands

The rates of carbon accumulation and the environmental controls on ecosystem photosynthesis and respiration in peatland ecosystems is poorly understood (Syed et al. 2006). This is in spite of the fact that peatlands cover approximately 21% of the western Canadian landscape and contain approximately 80% of the western Canadian stock of soil carbon (Syed et al. 2006). As part of the FCRN, Syed et al. continuously measured net ecosystem carbon dioxide exchange (NEE) using the eddy covariance technique in a treed fen in Alberta dominated by stunted black spruce (*Picea mariana*) and larch (*Larix laricina*) from August 2003 through December 2004. They found ecosystem respiration was highly correlated with changes in ecosystem photosynthesis during the growing season, suggesting important links between plant activity, mycorrhizae[3] and microbial activity in the shallow layers of the peat.

[3] A symbiotic association between a fungus and the roots of a vascular plant.

Bubier et al. (1998) also studied seasonal patterns and environmental controls for NEE in boreal peatlands; Schreader et al. (1998) studied the response of a northern fen to drought. Both of these studies occurred in the sub-arctic boreal wetlands of Manitoba, and are not necessarily applicable to the HBMP area of interest. However, these studies found the following:

- During July/August, the highest rates of NEE followed the trophic sequence bog < poor fen < intermediate fen < rich fen, but in spring and fall ericaceous vegetation[4] and sedges communities[5] found in poor and intermediate fens had higher CO_2 fixation rates than the deciduous shrub communities[6] found in rich fens (Bubier et al. 1998).
- Timing of snowmelt and differential thaw due to micro-topography controlled the onset of carbon uptake in spring, while soil temperature above the water table and timing of the surface thaw in spring, and freeze-up in fall, were the most important factors controlling net annual CO_2 exchange (Bubier et al. 1998).
- During the significant drought of 1994 (at the time, 1994 was the second driest and warmest year since 1943), a deep warm soil aerobic layer promoted respiration fluxes that exceeded the CO_2 uptake of the stressed sedge community (Schreader et al. 1998).
- Under climate warming scenarios, these peatlands (i.e., subarctic peatlands of Manitoba) are expected to become net sources of CO_2 to the atmosphere unless warmer air and soil temperatures are offset by increased precipitation (Schreader et al. 1998).

3.6.1.4 Northern Temperate Grasslands

The data available for the Alberta Grassland FCRN site (Table 3.6-1) is considered highly relevant to the HBMP. The site is located 1.5 km west of Lethbridge, Alberta, and is characterized as moist mixed grassland growing on a dark-brown chernozem soil type. The major objective of the Lethbridge study was to analyze how NEE and total ecosystem respiration vary seasonally, interannually, and in response to changes in precipitation. This information is critical to understanding carbon sink/sources associated with the Canadian prairie because plant productivity in the grassland ecosystems of continental North America is primarily controlled by variations in annual precipitation (Sala et al. 1988). Flanagan et al. (2002) investigated seasonal and interannual variations in CO_2 exchange at this northern temperate grassland site in the years 1998 to 2000.

Flanagan et al. (2002) found that the greatest interannual differences in NEE were due to the amount of local precipitation, and that changes in soil moisture were the most important ecological factor controlling carbon loss/gain in this grassland ecosystem. Seasonally the NEE at Lethbridge is positive (i.e., CO_2 release to the atmosphere) until early May when gross photosynthesis overtakes ecosystem respiration and NEE becomes negative (i.e., CO_2 removed from the atmosphere). By early September rates of gross photosynthesis decline below respiration and the system shifts back to a net release of CO_2 to the atmosphere. However, moisture stress and episodic rainfall during the growing season can lead to large changes in the rates of photosynthesis and respiration. This can result in the ecosystem oscillating between being a net source or a net sink of CO_2 on timescales of days to weeks (Austin et al. 2004). Integrated over the whole year, the NEE values for Lethbridge

[4] Heath or heather family of flowering plants.

[5] *Carex* spp.

[6] *Salix* spp. And *Betula* spp.

are near zero (-21 grams [g] Carbon [C] m^{-2} yr^{-1} in 1999; +18 g C m^{-2} yr^{-1} in 2000) indicating the system is neither a strong source nor a strong sink for CO_2.

The measurements at Lethbridge are put into context in Table 3.6-2 by comparing the southern Alberta results to those of a broader global assessment by Gilmanov et al. (2010). The Lethbridge site is most comparable to the "Extensively Managed Grassland" category in Gilmanov et al. The HBMP "Pastures" and "Annual Crop" vegetation plots are most similar to the "Intensively Managed Grasslands" and "Croplands" categories described in Gilmanov et al. Globally, grassland and agricultural systems appear to be net sinks of CO_2. However, the global data have large standard deviations and, except for croplands, at least 15% of the ecosystems within each ecosystem type appear to be net CO_2 sources rather than sinks. The 1999 and 2000 Alberta data clearly lie within the bottom quartile of the global data for NEE.

Other recent research has integrated measurements from the United States Department of Agriculture Agriflux Network (Svejcar et al. 1997), and the Ameriflux Network (Baldocchi 2003), with remote sensing data to potentially extrapolate eddy covariance tower measurements of CO_2 flux from the Northern Great Plains to larger spatial extents (Gilmanov et al. 2005).

Table 3.6-2: Comparison of Lethbridge Data to Global Data

Variable	Statistic	Lethbridge[a]		Global[b]			
		Mixed Prairie: 1999	Mixed Prairie: 2000	Grasslands: Extensively Managed[c]	Grasslands: Intensively Managed[d]	Wetlands	Croplands
		g CO_2 m^{-2} yr^{-1}					
GPP[e]	mean	287	272	565	6014	2328	4521
	st dev			1698	1133	1836	1365
Total Ecosystem Respiration	mean	267	290	2370	5296	1824	3588
	st dev			1469	1040	1373	909
Net Ecosystem Exchange	mean	-21	+18	255	700	504	933
	st dev			521	717	719	814

[a] Source: Flanagan et al. 2002.
[b] Source: Gilmanov et al. 2010.
[c] Ungrazed, lightly grazed, uncut or cut occasionally.
[d] Regularly cut, grazed, fertilized, irrigated.
[e] Gross Primary Productivity

3.6.1.5 Fluxnet-Canada Research Network Summary and Recommendations

The objective of the FCRN literature review was to determine whether or not the available data could be used to provide context for the Shell Quest HBMP surface CO_2 flux measurements. The FCRN data availability summarized in Table 3.6-1 indicates that several relevant high-quality data sets are available, including many peer-reviewed publications which include findings based on the FCRN measurements. Unfortunately, many publications are focused on ecosystem processes that are too specific to be of general use to the HBMP or the publications integrate the FCRN data into broad assessments aimed at deriving ecosystem averages globally (mostly for climate change research). Notwithstanding, the available publications link variability in net ecosystem

CO_2 exchange to their controlling biotic and abiotic factors, providing a basis from which a robust scientific approach for analyzing FCRN data for the HBMP can be created.

3.6.2 Soil Gas and Surface CO_2 Flux Sampling Methods

3.6.2.1 Soil Gas Sampling

During each quarterly HBMP sampling event, field technicians sample soil gases at multiple depths (0.5, 1.0 and 1.5 m) at each of the injection well sites, and at a single depth (1.5 m) at each vegetation plot. Sampling plots supporting annual crops are sampled using temporary soil gas probes that are removed after each sampling event. All other plots are sampled using semi-permanent soil gas vapour implants that are installed for the duration of the HBMP. Each probe type was installed according to the suggested operating procedure for vapour intrusion investigations that have been modified for the measurement, monitoring and verification plan for the Shell Quest carbon capture and storage project.

To install temporary probes, field technicians drive disposable soil probes to the desired sampling depth using a manual slide hammer. Once at the desired depth, the drive shaft is removed and back filled with washed silica sand and hydrated bentonite clay to maintain a clean, airtight seal. The disposable probes have a metal mesh filter enabling sampling of soil gases through non-sorptive Teflon tubing that connects to the sampling train at ground surface. Each temporary soil gas probe was leak tested in the field using a helium-filled shroud and helium detector after installation (Figure 3.6-4). Probes that fail their helium leak check (i.e., those that are sampling a significant portion of atmospheric air rather than soil gases, as indicated by a leakage[7] rate greater than 2%) are removed and re-installed; those passing their helium leak check are sampled immediately.

Semi-permanent probes are installed at locations where their chance of physical disturbance is low; this approach facilitated efficient resampling season-to-season. Probes with a 15 centimetre (cm) long wire mesh gas vapour implant are installed at the target depth. The small hole created during probe installation is back filled with washed silica sand and hydrated bentonite clay to maintain a clean, air tight seal. The Teflon tubing is finished at the surface with a ball valve and protected at the surface by a flush-mounted aluminum well vault casing (Figure 3.6-4, photo on right). Semi-permanent soil gas probes are also helium leak checked after their installation, but are allowed to rest for a 24-hour period before being sampled for the first time.

[7] Leakage is defined as ratio of He concentration in soil gas divided by shroud concentration times 100%

Figure 3.6-4: Leak Test (left photo) – Flushmount Vault (right photo)

To sample the temporary and semi-permanent soil gas probes, a Swagelock sampling train is connected to the Teflon tubing (temporary probes) or ball valves (semi-permanent probes) at the surface. In fall 2012, a LandTec GEM2000 gas monitor was used to purge three volumes of sample tubing and the soil gas probe before sampling, and to simultaneously measure O_2, CO_2 and CH_4 concentrations. However, the GEM2000 instrument had insufficient precision for quantitative measurements of in situ soil gas concentrations (i.e., a precision of 0.1%, or 1,000 ppmv, for O_2, CO_2 and CH_4). In spring 2013, soil probe purging and monitoring of gas concentrations was accomplished using a Model 915-0011 ultra-portable Greenhouse Gas Analyzer (GGA) (Los Gatos Research, California).

After the probes were purged of air, discrete samples of soil gases were collected using pre-evacuated sampling media. In fall 2012, three soil gas samples consisting of 125 mL pre-evacuated glass vials were collected for offsite laboratory analysis. After analysis of the fall 2012 results, lower reportable detection limits for CO_2 and CH_4 were required to meet the measurement goals for the Quest HBMP. Thus, in 2013 a new commercial laboratory was retained to complete the offsite analysis of the HBMP soil gas samples.

In spring, summer and fall of 2013, three soil gas samples consisting of 250 mL pre-evacuated borosilicate glass bottles were collected. Similar to fall 2012, these samples were analyzed for the following compounds:

- H_2, He, O_2, N_2, CO_2, CH_4, CO, H_2S;
- non-methane hydrocarbons (C_1 – C_7+);
- halogenated hydrocarbons;
- $\delta^{13}C$ of CO_2, $\delta^{13}C$ of CH_4; and
- $\delta^{2}H$ of CH_4.

In summer 2013, laboratory samples returned anomalously high soil gas concentrations of CO, CH_4 and C_1-C_7+ hydrocarbons, as well as anomalously low concentrations of soil gas CO_2. Sample contamination was suspected, but the contamination source could not be conclusively determined. However, shortly after the start of the fall 2013 sampling event, field technicians noted a high percentage (approximately 30%) of the pre-evacuated glass bottles were not passing their pre-sampling check of negative pressure. For example, the

sample bottles had vacuum pressures of only -16 millimetres of mercury (mm Hg), a value less negative than the QA/QC threshold for the vacuum, i.e., -26 mm Hg. This observation indicated that the potential source of sample contamination in summer 2013 was a loss of the vacuum integrity in the sample bottles before soil gas sampling.

As a result, soil gas samples collected in fall 2013 included not only three 250 mL samples collected in pre-evacuated glass bottles at each location, but also one sample collected using a 1.4 L pre-evacuated SUMMA canister. The fall 2013 SUMMA canister samples were analyzed for the same suite of soil gases and isotope ratios as the spring, summer, and fall 2013 glass bottle samples. This adjustment to the sampling protocol effectively doubled the number of samples acquired in fall 2013; however, the results will be instrumental in evaluating the integrity of the soil gas samples being collected as part of the Quest HBMP.

After a laboratory soil gas sample is collected, a valve in the sampling train is switched allowing the GGA instrument to collect one to two additional minutes of real time in situ soil gas concentrations. Since atmospheric and soil gas concentrations of CO_2 and CH_4 differ by several orders of magnitude (see Section 3.6.3), large differences between the pre-sample and post-sample collection concentrations of CO_2 or CH_4 can be indicative of problems associated with the sample being collected (i.e., short-circuiting of atmospheric air into the probe).

3.6.2.2 Surface CO_2 Flux Sampling

Surface CO_2 flux measurements were conducted using a field-deployable LiCor Model 8100A survey CO_2 flux system (Figure 3.6-5) calibrated by the manufacturer on August 13, 2012. The instrument consists of a bowl-shaped chamber connected via pneumatic hoses and electronic cables to an infrared gas analyzer housed inside a durable Pelican™ case. A soil moisture probe and a soil temperature probe are connected through an analog-to-digital input/output circuit. To start the measurement sequence, the instrument is placed upon 20 cm diameter soil collars, which are installed 24 hours before the measurement period. Long grass and other vegetation that may interfere with the closing and sealing of the chamber on the rim of the collar are trimmed using scissors during collar installation. No vegetation, leaf litter or other material is removed from inside the collar unless it will interfere with the instrument, i.e., all efforts are made to minimize disturbance to the surface being analyzed.

Figure 3.6-5: LiCor Model 8100A – Green Gas Analyzer

The LiCor 8100A instrument is controlled wirelessly using an application installed on an Apple iPod™. The flux chamber begins in an elevated position where it is purged by ambient air currents for one minute. The chamber then closes for two minutes. While closed, the infrared gas analyzer is continuously measuring the concentrations of CO_2, and water vapour (H_2O) as a small pump circulates air from the chamber into the gas analyzer and back into the sealed chamber. Positive increases in the concentrations of CO_2 over time indicate a positive flux to the atmosphere; reductions in the concentrations of CO_2 indicate a negative flux. Approximately 6 to 10, three-minute long replicate measurements (1 minute purge, 2 minute sample) were collected at each soil collar. Three surface flux collars were installed within a 1-hectare (ha) area at each sampling location (injection well sites and vegetation plots). These 1-ha areas represent a single, relatively homogeneous land cover type,

so that, in the future, both intra-plot and inter-plot variability among land cover types could be assessed using statistics.

3.6.3 Soil Gas Results

The injection well (IW) and vegetation plot (TP) sites sampled for soil gases in fall 2012 through fall 2013 for the Quest HBMP are summarized in Table 3.6-3. Sites successfully sampled are denoted with an "**X**". Sites not sampled, but annotated with text, are explained as follows:

- **No Access**: the CO_2 injection well at 08-19 was being developed in fall 2012 and prevented sampling at this location.
- **Added Spring 2013**: several new vegetation plot sites were added in spring 2013.
- **Split Spring 2013**: some vegetation plots with multiple land cover types were split into smaller units with distinct land cover types in spring 2013.
- **Added Summer 2013**: two new vegetation plot sites were added in summer 2013.
- **Discontinued**: three sites were discontinued after fall 2012 and not sampled thereafter.
- **Probe Removed**: four semi-permanent soil gas well vault casings were tampered with and/or removed by an unknown third party and were not sampled in summer 2013.
- **Probe Flooded**: several locations in spring and summer 2013 had water tables above the probe installation depth and could not be sampled for soil gases.

Analysis of the HBMP soil gas chemistry data uses a process-based approach modified from Romanak et al. (2012). Using this approach, geochemical relationships are investigated to determine the dominant biotic and abiotic conditions presently occurring within the vadose zone of the injection well and vegetation plot soils. Present or future deviations from known or expected geochemical relations can be indicative of other subsurface processes, i.e., the presence of exogenous CO_2 from a leaking geological CO_2 storage site.

As part of this process based approach, the O_2 concentration deficit versus the CO_2 enrichment for the soil gases measured seasonally as part of the HBMP are plotted in Figure 3.6-6. The terms *deficit* and *enrichment* refer to the concentration of O_2 and CO_2 after removing the canonical background atmospheric values according to the following equations:

$$[O_2]' = [O_2]_{meas} - 20.9460\% \qquad \text{(Equation 3.6-1)}$$

$$[CO_2]' = [CO_2]_{meas} - 0.0400\% \qquad \text{(Equation 3.6-2)}$$

On Figure 3.6-6 a slope of minus one, i.e., 1:1 correspondence between an increase in CO_2 and a decrease in O_2, can indicate simple respiration of soil organic matter by soil microbes using only atmospheric O_2. For comparison, in August/September of 2011 soil gas measurements at Weyburn Saskatchewan produced a slope and offset values of $[O_2]' = 0.55 - 1.16*[CO_2]'$; no confidence interval for the slope was listed (Trium 2011).

During the fall 2012 and fall 2013 HBMP sampling events, O_2 versus CO_2 slopes ranged from -0.76 to -1.61. The slopes derived from the fall 2012 data (-0.78) and the fall 2013 data (-0.76 and -0.81) are indistinguishable based on their overlapping 95% confidence intervals. Slopes of O_2 deficit versus CO_2 enrichment were less than -1.0 in both spring and summer 2013. The HBMP summer 2013 slope (-1.08) is comparable to the summer 2011 Trium results. However, sample contamination was suspected in summer 2013 and the low R^2 value for O_2

versus CO_2 appears to support this conclusion. Soil conditions in spring 2013 were excessively wet and the potential role of saturated soils contributing to the slope of -1.61 is still being investigated as part of the HBMP.

In 2014, soil gas sampling events are planned in winter, spring, summer and fall. Repeat measurements in spring and fall will be important for evaluating seasonal differences between oxygen consumption and carbon dioxide production. Observations in spring 2014 will help to determine the biochemical processes potentially responsible for the excessive depletion of O_2, compared to CO_2 production, observed in spring 2013.

Table 3.6-3: Soil Gas Sampling Summary

Plot Name	Plot Type	Fall 2012	Spring 2013	Summer 2013	Fall 2013
05-35 (50 cm)	Injection Well	X	X	X	X
05-35 (100 cm)	Injection Well	X	X	X	X
05-35 (150 cm)	Injection Well	X	X	X	X
07-11 (50 cm)	Injection Well	X	X	X	X
07-11 (100 cm)	Injection Well	X	X	X	X
07-11 (150 cm)	Injection Well	X	X	X	X
08-19 (50 cm)	Injection Well	No Access	X	Probe Removed	X
8-19 (100 cm)	Injection Well	No Access	X	Probe Removed	X
8-19 (150 cm)	Injection Well	No Access	X	Probe Removed	X
01-11	Semi-Permanent	X	X	X	X
02-34	Semi-Permanent	X	X	X	X
03-36a	Semi-Permanent	Added Spring 2013	X	Probe Removed	X
03-36b	Semi-Permanent	Added Spring 2013	Probe Flooded	Probe Flooded	X
04-05	Semi-Permanent	X	X	X	X
04-33a	Semi-Permanent	X	Probe Flooded	Probe Flooded	X
04-33b	Semi-Permanent	Split Spring 2013	X	X	X
06-36	Semi-Permanent	X	Probe Flooded	Probe Flooded	X
07-33	Transient	X	Discontinued		
08-21	Semi-Permanent	X	X	Probe Flooded	X
09-15	Transient	X	Discontinued		
12-20	Semi-Permanent	Added Spring 2013	X	X	X
12-24	Semi-Permanent	Added Summer 2013		X	X
13-08	Semi-Permanent	Added Spring 2013	Probe Flooded	X	X
13-35a	Semi-Permanent	Split Spring 2013	Probe Flooded	X	X
13-35b	Semi-Permanent	X	Probe Flooded	Probe Flooded	x
16-08	Semi-Permanent	Added Summer 2013		Probe Flooded	X
16-19	Transient	X	Discontinued		

Note: Sites successfully sampled are denoted with an "**X**".

Figure 3.6-6: Seasonal Oxygen Deficit Plotted versus CO_2 Enrichment for Soil Gases Samples

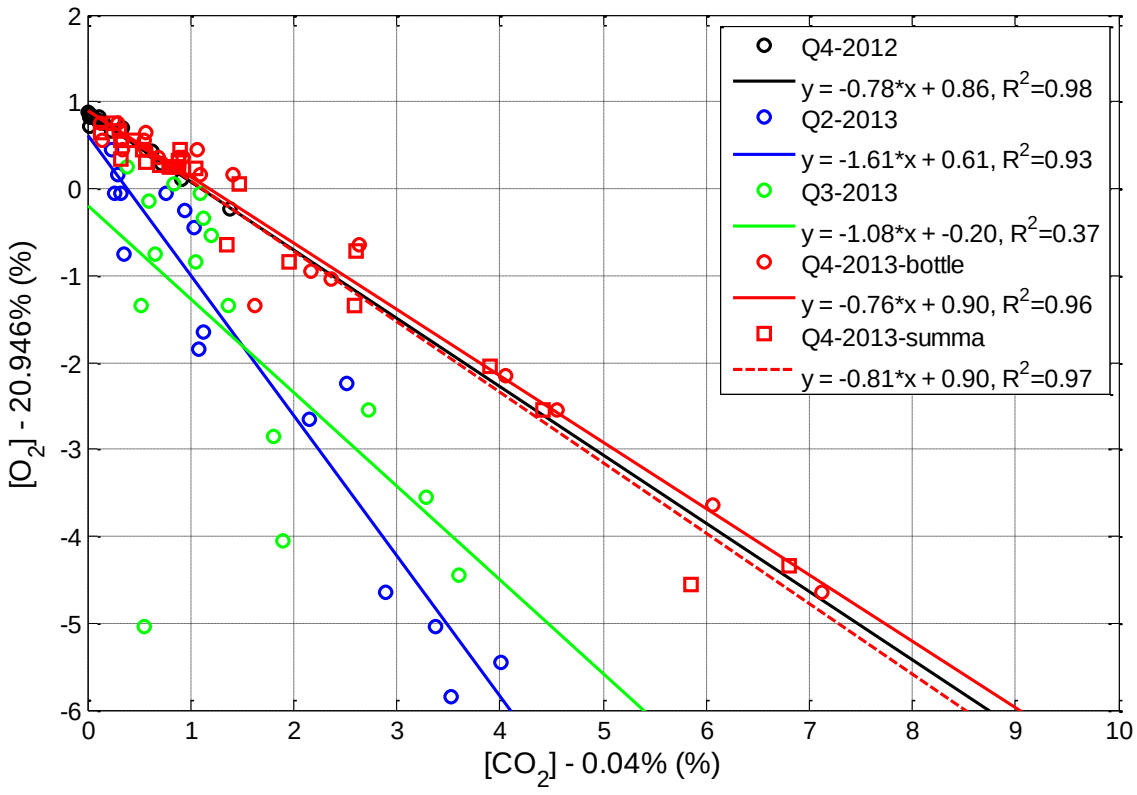

The isotopic composition of soil respired CO_2 can be estimated using a Keeling Plot (Pataki et al. 2003). In a 2-component system where soil gas CO_2 consists of a mixture of atmospheric CO_2 and respired soil gas CO_2, the y-intercept for a Keeling Plot indicates the isotopic composition of the respired CO_2. In a multi-component system, the y-intercept is a molar concentration-weighted average of the isotopic signatures for all sources and sinks of soil gas CO_2. Potential CO_2 sources and sinks can include the following:

- methane oxidation (source);
- dissolution into groundwater (sink);
- plant photosynthesis (sink);
- plant respiration (source);
- microbial autotrophy (sink);
- microbial respiration (source); and
- root respiration (source).

Keeling plots for the HBMP data for each season are provided on Figure 3.6-7. For each soil gas data point, an atmospheric CO_2 data point is added to force the linear regression to include the atmospheric CO_2 end member. The concentration inserted for atmospheric CO_2 is 400 ppmv; the $\delta^{13}C$ of the atmospheric CO_2 is assigned a value of -8.35‰ (+/- 0.31‰). The $\delta^{13}C$ value is the average (+/-1σ) recorded at the Mauna Loa Observatory in Hawaii between January 2008 and December of 2012 (NOAA/ESRL 2013).

The Keeling Plot analysis employs Model II linear regression to account for the following:

- the isotopic composition of CO_2 is not independent from the concentration of CO_2; and
- there is error associated with the measurement of the concentration of CO_2, a violation of the assumptions inherent to standard, Model I linear regression (Laws 1997).

Keeling intercepts derived from the HBMP data vary between -20.58‰ and -23.11‰ and the 95% confidence intervals for these intercepts on average are +/-0.55 ‰. Keeling intercepts may also be used to infer the $\delta^{13}C$ composition of the soil organic matter that was respired to create the soil gas CO_2. Differing diffusion rates for $^{12}CO_2$ versus $^{13}CO_2$ leads to isotopic fractionation and soil gas CO_2 can be approximately 4.4‰ higher than the soil organic matter from which it was derived (Cerling 1984; Cerling et al. 1991). Adjusting the HBMP Keeling intercepts for this observation yields $\delta^{13}C$ values of -24.98‰ to -27.51‰. These isotopic ratios are indicative of soil gas CO_2 derived predominantly from the respiration of soil organic matter formed from C3 plants ($\delta^{13}C$ ~= -27‰) rather than C4 plants ($\delta^{13}C$ ~= -13‰) (Henderson et al. 2004).

In all samples collected for the HBMP the soil gas concentrations of CH_4 were too low to accurately determine $\delta^{13}C$ of CH_4 or $\delta^{2}H$ of CH_4.

Figure 3.6-7: Keeling Plot for Soil Gas CO_2 Measured Seasonally

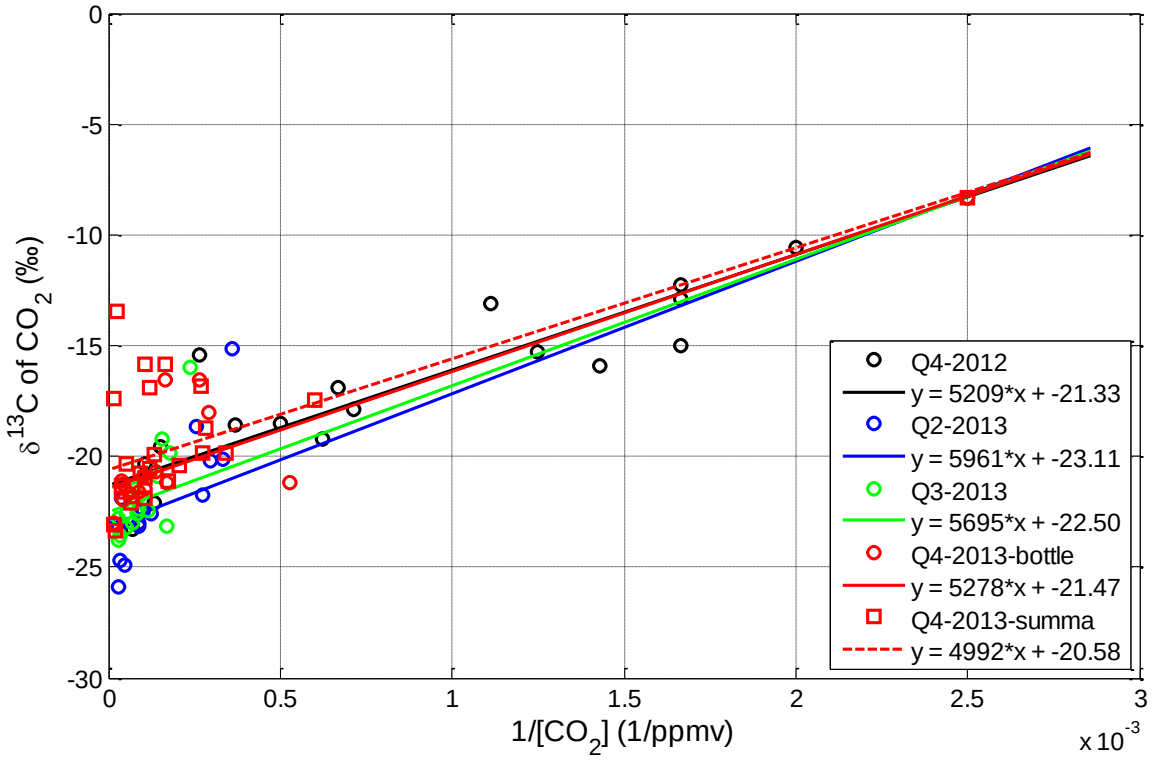

Seasonal vertical profiles of CO_2 and CH_4 measured with the GGA above and below the ground surface are presented on Figure 3.6-8. Each data point represents the average concentration measured by the GGA instrument prior to and after discrete sample collection for laboratory analysis (i.e., each point is the average of approximately 180 1-Hz measurements). These site averages are then pooled and the seasonal median calculated and shown on Figure 3.6-8. The left panel of the figure plots the vertical profiles of CO_2 concentration; the right panel plots the vertical profiles of CH_4. Note the logarithmic scale for CO_2 concentrations is in ppmv, and for CH_4 concentrations the units are parts per billion volumetric (ppbv). The HBMP results indicate CO_2 concentrations in soil gases in the study area are typically 25 to 100 times higher than the concentrations measured in the ambient atmosphere. Conversely, the concentrations of soil gas CH_4 are typically 10 to 100 times lower than the concentrations measured in the ambient atmosphere. Although the soil gas profiles appear continuous, the number of samples at 0.5 and 1.0 metre depths suffer from low sample numbers (being collected at injection well sites only). Repetition of the seasonal HBMP sampling program in 2014 will improve these statistics and aid in the interpretation of these results.

Figure 3.6-8: Vertical Profiles of Hydrosphere and Biosphere Monitoring Program Atmospheric and Soil Gas CO_2 (left) and CH_4 (right)

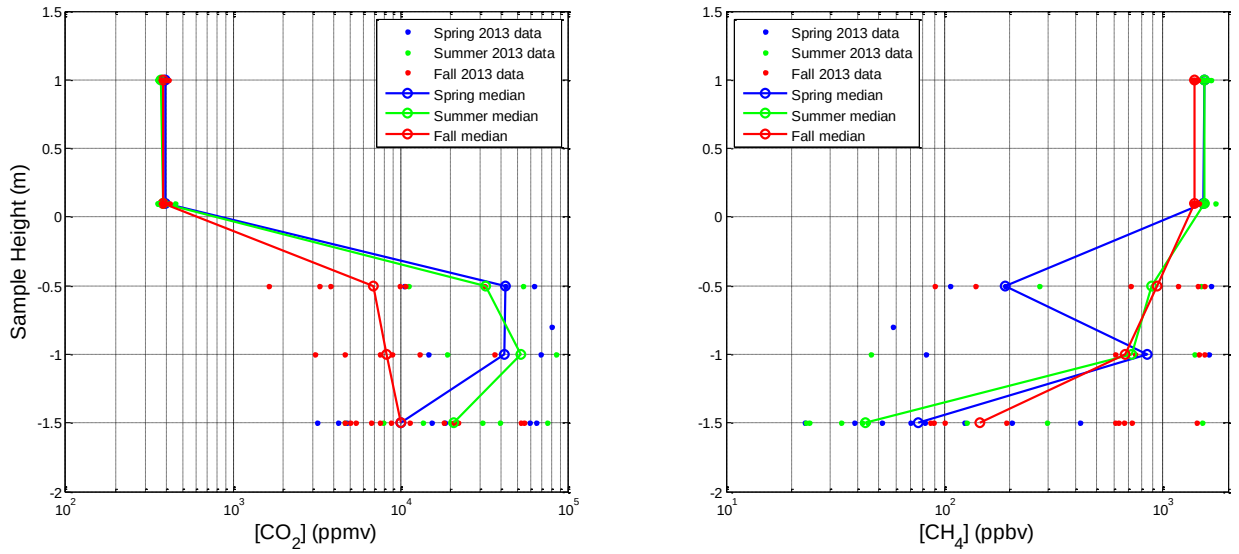

The median seasonal vertical profiles of CO_2 and CH_4, separated into the dominant land cover types, i.e., annual crops, pastures and meadows, and forests and wetlands, are plotted in Figure 3.6-9 and Figure 3.6-10. While these profiles, grouped by land cover type, still suffer from low sample number, some trends emerge. For example, CO_2 concentrations and CH_4 concentrations below the surface of annual crops are higher and lower, respectively, than their concentrations below pastures/meadows and forests/wetlands. These preliminary results should not be over-interpreted because they are affected by low sample number. Repetition of the seasonal HBMP sampling program in 2014 will improve these statistics and aid in the interpretation of these results.

Figure 3.6-9: Seasonal Atmospheric and Soil Gas CO_2 Profiles Separated by Land Cover Type

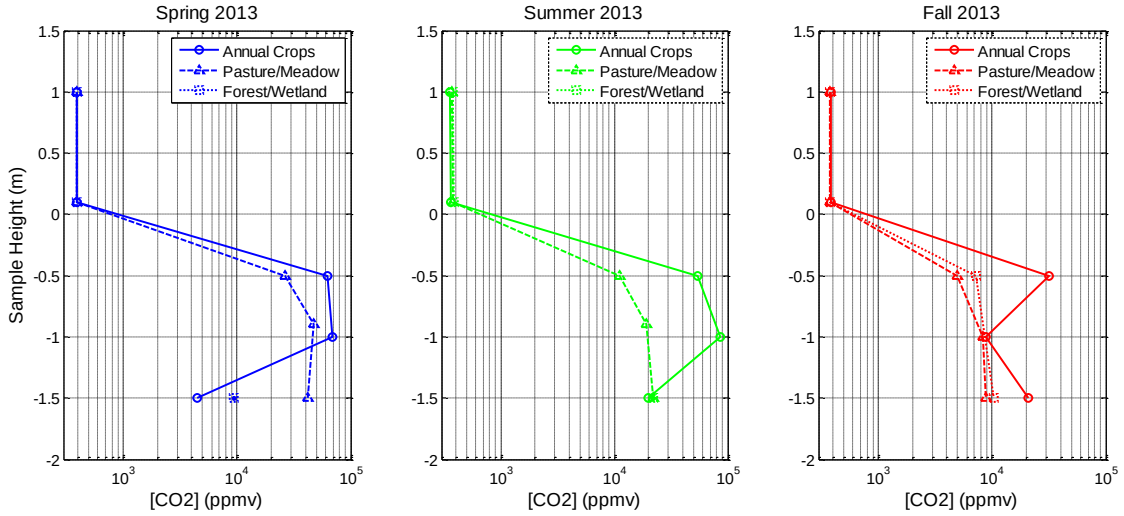

Figure 3.6-10: Seasonal Atmospheric and Soil Gas CH_4 Profiles Separated by Land Cover Type

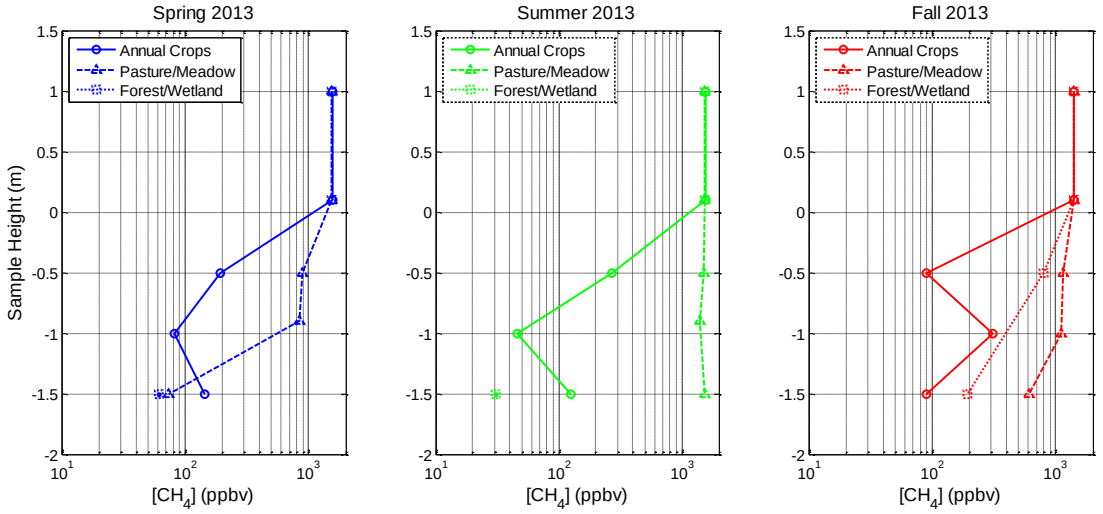

3.6.4 Surface CO_2 Flux Results

The number of individual flux measurements collected during each season (N) and their mean, median, standard deviation, minimum, and maximum values for each season are summarized in Table 3.6-4. The median, mean and one standard deviation (1σ) for seasonal surface CO_2 fluxes after grouping the measurements by land surface type are summarized in Table 3.6-5.

The same results are illustrated graphically on Figure 3.6-11, which plots the surface CO_2 flux data grouping the results by season; and Figure 3.6-12, which separates seasonal flux results according to land cover type. The red line in each box plot corresponds to the median concentration, the box the 25th and 75th quartiles, the whiskers the 95% confidence interval of the arithmetic mean, and any red crosses are considered statistical outliers at α=0.05.

The HBMP surface CO_2 flux measurements clearly capture a seasonal trend with additionally important differences when the data are separated by land cover type. Because the number of plots and some of their locations differed in fall 2012 and fall 2013, quantitative comparisons between these two seasonal events should be approached with caution.

Pastures/meadows consistently displayed higher surface CO_2 flux values than both annual crops and forests/wetlands. The exception appears to be winter 2013 when annual crops displayed marginally higher average surface CO_2 fluxes, but with a high coefficient of variation. This higher mean value, and its large standard deviation, is being driven by a few higher flux values observed during winter (Figure 3.6-12). Median surface CO_2 fluxes from forests/wetlands were below those of annual crops in fall 2012 and winter 2013, but were higher than annual crops in spring, summer and fall 2013. Repetition of these seasonal measurements in 2014 will enable better determination of median surface CO_2 fluxes and their variability within the Project area.

Table 3.6-4: Surface CO_2 Flux Statistics Grouped by Sampling Event

Sampling Event	N	Mean	Median	Standard Deviation	Min	Max
	#	μmol cm^{-2} s^{-1}	μmol cm^{-2} s^{-1}	μmol cm^{-2} s^{-1}	μmol cm^{-2} s^{-1}	μmol cm^{-2} s^{-1}
Fall 2012	246	2.3	2.5	1.0	0.0	3.5
Winter 2013	165	1.0	0.6	1.0	0.2	3.6
Spring 2013	345	4.7	3.8	2.6	1.6	10.2
Summer 2013	378	9.4	8.3	5.0	3.4	25.3
Fall 2013	381	2.5	2.4	1.3	0.6	6.2

Table 3.6-5: Seasonal Surface CO_2 Flux Statistics Grouped by Land Cover Type

Land Cover Type	Surface CO_2 Flux (µmol cm^{-2} s^{-1})														
	Fall 2012			Winter 2013			Spring 2013			Summer 2013			Fall 2013		
	Median	Mean	1σ	Median	Mean	1σ	Median	Mean	1σ	Median	Mean	1σ	Median	Mean	1σ
Annual Crops	2.4	2.1	0.8	0.7	1.2	1.2	2.2	3.3	2.2	4.6	5.0	1.3	1.0	1.5	0.8
Pastures/ Meadows	3.3	3.2	0.2	0.66	0.71	0.34	6.8	7.3	1.6	13.2	14.7	4.3	3.4	3.2	1.3
Forests/ Wetlands	0.78	0.78	0.05	0.23	0.28	0.12	2.9	3.0	0.8	8.3	8.6	2.4	3.1	2.9	1.0

1σ = one standard deviation of the arithmetic mean

Figure 3.6-11: Seasonal Surface CO_2 Fluxes for all Land Cover Types

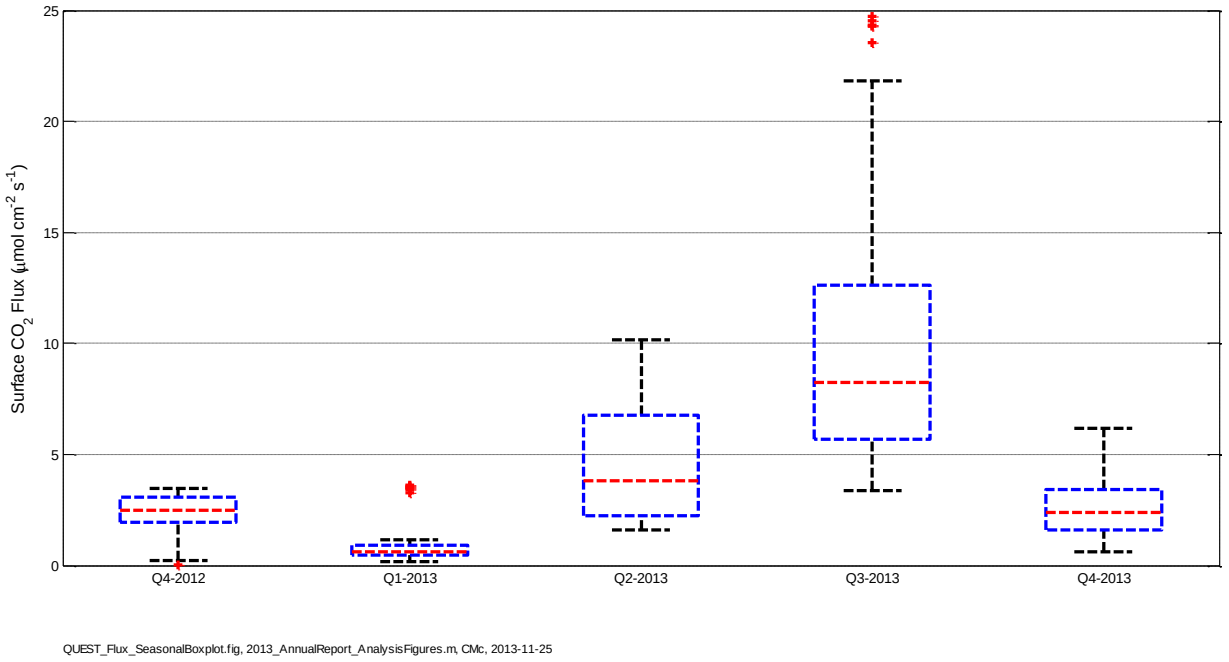

QUEST_Flux_SeasonalBoxplot.fig, 2013_AnnualReport_AnalysisFigures.m, CMc, 2013-11-25

Figure 3.6-12: Seasonal Surface CO_2 Fluxes Grouped by Land Cover Type

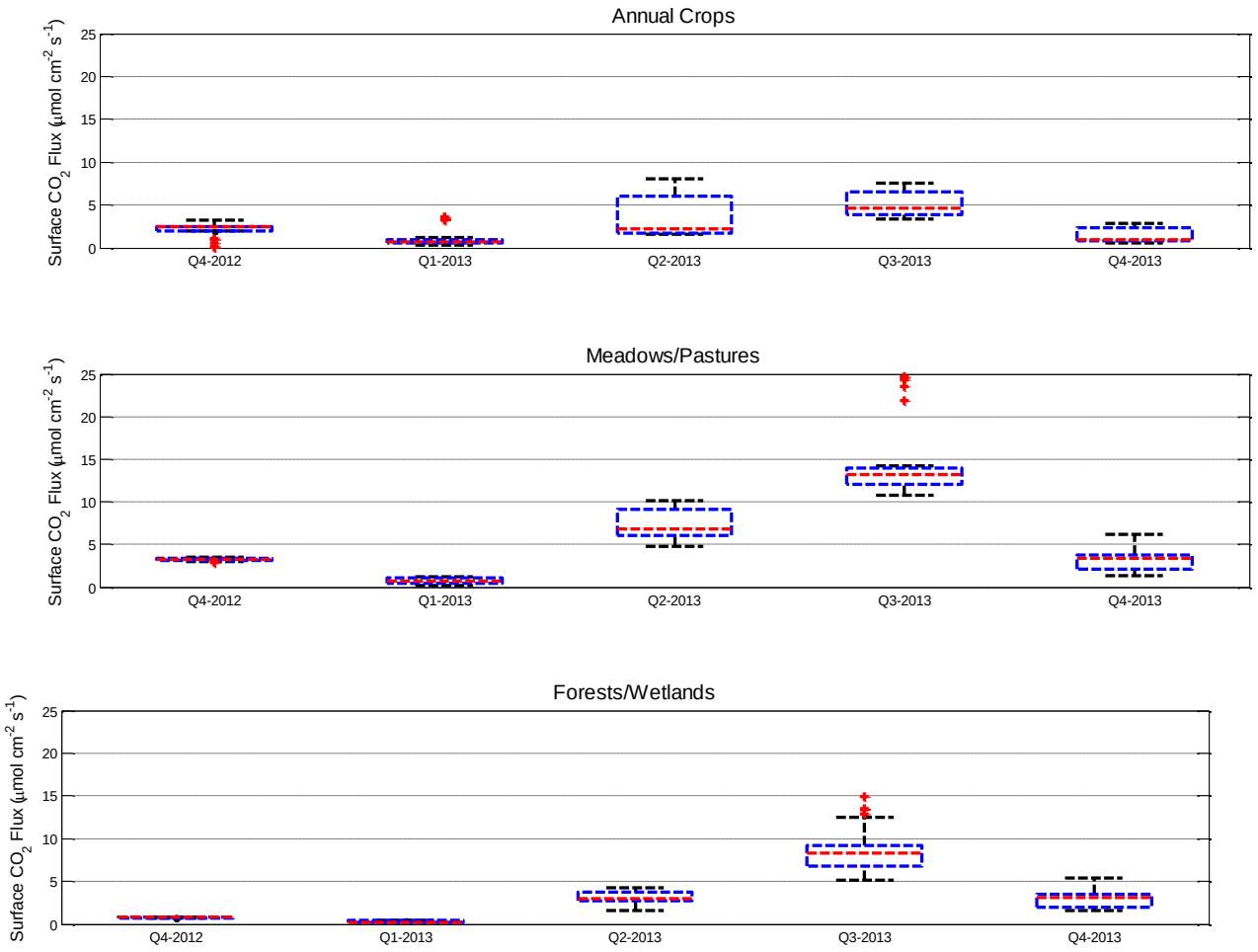

3.6.5 Summary of Key Findings

The key finding related to the literature review of the available FCRN data is the following:

- Several high-quality, highly relevant FCRN data sets are available that can be used to link diurnal, seasonal and interannual variability in net CO_2 exchange for ecosystems in Alberta and Saskatchewan to their controlling biotic and abiotic factors. Expert analysis of the available FCRN data, in particular the longer time series data, could aid in the interpretation of the HBMP's chamber-based surface CO_2 flux data.

Key findings related to soil gas and surface CO_2 flux sampling methods during the 2013 Shell Quest HBMP include the following:

- a reportable detection limit of less than 0.1 ppmv, preferably better than 0.01 ppmv, is required for the measurement of soil gas CH_4; and
- high concentrations of CO and non-methane hydrocarbons together with low concentrations in CO_2 in soil gas samples collected in summer 2013 indicate possible sample contamination.

Key findings related to soil gas and surface CO_2 flux results from the 2013 Shell Quest HBMP include the following:

- Linear regressions of seasonal soil gas O_2 depletion versus CO_2 enrichment have slopes that ranged from -0.76 to -1.61. The fall 2012 slope (-0.78) and the fall 2013 slopes (-0.76 and -0.81) are indistinguishable, the summer 2013 slope is likely affected by sample contamination leading to the low R^2 value, and excessively wet subsurface conditions in spring 2013 may have contributed to its slope of -1.61.
- Keeling Plot intercepts derived from the HBMP data using Model II linear regression vary between -20.58‰ and -23.11‰ and the 95% confidence intervals for these intercepts on average is +/-0.55 ‰. After adjusting the HBMP Keeling intercepts by -4.4‰ to account for soil organic matter to soil gas CO_2 isotopic fractionation in situ, the HBMP isotopic ratios are indicative of soil gas CO_2 derived predominantly from the respiration of soil organic matter formed from C3 plants ($\delta^{13}C$ ~= -27‰) rather than C4 plants ($\delta^{13}C$ ~= -13‰).
- HBMP soil gas CO_2 concentrations are typically 25 to 100 times higher than the concentrations measured in the ambient atmosphere. Conversely, the concentrations of soil gas CH_4 are typically 10 to 100 times lower than the concentrations measured in the ambient atmosphere.
- The HBMP surface CO_2 flux measurements clearly capture a seasonal trend with additionally important differences observed when the data are separated by season and by land cover type.
- Pastures/meadows consistently displayed higher surface CO_2 fluxes than annual crops and forests/wetlands, with the exception of winter 2013 where annual crops displayed marginally higher average surface CO2 fluxes, but with a high coefficient of variation.
- Median surface CO_2 fluxes from forests/wetlands were below those of annual crops in fall 2012 and winter 2013, comparable to annual crops in spring 2013, and higher than annual crops in summer and fall 2013.

3.7 Remote Sensing

Remote sensing describes the science of acquiring information about the Earth's surface without being directly in contact with it, through detecting and recording the emitted or reflected energy, analyzing it, and applying that information to better understand the target features or processes. The general principles of remote sensing are valid for measurements done from millimetres away, to those done using sensors on airborne or space-borne platforms tens or hundreds of kilometres away. To capture the necessary information of the target vegetation communities, this study used a hand-held spectrometer along with multi-spectral RapidEye satellite imagery.

3.7.1 Methodology and Field Program

Field methodology was designed with the objective of collecting specific data to apply an empirical line calibration to the RapidEye satellite imagery. An empirical line calibration is a method of removing the atmospheric effects from satellite imagery or aerial photographs by forcing the spectral reflectance in the imagery to match that of known ground locations (Conel et al. 1987). To perform the calibration, spectral reflectance of large spectrally homogeneous areas observable in the imagery and accessible on the ground must be measured within a few days of satellite image collection. For this Project, spectral signatures of vegetation and key ground locations were done in conjunction with satellite imagery collection.

Ground targets were selected based on the criteria of size, spectral homogeneity and spatial distribution across the Project area. To be observable in the RapidEye imagery with a 5 m spatial resolution (pixel size), the target features must be at least 20 m × 20 m and completely spectrally homogeneous. Thus, two white artificial targets made from geotextile fabric were set-up during each of the imagery collection periods. To aid in calibration of darker objects, two black targets of the same size and construction were set-up during the 2013 satellite imagery collection periods.

In addition to the artificial targets, several Pseudo-Invariant Features (PIFs) were identified throughout the Project area. The PIFs are pseudo-Lambertian reflectors such as asphalt, shale baseball diamonds, concrete or uniform gravel roads. Like the artificial targets, PIFs must be of sufficient size (20 m × 20 m), spectrally homogeneous, unobstructed, and located where the surrounding land cover has minimal influence on the spectral characteristics of the target feature. During each imagery collection period, spectral signatures of at least four PIFs were collected.

Spectral signatures were also collected at vegetation plots. These measurements were used to develop a full spectral description of the vegetation type and incorporated into the spectral library database.

To account for strong angular effects on the measured reflectance of the target, multiple measurements were made at each location. The concept of the bidirectional reflectance distribution function suggests that certain terrain covers may have strongly varying spectral signatures dependant on the azimuth and zenith angles of the incident light and the sensor (Jensen 2005). This concept is exemplified by the differing reflectance of a freshly mowed lawn, which is a result of the direction in which the grass was cut.

Spectral measurements were obtained using an Ocean Optics Jaz^{TM} Spectrometer. This unit was chosen based on its small size, ease of operation, battery support, and ability to measure wavelengths in the range of 350 to 1,000 nanometres (nm) with a spectral resolution of 0.35 nm. The spectrometer was fitted with a cosine diffuser foreoptic lens and calibrated by Ocean Optics before being delivered and used in the field for the September 2012 survey.

3.7.2 Data Collected

Data collected during the field programs included spectral measurements of artificial targets, PIFs and vegetation plots, their locations (GPS coordinates) as well as photographs of each feature.

3.7.3 Empirical Line Calibration Analytical Results

To determine the calibration equations for each image, reflectance values were calculated for the geotextile targets and PIFs from the spectrometer raw files collected during the time of image acquisition. These values were then grouped into categories corresponding with the five RapidEye bands: 440 to 510 nm (blue band); 520 to 590 nm (green band); 630 to 685 nm (red band); 690 to 730 nm (red edge band); and 760 to 850 nm (near-infrared band). The average image digital number value for each of the geotextile targets and PIFs were extracted from the RapidEye image for a four pixel area in the centre of each target feature. A linear regression equation relating the digital number values to the measured reflectance of each feature was generated for each of the five RapidEye bands. This equation was then applied to the image to create a calibrated image dataset showing the at-surface average reflectance across the whole image. An example of a linear regression equation is shown on Figure 3.7-1.

Figure 3.7-1: Linear Regression for the RapidEye Green Band, July 2013 Image

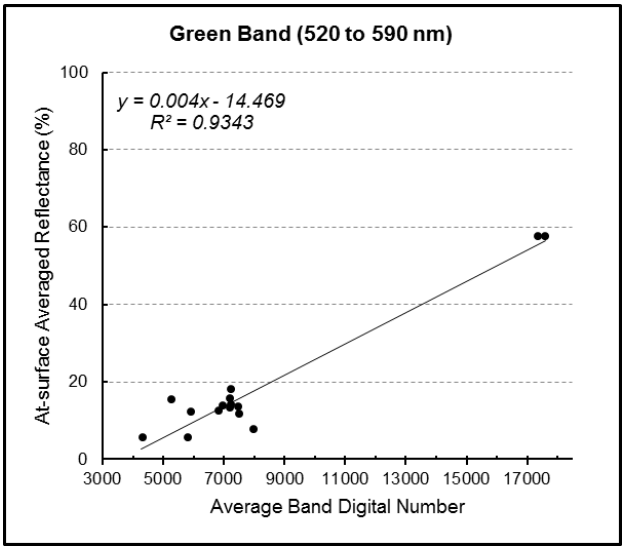

3.7.4 Spectral Data Analytical Results

Spectral signatures were collected for three of the five (annual crop, pasture and wetland) land covers at different times of the year in order to understand the natural spectral variance that occurs in these landscapes. During the fall 2012 field program, understorey spectral sampling was also done at the broadleaf and coniferous plots, with the expectation that the measurements would capture changes in the sub-canopy vegetation at these sites. Due to inconsistent results and the inability to relate them to the imagery, these samples were discontinued in the 2013 field programs.

3.7.4.1 Background on Spectral Signatures

When electromagnetic radiation (EM) hits an object, specific wavelengths are absorbed, transmitted or reflected back into the environment. The manner in which the object interacts with EM is unique to the composition or surface characteristics of an object. Using a spectrometer, the spectral signature of the object can be measured. By comparing spectral signatures of objects across a broad range of the electromagnetic spectrum, it is possible to differentiate one object from another. Understanding the general characteristics of the interaction between different land cover types and EM is integral for interpretation of spectral signatures. For example, clear water is a strong absorber of EM across most wavelengths, but does feature some reflectance in the blue and green portions of the spectrum. In contrast, soil is generally highly reflective across the EM spectrum, but the magnitude of the reflectance can vary with soil moisture, particle size, iron oxide content, mineralogy, organic matter content, as well as other factors. The spectral signatures of some common land cover types are shown on Figure 3.7-2.

Vegetation has a very specific spectral signature that can be used to identify not only different species, but also health and water content within the same species. Chlorophyll, a chemical compound that is found in all vegetation, absorbs wavelengths in the blue and red portions of the EM spectrum, and reflects wavelengths in the green and near-infrared. As a result, leaves appear green. The presence of chlorophyll is defined by the dip in reflectance values starting at approximately 600 nm and an increase in reflectance starting at approximately 700 nm, as shown by the *grass* line on Figure 3.7-2. In autumn, when vegetation is senescing, less chlorophyll is present in the leaves, thus resulting in less absorption in the 600 to 700 nm range. For this reason leaves turn yellow, orange and red. Absorbance in the near-infrared wavelengths can also be an indicator of plant stress.

For non-homogeneous plots, where more than one type of surface can be measured by the sensor, spectral signatures will be influenced by the proportion and spectral characteristics of those individual surfaces.

Figure 3.7-2: Spectral Signatures of Common Land Cover Types

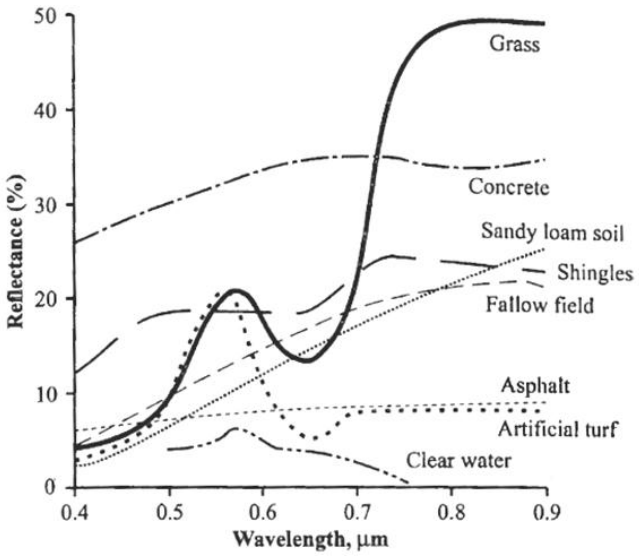

3.7.4.2 Annual Crops

Consisting exclusively of agricultural fields, the annual crop land cover shows the most dramatic interseasonal spectral variance, because the fields are fallow or just seeded in the spring, crops are fully grown in the summer, and the fields are again barren or covered with post-harvest detritus in the fall. Five such sites were analyzed during each field program in 2012 and 2013 (Section 3.1). An overview of the vegetation at these sites is provided in Section 3.3.2.1.

Spectral response at each of the agricultural sites is very similar, and exemplified by the curves shown on Figure 3.7-3. Spectral signatures in the shoulder seasons (i.e., spring and fall) show a lack of live or healthy vegetation, and are dominated by the spectral characteristics of exposed soil and detritus. In the spring, moist soil and agricultural practices such as tilling contribute to the overall low reflectance of the sites. Fall spectral signature, albeit similarly affected by the percentage of exposed soil, is more influenced by the senesced vegetation left behind after harvesting and the drier soil conditions in the fall. This is evidenced by the higher overall reflectance of the curve, as well as the slight vegetation signature in the chlorophyll absorption band (650 to 750 nm).

In the summer measurements, however, the presence of healthy crops dominates the spectral characteristics at these sites. A clear and well-defined vegetation signature can be observed at all sites, except at the semi-permanent plot 02-34 which was left fallow in 2013.

Figure 3.7-3: Spectral Signature of an Annual Crop Plot, 08-21

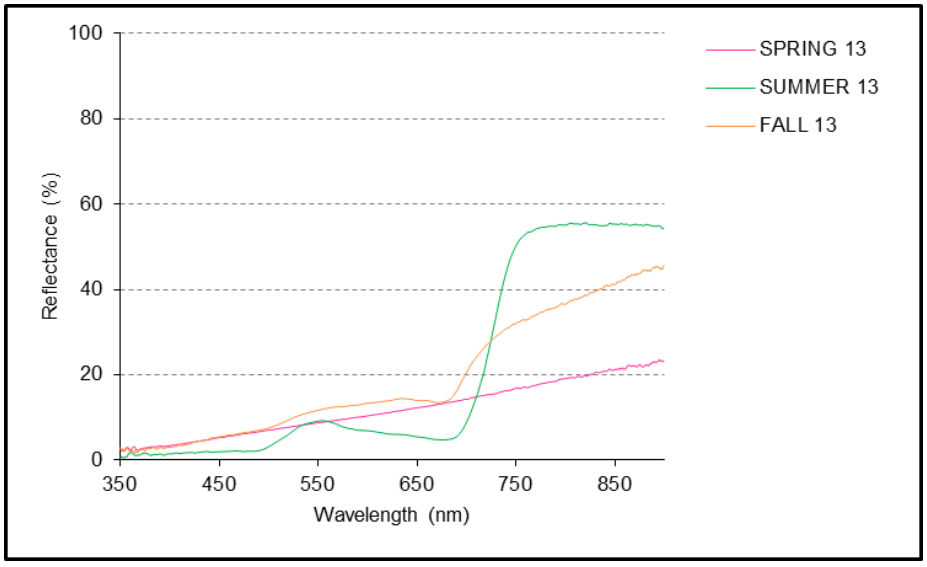

3.7.4.3 Pastures

As observed in the vegetation surveys, detailed in Section 3.3.2.2 the pasture land cover is dominated by native graminoid species, and unlike annual crops, tends to be resistant to cooler temperatures. This is evidenced by the predominantly live vegetation observed at the plots in every field program. Thus, as expected, the spectral characteristics of the pasture plots remain fairly similar throughout the non-snowy seasons. The typical spectral curves observed at a pasture site are shown on Figure 3.7-4. In each season, clear vegetation signatures are observed. Overall spectral reflectance of the site is a bit higher in the summer months because the vegetation is greener (and arguably healthier) than in the shoulder seasons. Three pasture sites were analyzed during each field program in 2012 and 2013.

Figure 3.7-4: Spectral Signature of a Pasture Plot, 03-36a

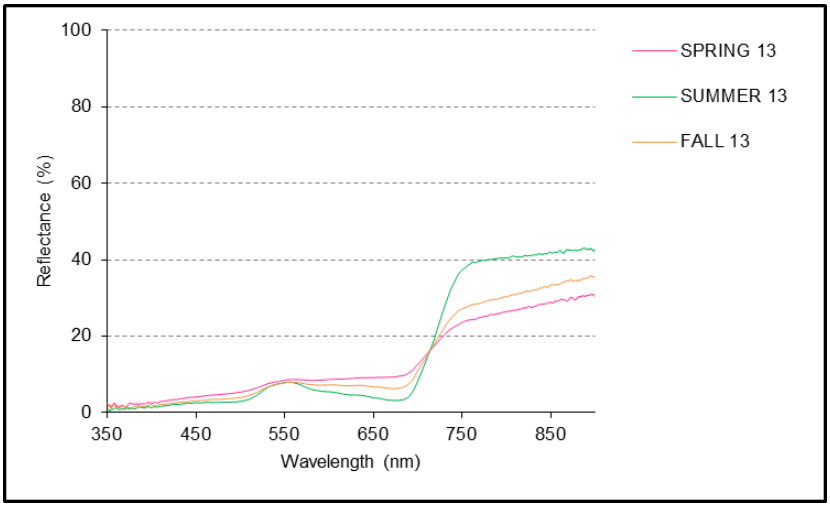

3.7.4.4 Wetlands

The wetland land cover class in the Project area is primarily composed of sedges and graminoid species adapted to growth in wet environments. Similar to the pasture sites, live vegetation was observed in every field program. Senesced grasses were only seen at the semi-permanent plot 16-08 during the May 2013 field program, and are thought to be due to lack of early season growth at this site. The vegetation composition of wetland plots is detailed further in Section 3.3.2.5. Spectral characteristics of a typical wetland site are shown on Figure 3.7-5. The spectral response in the spring measurements is fairly low, but a slight vegetation signature can be observed. Overall low reflectance is primarily driven by the exposed moist (or wet) soil as well as some presence of standing water. In the summer measurements, the overall reflectance increases with the decrease of exposed soil and filling-in of the live, healthy vegetation. A clearly defined vegetation signature can be seen in the summer and fall spectral curves. Depending on the vegetation composition of the site, and the growing characteristics of that vegetation, the overall reflectance in fall measurements may be higher or lower than those in the summer.

Figure 3.7-5: Spectral Signature of a Wetland Plot, 03-36b

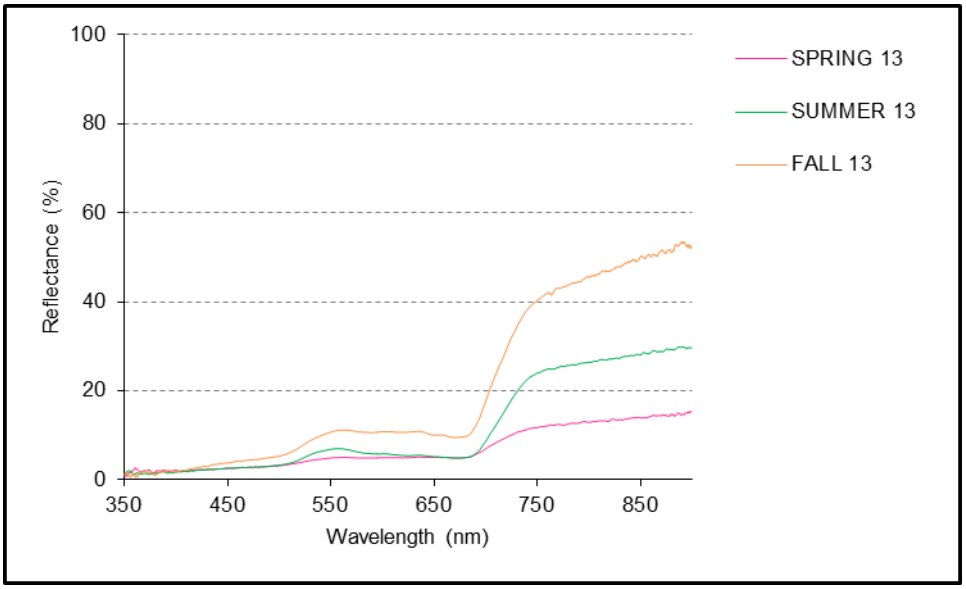

3.7.5 Summary of Key Findings

- The spectral distribution of artificial targets and PIFs was sufficient to be used for empirical line calibration of RapidEye imagery.
- Spectral signatures of vegetation plots were consistent across the same vegetation types, and all displayed expected interseasonal spectral variability.

4.0 HYDROSPHERE

The hydrosphere component of the HBMP for the Shell Quest Carbon Capture and Storage Project has included baseline groundwater and wellhead gas sampling and data logging over five quarterly sampling events to date. The data collected will be used to define baseline conditions against which future monitoring results can be assessed.

The wells sampled for groundwater and gas analyses are located within and surrounding the Sequestration Lease Area. Samples are collected from two types of wells: Project wells and Landowner wells. Landowner wells include participating private landowner wells located within the Sequestration Lease Area. Project wells are monitoring wells located at one of Shell's three Project injection well sites: 07-11-59-20 West of the Fourth Meridian (W4M) (07-11), 08-19-59-20 W4M (08-19) and 05-35-59-21 W4M (05-35).

In addition to groundwater and wellhead gas sampling, Golder has also undertaken the operation, quarterly download, maintenance and calibration of In-Situ® Multi-Parameter TROLL 9500 data loggers which are used to collect continuous water level and basic water chemistry in the nine Project monitoring wells.

This section provides a summary of field work activities completed, and analytical results obtained since initiating the hydrosphere sampling program in November 2012 (Q4-2012). To date, five quarterly data collection events have been completed (Q4-2012, Q1-2013, Q2-2013, Q3-2013 and Q4-2013).

4.1 Baseline Monitoring Well Network

4.1.1 Landowner Wells

A Landowner well inventory list, consisting of approximately 160 private wells, was used to identify potential wells to include in the baseline groundwater monitoring program. The list was compiled from the Alberta Water Well Database (AWWDB) maintained by Alberta Environment and Sustainable Resource Development, supplemented by information provided by Shell. Additions to the list were made as new wells were identified in the area. To date, over 300 possible Landowner wells have been identified in the well inventory. However, not all the wells in the inventory could be located and/or sampled. The ability to collect samples from landowner wells is subject to several factors including landowner consent and/or availability, site accessibility, health and safety considerations (i.e., confined entry), as well as difficulties experienced in attempting to locate wells lacking GPS coordinates, in particular older wells included in the AWWDB.

The Landowner wells are subdivided into three types: Local, Legacy and Regional wells, described below. Well selection and sampling for each of these well types differed slightly and are described as follows:

- *Local Wells*: Landowner wells that are located within a 3.2 kilometre radius of the three Project injection well sites. As many wells as possible were included in this category.
- *Legacy Wells*: Landowner wells that are near four known legacy oil and gas wells. These oil and gas wells are located within the Sequestration Lease Area and drilled into the Basal Cambrian Sand, the formation targeted for CO_2 storage:
  - 06-36-058-23 W4M (06-36);
  - 01-34-057-22 W4M (01-34);
  - 09-31-062-19 W4M (09-31); and
  - 16-19-062-19 W4M (16-19).

  Wells of this type were selected based on well geology and proximity to legacy wells. Where possible, a well representing each of the three major aquifers present in the area (surficial, Oldman Formation and Foremost Formation) was selected for sampling.
- *Regional Wells*: These wells were selected to provide a regional groundwater monitoring network for the Sequestration Lease Area. Wells were selected at a nominal density of one per township for a total of 34 wells.

4.1.2 Project Wells

The Project wells are Shell-owned groundwater monitoring wells located at the three proposed injection sites:

- 07-11-59-20 W4M (07-11);
- 08-19-59-20 W4M (08-19); and
- 05-35-59-21 W4M (05-35).

A total of nine Project groundwater monitoring wells have been installed; five are located at the 08-19 injection well site and two wells each are located at the 05-35 and 07-11 injection wells. Well coordinates and information for each of the Project monitoring wells is provided in Table 4.1-1.

Table 4.1-1: Project Injection Wells

Well ID	UTM Coordinates		Total Depth (mbgl)	Geology	Screen Length (m)
	Easting (NAD83)	Northing (NAD83)			
1F1-08-19-059-20W4/00	370669	5997943	158.7	Foremost Fm	3.0
1F1-08-19-059-20W4/01	370665	5997937	101.0	Foremost Fm	3.0
1F1-08-19-059-20W4/02	370654	5997934	62.8	Foremost Fm	3.0
1F1-08-19-059-20W4/03	370658	5997941	37.5	Foremost Fm	3.0
1F1-08-19-059-20W4/04	370663	5997947	20.0	Oldman Fm	3.0
1F1-07-11-059-20W4/00	376596	5994619	127.5	Foremost Fm	3.0
UL1-07-11-059-20W4/00	376595	5994609	30.7	Foremost Fm	3.0
1F1-05-35-059-21W4/00	366367	6001348	118.0	Foremost Fm	3.0
UL1-05-35-059-21W4/00	366368	6001359	23.0	Foremost Fm	3.0

4.1.3 Laboratory Analyses

4.1.3.1 Groundwater Analyses

Laboratory analyses for groundwater samples collected for the HBMP are listed in Table 4.1-2. Sample analyses included routine parameters and dissolved metals (Tier 1 + 2 analytes) and isotopes (Tier 3 analytes). Routine chemistry and metals analyses were performed by AGAT Laboratories. Isotope analyses were performed by Isobrine Solutions Ltd. for samples collected in Q4-2012; and by the University of Calgary (UC) and University of Waterloo (UW; 2013 δ^{37}Cl analyses only) for samples collected in 2013. Determination of δ^{81}Br was only done by Isobrine for Tier 3 samples collected in Q4-2012. Sampling for δ^{81}Br was not done in 2013 because the large sample volume required could not be supported by the low-flow sampling method employed.

Table 4.1-2: Laboratory Analyses – Groundwater

Analysis Type	Laboratory	Method
Tier 1+2		
Routine water[(a)]	AGAT	various
Low level metals[(b)]	AGAT	High Resolution Inductively Coupled Mass Spectrometry
Tier 3 - Isotopes		
$\delta^{11}B$	Isobrine, UC[(c)]	Isotope-Ratio Mass Spectrometry
$\delta^{13}C$ for dissolved inorganic carbon	Isobrine, UC	Isotope-Ratio Mass Spectrometry
$\delta^{18}O$ & $\delta^{2}H$ for H_2O	Isobrine, UC	Isotope-Ratio Mass Spectrometry
$\delta^{37}Cl$	Isobrine, UW[(d)]	Isotope-Ratio Mass Spectrometry
$\delta^{81}Br$[(e)]	Isobrine	Isotope-Ratio Mass Spectrometry
$^{87/86}$ Sr	Isobrine, UC	Thermal Ionisation Mass Spectrometry

(a) Includes pH, electrical conductivity, TDS, alkalinity, ion balance, total hardness, Na, K, Ca, Mg, HCO_3, CO_3, OH, SO_4, NO_2, NO_3, P, dissolved inorganic carbon.
(b) Low level dissolved metals: includes Al, Sb, As, Ba, Be, B, Cd, Ca, Cr, Co, Cu, Fe, Hg, Pb, Li, Mg, Mn, Hg, Mo, Ni, K, Se, Si, Ag, Sr, Tl, Sn, Ti, U, V, Zn.
(c) University of Calgary.
(d) University of Waterloo.
(e) $\delta^{81}Br$ was measured by Isobrine in Q4-2012, but was not determined in 2013.

4.1.3.2 Wellhead Gas Analyses

Laboratory analyses for wellhead gas samples collected for the HBMP are listed in Table 4.1-3. Sample analyses included standard gas composition and isotopic analyses. Compositional analyses were conducted by AGAT Laboratories. Isotopic analyses were performed by Isobrine Solutions Ltd. for samples collected in 2012 and by the University of Alberta (U Alberta) for samples collected in 2013.

Table 4.1-3: Laboratory Analyses – Wellhead Gas

Analysis Type	Laboratory	Method
Composition		
CO_2, N_2, O_2, He, C_1 to C_{10} hydrocarbons	AGAT	various
Isotopes		
$\delta^{13}C$–CO_2 and CH_4	U Alberta	GC-C-IRMS[(a)]
$\delta^{2}H$–CH_4	U Alberta	GC-C-IRMS

(a) Gas Chromatography–Combustion–Isotope Ratio Mass Spectrometry

4.1.3.3 2012-2013 Sampling Schedule

The planned 2012-2013 groundwater and wellhead gas sampling schedule is presented in Table 4.1-4. A total of five quarterly sampling events were conducted in 2012 and 2013. Where possible, both groundwater and wellhead gas samples from Project, Legacy and Regional wells were collected from each sampling event. Samples from Local wells were collected at least once over the 2012-2013 period.

Table 4.1-4: 2012-2013 Groundwater and Wellhead Gas Sampling Schedule

Tier 1 and 2 – Composition

	Q4 - 2012		Q1- 2013		Q2 - 2013		Q3 - 2013		Q4 - 2013	
Well Type	**GW[(c)]**	**WHG**	**GW**	**WHG**	**GW**	**WHG**	**GW**	**WHG**	**GW**	**WHG**
Project	9	9	9	9	9	9	9	9	9	9
Local	154	154	47	47	43	43	0	0	9[(a)]	9[(a)]
Legacy	10	10	9[(b)]	9[(b)]	10[(b)]	10[(b)]	3[(a)]	3[(a)]	3[(a)]	3[(a)]
Regional	34	34	34	34	34	34	34	34	34	34
Total Wells	**207**	**207**	**99**	**99**	**96**	**96**	**46**	**46**	**55**	**55**

Tier 3 - Isotope Analysis

	Q4 - 2012		Q1- 2013		Q2 - 2013		Q3 - 2013		Q4 - 2013	
Well Type	**GW**	**WHG**	**GW**	**WHG**	**GW**	**WHG**	**GW**	**WHG**	**GW**	**WHG**
Project	9	9	9	9	9	9	9	9	9	9
Local	9	9	0	0	9[(b)]	9[(b)]	0	0	3[(a)]	3[(a)]
Legacy	9	9	3[(a)]	3[(a)]	9[(b)]	9[(b)]	3[(a)]	3[(a)]	3[(a)]	3[(a)]
Regional	9	9	9	9	9	9	9	9	9	9
Total Wells	**36**	**36**	**21**	**21**	**36**	**36**	**21**	**21**	**24**	**24**

[(a)] Well selection based on geology - wells completed in the Foremost Formation.
[(b)] Well selection based on geology - one well per surficial/Oldman/Foremost Formations.
[(c)] GW= groundwater; WHG = wellhead gas.

To the extent possible, samples were collected for the full suite of wells targeted for sampling in the quarter. However, for a variety of circumstances (i.e., landowner refusal or absence, well located in an enclosed space) it was not always possible to collect the total number of samples indicated in Table 4.1-4 during a given quarter.

4.2 Methodology

Prior to starting each quarterly sampling event, well owners were contacted for permission to access their property and conduct groundwater sampling. The sampling procedures used to collect groundwater and gas samples from Landowner and Project wells are described below.

Groundwater and gas samples collected from Landowner and Project wells were placed in an ice chest and submitted under chain-of-custody to AGAT Laboratories in Edmonton. Where possible, samples were collected and delivered to the laboratory on the same day. Analyses for routine chemistry and metals were conducted by AGAT. In Q4-2012, groundwater samples for isotopic analyses were forwarded by Golder directly to Isobrine Solutions Ltd. (Q4-2012 samples only). In 2013, samples for isotopic analyses were shipped to AGAT, who then forwarded them to the University of Calgary and the University of Waterloo (Q1-2013 to Q4-2013). Wellhead gas

samples for isotopic analyses were forwarded to either Isobrine Solutions Ltd. (Q4-2012 samples only) or, in 2013, by AGAT to the University of Alberta.

4.2.1 Groundwater Sampling

4.2.1.1 Landowner Wells

Groundwater samples from Landowner wells were collected via a raw water sampling outlet (i.e., an outdoor spigot or kitchen tap), upstream of water treatment or softening systems. The water was first run through the tap for about 5 to 15 minutes, and field parameters (pH, conductivity, temperature and dissolved oxygen) were monitored and recorded during that time. Once field parameters had stabilized (indicating representative groundwater conditions), samples were collected directly into laboratory-grade bottles. Additional data collected during sampling included well location coordinates, photos and site description, a description of the water supply system (including the presence/absence of any water treatment), and well construction information (i.e., installation date, total depth, geology and water level).

Where possible, manual water level data were also collected at Landowner wells. However, to collect water level data, unobstructed access to the wellhead and into the well is required. Where access was not available, or where infrastructure (i.e., wiring, pumps) was present, a manual water level measurement could not be collected.

4.2.1.2 Project Wells

Groundwater samples from Project wells were collected with a portable bladder pump, following a a low-flow sampling protocol. Low-flow sampling is an alternative approach to traditional sampling that significantly reduces necessary purge volumes by minimizing mixing and dilution within the wellbore, thereby avoiding alterations in water chemistry during the sampling process. Before conducting the low-flow groundwater sampling, manual water level measurement, wellhead gas sampling and data logger removal/download were first performed.

The Project wells were purged at a low flow rate (between 0.1 to 0.5 litres per minute (L/min)), with the water intake placed approximately at the mid-point of the well screen. Field parameters and water levels were monitored/recorded during purging. Once field parameters had stabilized (indicating representative groundwater conditions), a sample was collected directly into laboratory-grade bottles supplied and prepared by the analytical laboratory.

4.2.2 Gas Sampling

Gas sampling was conducted at all Project wells and at Landowner wells where there was unobstructed access to the well bore and where the wellhead was not located in a confined space. Two different gas sampling methods have been used for gas sampling. The first method is wellhead gas (WHG) sampling which involves collecting gas samples from within the wellbore, just above the level of the water in the well. The second method used involded a a flow-through gas separator, which collects the free gas released from the stream of water pumped from the well.

4.2.2.1 Wellhead Gas Sampling

Wellhead gas samples were collected at both Landowner and Project wells from Q4-2012 to Q4-2013. The original WHG sampling protocol required that the well be sealed during sampling. A sampling tube was to be inserted through a gas-tight port into the well and a sample collected using a pump and lung sampler to fill a gas-tight 1-litre Tedlar bag with sufficient sample for chemical and, if required, isotopic analyses. At Project wells, samples were collected before water sampling to avoid contamination of the wellbore by inflowing ambient air

and to ensure an adequate quantity of sample could be collected. A portable gas detector was used to continuously monitor and record concentrations of wellhead gases throughout the sampling process.

WHG gas sampling was modified in Q2-2013 in an attempt to improve results which had shown that significant atmospheric air was being entrained in the samples collected using the WHG sampling protocol. Under no circumstances at either the Project or the Landowner wells could the requirement for a gas-tight seal be met and almost all Landowner wells contained in-well infrastructure (i.e., downhole pumps, electrical wiring, tubing) that prevented access to the well and gas-tight sealing of the well.

From Q2-2013 to Q4-2013, a modified WHG sampling procedure utilizing low-flow sampling rates and a baffle to minimize air entrainment was developed and followed. The low-flow technique was successful in reducing air-entrainment in the deepest Project wells, but was less successful in shallower Project and Landowner wells.

4.2.2.2 Flow-Through Gas Sampling

In Q4-2013 a flow-through gas separator was tested in an attempt to improve the quality of gas samples by reducing the amount of air entrained during sampling. The gas separator was designed for use in separating free gas from groundwater during sampling of coalbed methane wells and is described by Jones et. al (2009). The flow-through separator operates by capturing free phase gas bubbles that enter the separator or are released within the separator. The detailed protocol adopted for flow-through sampling is provided by Jones et. al (2009).

In most wells, the gases are fully dissolved at depth and there is no free gas phase. However, as the sample is pumped to surface, gas bubbles may form in response to the reduced pressure. These bubbles are captured in the gas separator and sampled for chemical and isotopic analysis. A comparison of the preliminary gas phase chemistry results from samples collected using the flow-through separator shows that this sampling method is less prone to air entrainment than the WHG sampling method described above.

4.2.3 Water Quality Data Loggers

In addition to water and gas sampling, water quality data loggers were installed in each of the nine Project wells to provide a continuous record of groundwater levels and select hydrochemical parameters. In-Situ® Multi-Parameter TROLL 9500 probes are used to collect water level and basic water chemistry (pH, temperature, conductivity and oxidation-reduction potential) from the Project wells on a daily basis. The data loggers were installed at two wells (8-19/03 and 8-19/04) in early 2011; the remaining loggers were installed in early 2013. Download and maintenance (i.e., calibration, inspection and battery replacement) were performed by Golder each quarter.

4.2.4 Quality Assurance/Quality Control

The groundwater quality assurance/quality control (QA/QC) program consisted of collecting duplicate samples and field blanks during each quarterly sampling event.

Field duplicates were collected and used to assess the reliability of field sampling procedures. Duplicates were collected for every 10 to 12 wells sampled and were submitted with the original sample for laboratory analyses. Analytical results of the original and duplicate samples were then compared by calculating the relative percent difference (RPD) between the two analyses to assess the reproducibility or precision of the sampling procedure. Theoretically, the duplicate sample should have the same concentrations as the original sample. A maximum acceptable RPD of 20% for analyses where the analytical results were greater than 5 times the lower limit of detection was used to meet the data quality objectives of the Project (Mitchell, 2006).

Field blanks were collected to assess potential contamination introduced in the field during the sampling process. Field blank samples were generated by rinsing cleaned sampling equipment using laboratory-supplied distilled water. The samples were filled in the field, exposing them to the sampling environment. Theoretically, sample concentrations in field blank samples should be below reportable detection limits.

4.3 Results

4.3.1 Groundwater

The numbers of groundwater samples collected during each of the five quarterly sampling events are summarized in Table 4.3-1. Sampling sites and total number of samples collected in 2012-2013 are shown on Figure 4.3-1. To date, a total of 246 groundwater samples have been collected from 121 wells and submitted for Tier 1 + 2 analysis and a total of 132 groundwater samples have been collected and submitted for Tier 3 (isotopic) analysis.

Figure 4.3-1: Well Sampling Locations

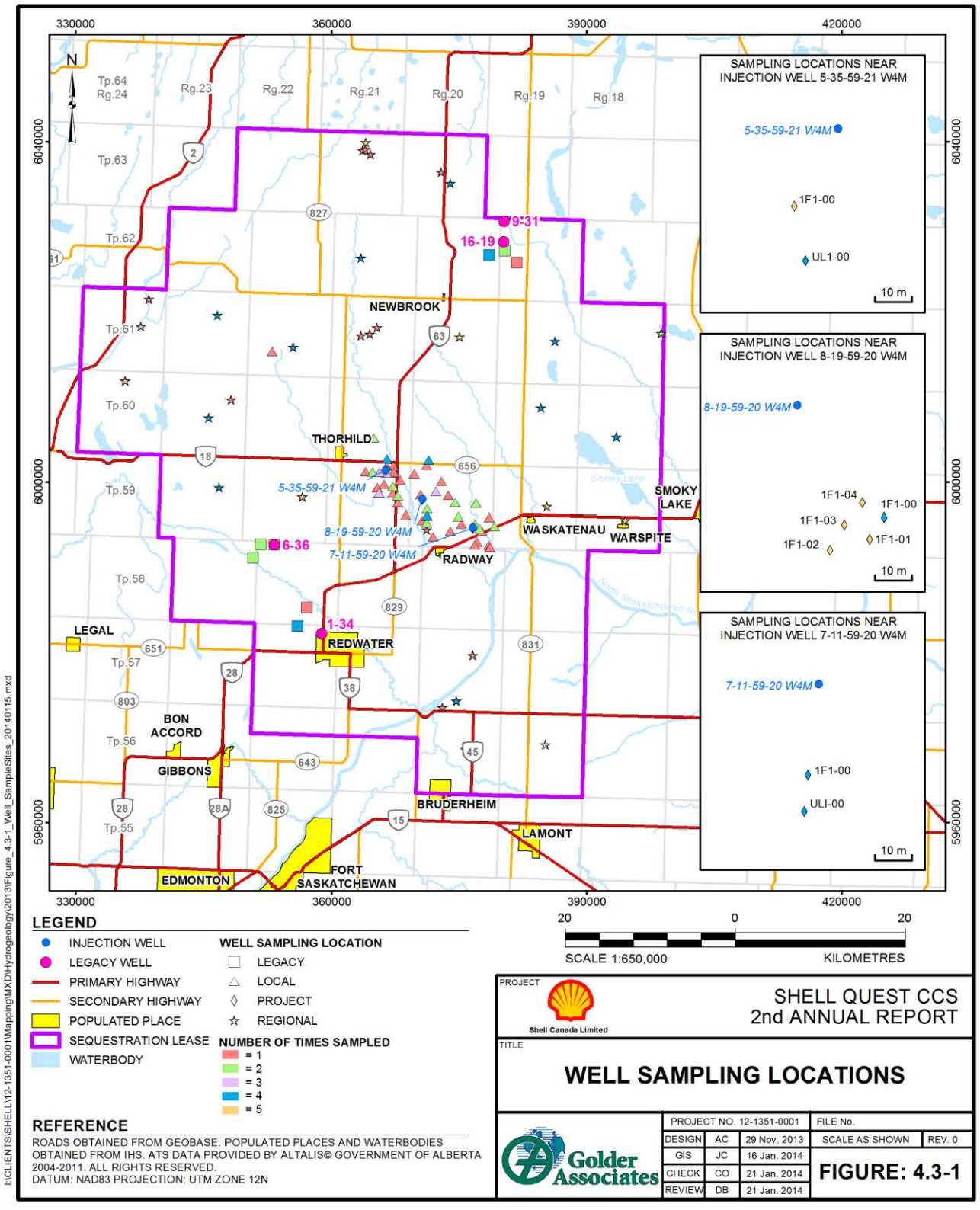

Table 4.3-1: 2012-2013 Groundwater Sampling Summary

Year	Sampling Event	Analysis Type	Wells Sampled				
			Regional	Legacy	Local	Project Monitoring Wells	**Total**
2012	Q4	**Tier 1 + 2**	9	3	41	4	**57**
		Tier 3	9	3	33	4	**49**
2013	Q1	**Tier 1 + 2**	31	8	10	9	**58**
		Tier 3	5	3	0	9	**17**
	Q2	**Tier 1 + 2**	21	7	17	9	**54**
		Tier 3	5	6	7	9	**27**
	Q3	**Tier 1 + 2**	21	3	4	6	**34**
		Tier 3	6	3	1	6	**16**
	Q4	**Tier 1 + 2**	22	3	10	8	**43**
		Tier 3	9	3	3	8	**23**
Total			**138**	**42**	**126**	**72**	**378**

As noted previously, not all wells provided on the inventory list could be sampled. For those wells not sampled, one or more of the following issues typically were encountered:

- Unable to contact landowner (after multiple attempts);
- Landowner unavailable during the period of sampling;
- Unable to locate Landowner's well at the specified location;
- Unsafe or inaccessible location due to conditions such as snow, heavy vegetation or confined space;
- Wells without a pump or inoperative pumps; and
- Access to property denied by Landowner.

4.3.1.1 Laboratory Results

The groundwater analytical results are compared to Health Canada's *Guidelines for Canadian Drinking Water Quality* (Health Canada 2012) in Table 4.3-2; with concentrations above guidelines indicated in bold. The Tier 1 + Tier 2 analytical data, including the total number of samples above each reported detection limit, maximum observed concentrations and number of drinking water exceedances for each analyte, are summarized in Table 4.3-2.

Table 4.3-2: 2012-2013 Groundwater Chemical Analysis Summary

Parameter	Reported Detection Limit (RDL)	Health Canada 2012 Drinking Water Guidelines [a]		Maximum Concentration Detected	Number of Samples Above RDL	Drinking Water Exceedances[d]
		MAC [b]	AO [c]			
Units	**mg/L**	**mg/L**	**mg/L**	**mg/L**		
pH - Field	N/A	-	-	10.5	233	72
pH - Lab	N/A	-	6.5-8.5	11.9	246	133
Alkalinity, phenolphthalein	5.0 as $CaCO_3$	-	-	742	167	-
Alkalinity, Total	5.0 as $CaCO_3$	-	-	1060	246	-
Aluminum	0.002	0.1	-	0.547	187	10
Antimony	0.001	0.006	-	0.026	34	5
Arsenic	0.001	0.01	-	0.12	140	50
Barium	0.05	1	-	32.5	149	21
Beryllium	0.001	-	-	n.d.	0	-
Bicarbonate	5	-	-	1220	243	-
Bismuth	0.001	-	-	0.009	9	-
Boron	0.01	5	-	2.19	246	0
Bromide	0.1	-	-	88.6	122	-
Cadmium	0.000016	0.005	-	0.00088	56	0
Calcium	0.3	-	-	445	246	-
Carbonate	5	-	-	141	169	-
Chloride	1	-	250	11500	237	41
Chromium	0.001	0.05	-	0.018	138	0
Cobalt	0.001	-	-	0.006	47	-
Conductivity – Field (uS/cm)	-	-	-	32,062	233	-
Conductivity - Lab (uS/cm)	-	-	-	29,000	246	-
Copper	0.002	-	1	0.131	218	0
Dissolved Inorganic Carbon	3	-	-	243	243	-
Hydroxide	5	-	-	233	2	-
Iodide	0.1	-	-	26	71	-
Iron	0.1	-	0.3	17.8	134	72
Lead	0.001	0.01	-	0.027	12	3
Lithium	0.001	-	-	0.69	246	-
Magnesium	0.2	-	-	188	245	-
Manganese	0.005	-	0.05	1.36	204	116
Mercury	0.000025	0.001	-	0.000098	9	0
Molybdenum	0.003	-	-	0.066	68	-

Parameter	Reported Detection Limit (RDL)	Health Canada 2012 Drinking Water Guidelines [a]		Maximum Concentration Detected	Number of Samples Above RDL	Drinking Water Exceedances[d]
		MAC [b]	AO [c]			
Units	**mg/L**	**mg/L**	**mg/L**	**mg/L**		
Nickel	0.003	-	-	0.226	97	-
Nitrate-N	0.113	-	1	11.4	12	2
Nitrite-N	0.015	-	10	2.24	4	1
Dissolved Phosphorus	0.005	-	-	3.26	218	-
Potassium	0.6	-	-	782	246	-
Selenium	0.001	0.01	-	0.18	82	38
Reactive Silica	0.05	-	-	60.7	209	-
Silicon	0.032	-	-	27	246	-
Silver	0.00005	-	-	0.00059	23	-
Sodium	6	-	200	5810	246	205
Strontium	0.01	-	-	24.8	246	-
Sulphate	1	-	500	2500	218	48
Thallium	0.0005	-	-	n.d.	0	-
Tin	0.00025	-	-	0.00581	57	-
Titanium	0.0005	-	-	0.0636	241	-
Total Dissolved Solids	5	-	-	18300	201	228
Total Suspended Solids	2	-	-	1480	110	-
Uranium	0.001	0.02	-	0.034	68	3
Vanadium	0.001	-	-	0.007	125	-
Zinc	0.001	-	5	15.7	238	2

[a] Health Canada (2012). *Guidelines for Canadian Drinking Water Quality - Summary Tabl*e. Water, Air and Climate Change Bureau, Healthy Environments and Consumer Safety Branch, Health Canada, Ottawa, Ontario.
[b] Health Canada's Maximum Acceptable Concentration (MAC) for Drinking Water.
[c] Health Canada's Aesthetic Objectives (AO) for Drinking Water.
[d] The number of samples that exceed Health Canada's Drinking Water Guidelines.
n.d.= not detected; no concentrations observed above parameter RDL.

A large amount of hydrochemical and gas compositional and isotopic data was collected over the five quarters of sampling. As an example of the information collected, maps depicting pH values obtained from Regional wells completed in the Foremost Formation, during each successive quarterly sampling event, are presented in Figure 4.3-2 to Figure 4.3-6.

Figure 4.3-2: PH Values for Regional Wells Completed in the Foremost Formation – Quarter 4, 2012

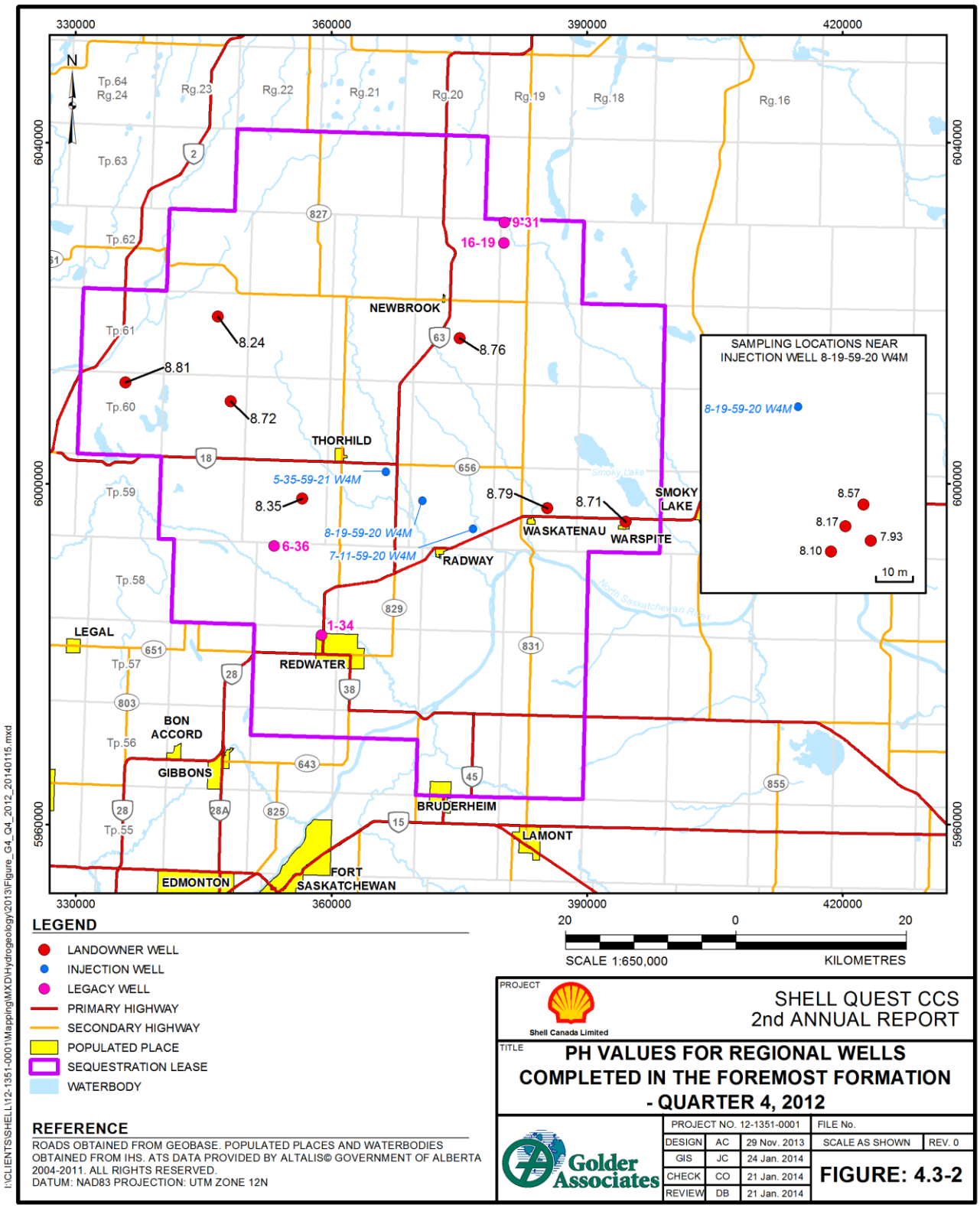

Figure 4.3-3: PH Values for Regional Wells Completed in the Foremost Formation – Quarter 1, 2013

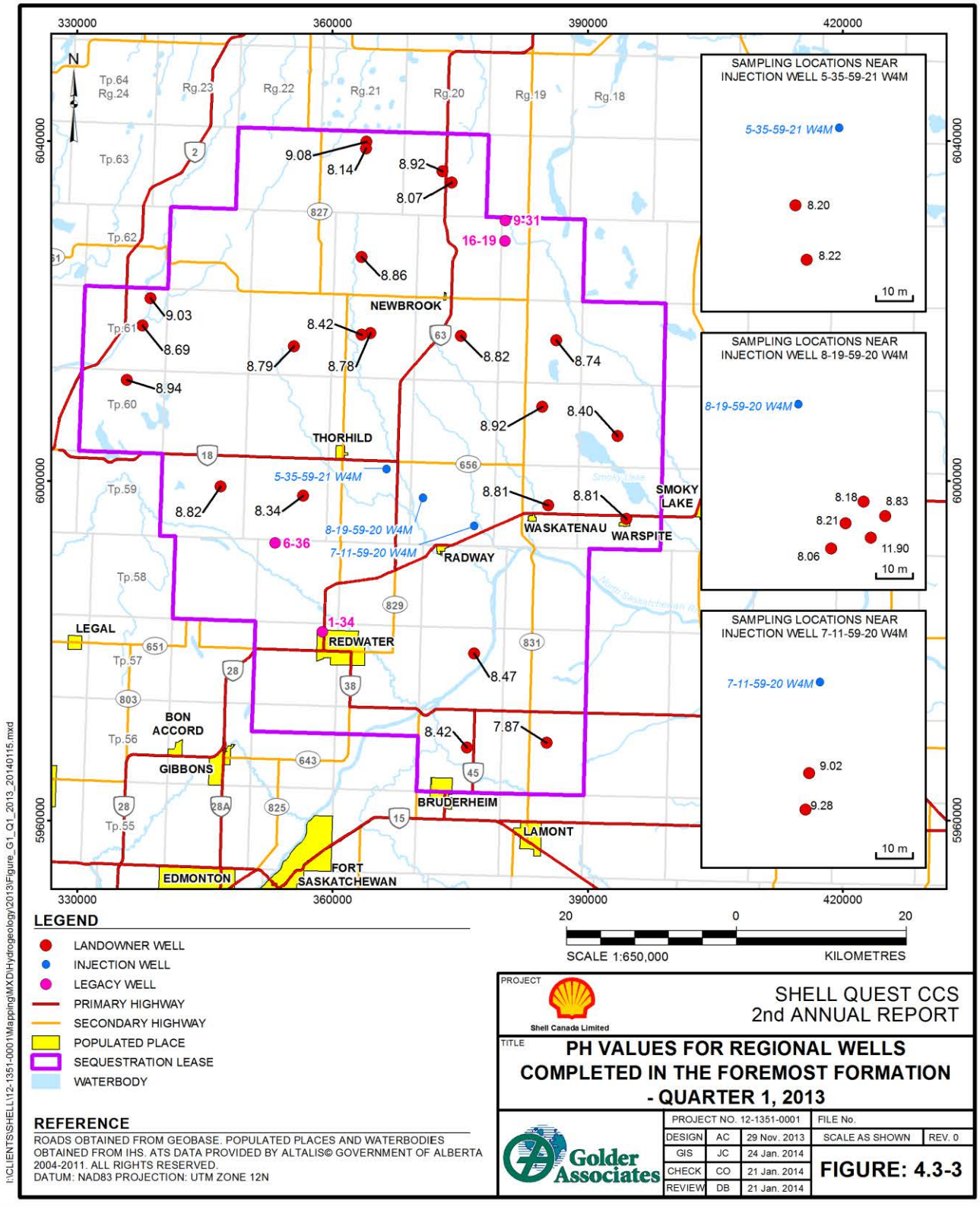

Figure 4.3-4: PH Values for Regional Wells Completed in the Foremost Formation – Quarter 2, 2013

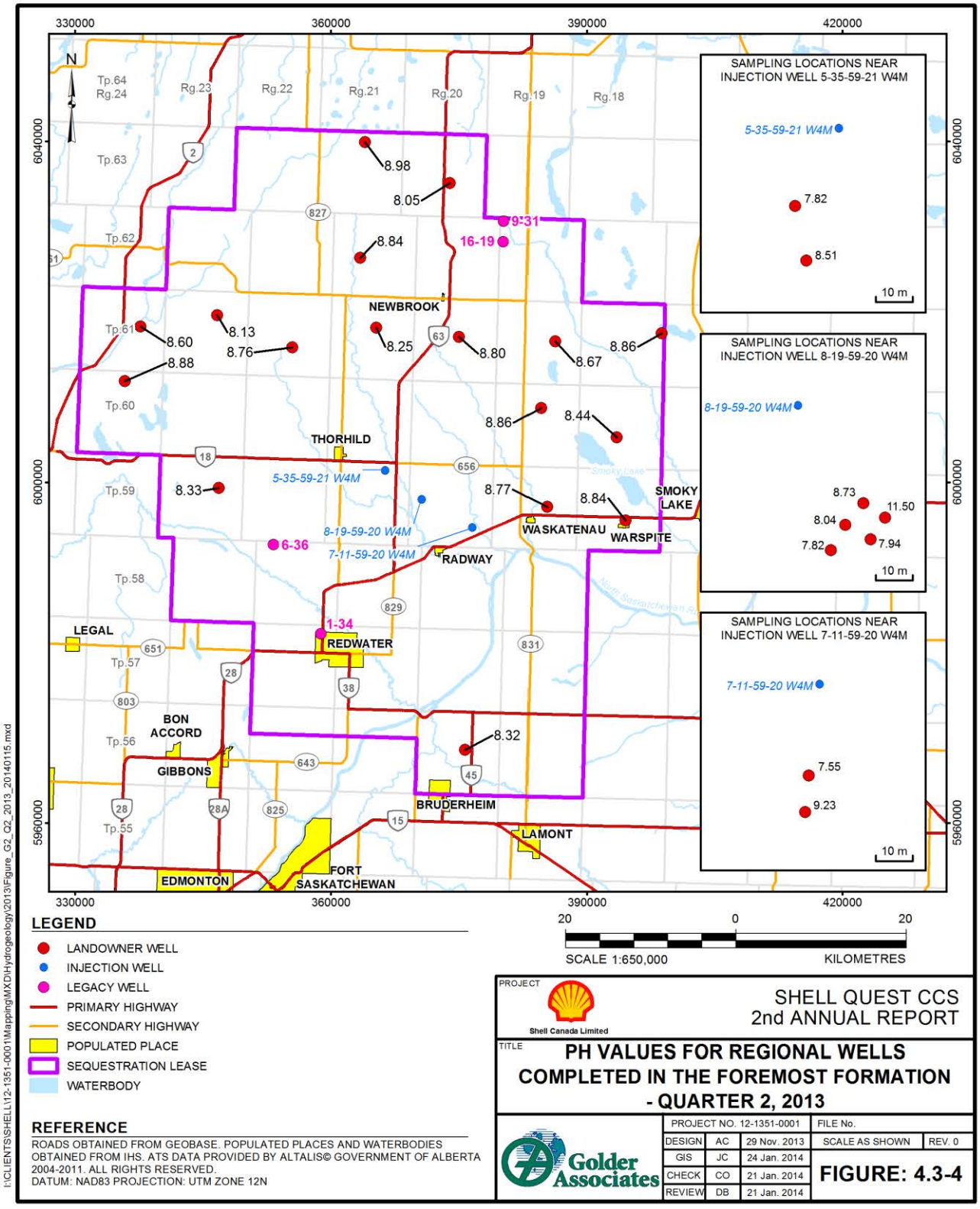

Figure 4.3-5: PH Values for Regional Wells Completed in the Foremost Formation – Quarter 3, 2013

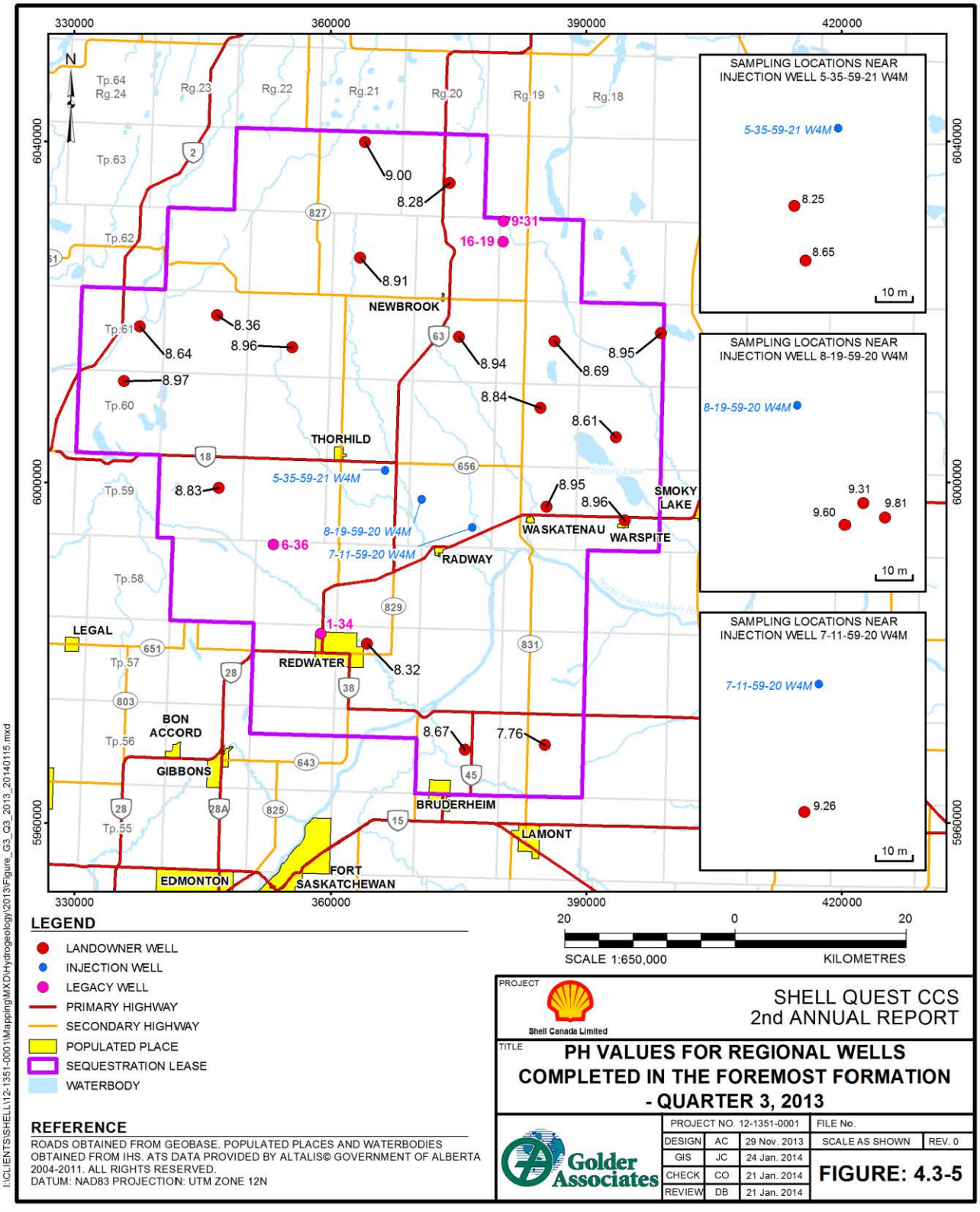

Figure 4.3-6: PH Values for Regional Wells Completed in the Foremost Formation – Quarter 4, 2013

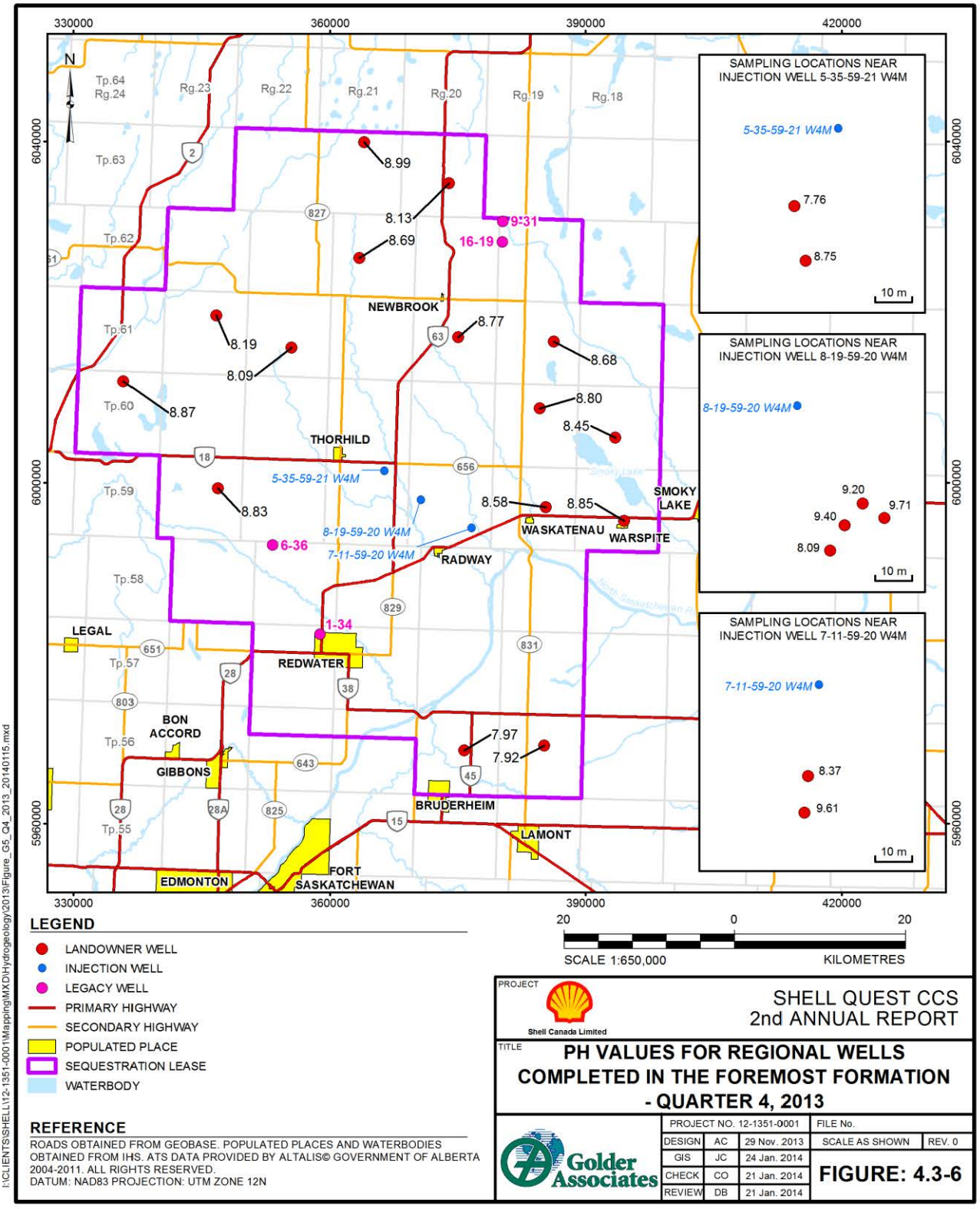

Major ion chemistry from groundwater samples collected in 2012 and 2013 were plotted on a Piper diagram (Figure 4.3-7) and grouped by geological formation as inferred from well depths. The geological formations assigned to specific wells will be reassessed by Shell during the course of the HBMP and may, therefore, change from those portrayal on Figure 4.3-7.

The Piper plot illustrates the range of water quality observed from the groundwater samples collected over the Sequestration Lease Area. Groundwaters trend from the immature calcium-magnesium-bicarbonate (Ca-Mg-HCO_3) composition type to more evolved compositions, as indicated by the trend from calcium-magnesium to sodium dominated compositions in the lower left cation ternary. Groundwater in surficial deposits trends from immature Ca-Mg dominated to more evolved sodium dominated compositions. However, two types of sodium-rich surficial groundwaters are evident; one is sodium-sulphate-bicarbonate (Na-SO_4-HCO_3) type and the second is sodium-bicarbonate (Na-HCO_3) type. The former (Na-SO_4-HCO_3) groundwater type is typical of prairie soils originating from Laurentide glacial tills (derived from the Canadian Shield), where oxidation of pyrite contributes sulphate to the groundwater. The latter Na-HCO_3 type surficial groundwater is probably related to the former, but may be indicative of reduction of sulphate to sulphide by bacterial sulphate reduction or methane oxidation. Additional work to estalish the origins and controls on surficial water types is considered warranted.

Figure 4.3-7: Piper Plot – 2012-2013 Groundwater Samples

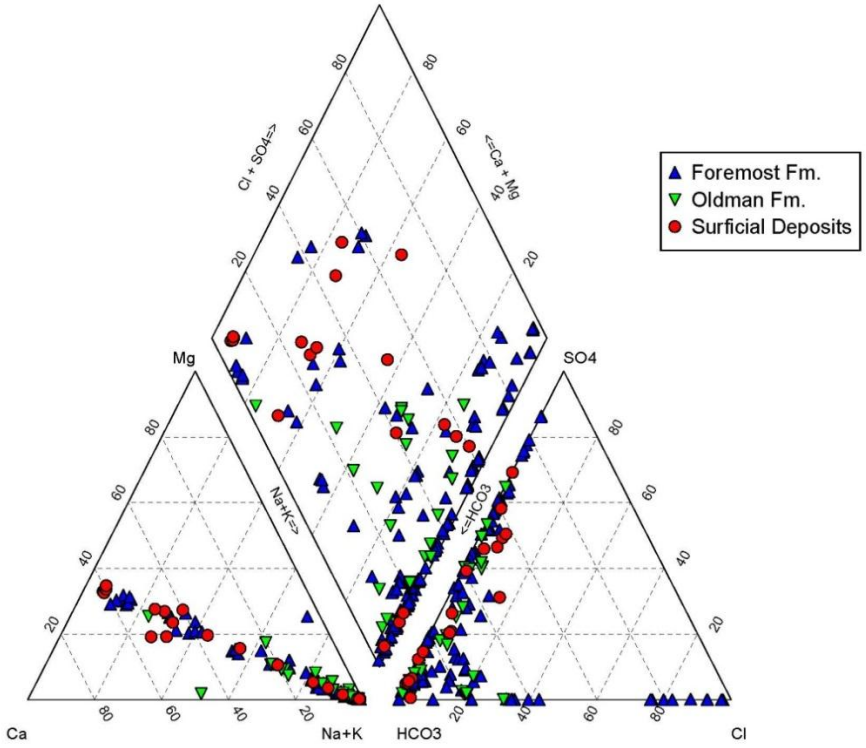

The majority of groundwaters derived from the Oldman and Foremost formations show similar behaviour to the surficial deposits with Foremost Formation samples showing the highest proportion of sulphate. However, a subset of Foremost Formation samples and some Oldman Formation samples show increasing proportions of chloride (Cl), with a number of Foremost Formation samples ranging to mature Na-Cl-(HCO_3) type groundwater compositions. This composition type is indicative of a connection to deeper sedimentary basin groundwaters. Additional work to estalish the origins and controls on Oldman and Foremost groundwater types is considered warranted, including using stable and radiogenic isotopes to characterise the groundwaters and constrain their origins..

Water samples collected in 2013 for isotope analyses were submitted to the University of Waterloo and University of Calgary for analysis. Isotope analyses were performed by Isobrine Solutions Ltd. for samples collected in Q4-2012. The Tier 3 data, including maximum and minimum reported values for each analyte, are summarized in Table 4.3-2.

Table 4.3-2: 2012-2013 Groundwater Isotopic Analysis Summary (to Dec. 2013)

Isotope	Unit	Standard	Number	Maximum	Minimum
[a] $\delta^{13}C$_DIC	‰	V-PDB	67	13.8	-33.4
[b] $\delta^{18}O$_H2O	‰	V-SMOW	47	-13.8	-21.47
[c] $\delta^{2}H$_H2O	‰	V-SMOW	47	-118	-166.77
[d] $\delta^{11}B$	‰	NIST SRM 951	36	59.2	-35.4
[e] $\delta^{37}Cl$	‰	SMOC	39	-0.24	-4.93
[f] $\delta^{81}Br$	‰	SMOB	15	1.17	-2.12
[g] $^{87}Sr/^{86}Sr$	mass ratio	n/a	43	0.7082	0.7054

Notes:
[a] $\delta^{13}C$ - dissolved inorganic carbon; V-PDB - Vienna Peedee belemnite
[b] $\delta^{18}O$ – water; V-SMOW – Vienna standard mean ocean water
[c] $\delta^{2}H$ – water
[d] $\delta^{11}B$ – solute in water; NIST SRM 951 – NIST Standard Reference Material 951
[e] $\delta^{37}Cl$ – solute in water; SMOC – standard mean ocean chlorine
[f] δ^{81} – solute in water; SMOB – standard mean ocean bromine
[g] $^{87}Sr/^{86}Sr$ – solutes in water

Due to lengthy turnaround times experienced for isotopic analyses (between 12 and 30 weeks after submission), the complete 2013 isotope dataset is not available as of the date of this report.

4.3.1.2 Data Logger Results

Data collected from the In-Situ® Multi-Parameter TROLL 9500 data loggers are summarized in Table 4.3-3. Minimum, maximum and average data values for water level, temperature, barometric pressure and oxidation-reduction potential, by project well, are provided. Quality checks (QA/QC) of conductivity and pH have identified issues with some data related to instrument drift and sensor performance and failure, possibly resulting from lightning strikes.

Table 4.3-3: 2013 Troll 9500 Data Logger Summary

Well-ID	Troll S/N	Geology	Time Period Sampled	Descriptive Statistics	Water Level (masl)*	Bar. Pressure (inches Hg)	Temp (°C)	ORP (V)	pH	Electrical Conductivity (uS/cm)
1F1-08-19-059-20W4/00	SN51087	Foremost	May 16th 2013 - Oct. 26th 2013	Minimum:	601.4	26.84	8.09	-0.88	10.85	16,998
				Maximum:	601.75	28.52	8.21	-0.72	12.42	20,238
				Average:	601.61	28.08	8.15	-0.78	12.13	18,274
				Number of Data Points:	132	87	87	87	87	99
1F1-08-19-059-20W4/01	SN51065	Foremost	Mar. 28th 2013 - Oct. 26th 2013	Minimum:	543.13	27.24	6.34	-0.35	7.41	6,696
				Maximum:	622	28.58	7.26	0.46	10.47	13,178
				Average:	601.08	28.08	6.58	-0.12	8.10	7,461
				Number of Data Points:	201	209	209	209	209	62
1F1-08-19-059-20W4/02	SN51070	Foremost	Mar. 28th 2013 - Aug. 21st 2013	Minimum:	583.9	27.53	5.41	-0.48	8.61	8,191
				Maximum:	636.01	28.46	5.57	-0.09	13	8,456
				Average:	633.42	28	5.44	-0.33	9.99	8,415
				Number of Data Points:	141	141	141	141	92	92
1F1-08-19-059-20W4/03	SN50248	Foremost	Apr. 5th 2013 - Oct. 26th 2013	Minimum:	636.28	27.23	5.03	-0.61	5	3,396
				Maximum:	636.47	28.2	5.11	0.22	10.29	3,567
				Average:	636.35	27.73	5.06	-0.32	9.10	3,501
				Number of Data Points:	72	77	77	77	67	77
1F1-08-19-059-20W4/04	SN50249	Oldman	Apr. 5th 2013 - Oct. 26th 2013	Minimum:	634.17	27.4	4.86	-0.56	5.06	1,072
				Maximum:	635.63	28.17	4.98	-0.03	11.03	1,689
				Average:	635.33	27.76	4.9	-0.4	9.23	1,302
				Number of Data Points:	81	85	85	85	61	85
1F1-05-35-059-21W4/00	SN51069	Foremost	Mar. 28th 2013 - Oct. 15th 2013	Minimum:	613.62	27.25	6.31	-0.67	9.1	11,422
				Maximum:	613.86	28.64	6.41	-0.38	8.67	13,542
				Average:	613.75	28.13	6.36	-0.58	204	12,092
				Number of Data Points:	204	205	205	205	205	135
UL1-05-35-059-21W4/00	SN51067	Foremost	Jun. 10th 2013 - Aug. 25th 2013	Minimum:	638.64	27.36	4.65	-0.7	7.81	919
				Maximum:	638.75	28.28	4.66	-0.17	8.62	4,879
				Average:	638.69	27.82	4.67	-0.44	8.36	1,255
				Number of Data Points:	77	77	8	77	77	64
1F1-07-11-059-20W4/00	SN51066	Foremost	Mar. 28th 2013 - Oct. 15th	Minimum:	NA(b)	27.35	7.03	NA(b)	6.87	7,667
				Maximum:	NA(b)	28.69	7.1	NA(b)	9.84	7,903

Well-ID	Troll S/N	Geology	Time Period Sampled	Descriptive Statistics	Water Level (masl)*	Bar. Pressure (inches Hg)	Temp (°C)	ORP (V)	pH	Electrical Conductivity (uS/cm)
			2013	Average:	NA(b)	28.19	7.05	NA(b)	7.65	7,809
				Number of Data Points:	199	199	199	199	199	199
UL1-07-11-059-20W4/00	SN51062	Foremost	Mar. 29th 2013 - Oct. 17th 2013	Minimum:	627.8	27.04	5.08	-0.54	8.26	3,001
				Maximum:	631.42	28.35	5.12	-0.17	12.81	4,838
				Average:	630.76	27.87	5.09	-0.27	9.33	3,584
				Number of Data Points:	202	202	202	202	202	190

* masl = meters above sea level
(a) - Preliminary quality checks (QA/QC) of conductivity and pH have identified issues with the data logged.
(b) - Preliminary QA/QC identified issues with data accuracy; therefore the data are not presented at this time.

4.3.2 Wellhead Gas Results

The wellhead gas results for samples collected during the five quarterly sampling events are summarized in Table 4.3-4. To date, a total of 73 wellhead gas compositions have been collected of which 49 were submitted for isotopic analysis.

Table 4.3-4: 2012-2013 Wellhead Gas Sampling Summary

Year	Sampling Event	Analysis Type	Wells Sampled				
			Regional	Legacy	Local	Project Monitoring Wells	**Total**
2012	Q4	**composition**	0	0	0	4	**4**
		isotope	0	0	0	4	**4**
2013	Q1	**composition**	2	1	4	9	**16**
		isotope	0	1	0	9	**10**
	Q2	**composition**	3	0	10	9	**22**
		isotope	0	0	4	9	**13**
	Q3	**composition**	2	1	2	9	**14**
		isotope	0	1	1	9	**11**
	Q4	**composition**	3	0	5	9	**17**
		isotope	0	0	2	9	**11**
Total			**10**	**4**	**28**	**80**	**122**

4.3.2.1 Wellhead Gas Composition

The analyte data including total number of samples above reported detection limit and maximum observed concentration are summarized in Table 4.3-5.

Table 4.3-5: 2012-2013 Wellhead Gas Chemical Analysis Summary

Parameter	Units	Reported Detection Limit (RDL)	Samples Above RDL	Maximum Concentration Detected (ppm)
Helium (He)	%	0.001	38	0.236
Hydrogen (H_2)	%	0.001	60	0.814
Oxygen (O_2)	%	0.001	75	219900
Nitrogen (N_2)	%	0.001	75	786800
Carbon Dioxide (CO_2)	%	0.001	74	2000
Hydrogen Sulphide (H_2S)	%	0.0001	0	0
Methane (C_1)	%	0.001	37	9100
Ethane (C_2)	%	0.001	12	0.28
Propane (C_3)	%	0.001	7	0.018
I-Butane (IC_4)	%	0.001	5	0.049
N-Butane (NC_4)	%	0.001	6	0.064
I-Pentane (IC_5)	%	0.001	4	0.036
N-Pentane (NC_5)	%	0.001	3	0.055
Hexanes (C_6)	%	0.001	3	0.037
Heptanes (C_7)	%	0.001	3	0.044
Octanes (C_8)	%	0.001	3	0.033
Nonanes (C_9)	%	0.001	3	0.005
Decanes+ (C_{10+})	%	0.001	0	0

Gas samples collected for isotope analyses were submitted to the University of Alberta for analysis. The isotopic data, including maximum and minimum reported values for each analyte, are summarized in **Table 4.3-2**. Due to lengthy turnaround times by the university, a complete 2013 isotope dataset has not yet been received.

Table 4.3-6: 2012-2013Wellhead Gas Isotopic Analysis Summary (to Dec. 2013)

Isotope Ratio	Units	Standard	Number	Maximum	Minimum
$\delta^{13}C_{CH4}$	‰	V-PDB	19	-3.18	-68.12
$\delta^{13}C_{C2}$	‰	V-PDB	4	-42.6	-50.77
$\delta^{13}C_{C3}$	‰	V-PDB	1	-39.58	-39.58
$\delta^{13}C_{NC4}$	‰	V-PDB	3	-32.66	-226
$\delta^{13}C_{CO2}$	‰	V-PDB	29	-5.83	-40.67

4.3.3 Quality Assurance/Quality Control

The Quality Assurance/Quality Control (QA/QC) program consisted of collecting field blank and duplicate groundwater and wellhead gas samples during the 2012-2013 sampling events.

Field blanks are collected to assess potential contamination introduced during the sampling process and during transport to and from the site and provide a measure of accuracy in the results. Field blank samples were collected using laboratory-supplied de-ionized water that was filled into sample containers at a sampling location. Theoretically, laboratory results from field blanks will be identical to de-ionized water chemistry.

Duplicate samples are used to assess precision of field sampling procedures. The sample is collected successively to the original sample (i.e., two samples taken immediately following one another under identical conditions/procedures). Laboratory results between the original and the duplicate are then compared. Theoretically, duplicate samples should have the identical chemical composition; however, due to factors such as sample matrix heterogenieity, or natural variability, minor differences (typically up to 20%) in chemical concentration may occur.

QA/QC samples collected in 2012-2013 are summarized in Table 4.3-6. A total of 31 and 9, field duplicate samples and field blanks (groundwater and wellhead gas combined), respectively were collected in 2012-2013. Laboratory results of the QA/QC samples indicate that, in general, QA/QC samples are within acceptable quality criteria for both duplicate and field blank samples.

Table 4.3-6: 2012-2013 Quality Assurance/Quality Control Sampling

Year	Sampling Event	Analysis Type	QA/QC Sampling			
			Groundwater		Wellhead Gas	
			Duplicate Samples	Field Blanks	Duplicate Samples	Field Blanks
2012	Q4	**Chemical**	4	2	0	0
		Isotopic	4	0	0	0
2013	Q1	**Chemical**	2	1	1	0
		Isotopic	0	0	0	0
	Q2	**Chemical**	5	2	2	0
		Isotopic	2	0	1	0
	Q3	**Chemical**	3	2	0	0
		Isotopic	1	0	0	0
	Q4	**Chemical**	3	1	2	1
		Isotopic	0	0	1	0
Total			**24**	**8**	**7**	**1**

5.0 REFERENCES

ACIMS (Alberta Conservation Information Management System). 2013. *List of all Species and Ecological Communities in Alberta, within the ACIMS Database* – June 2013. Alberta Tourism, Parks and Recreation, Parks Division, Edmonton, AB.

ACMC (Alberta Clubroot Management Committee) 2010. Alberta Clubroot Management Plan, Alberta Clubroot Management Committee (revised May 2010) www1.agric.gov.ab.ca/$department/deptdocs.nsf/all/agdex11519

Amiro, B.D., Barr, A.G., Black, T.A., Iwashita, H., Kljun, N., McCaughey, J.H., Morgenstern, K., Murayama, S., Nesic, Z., Orchansky, A.L., Saigusa, N., 2006. Carbon, energy and water fluxes at mature and disturbed forest sites, Saskatchewan, Canada. Agricultural and Forest Meteorology 136, 237–251.

Austen, A. T., L. Yahdjian, J. M. Stark, J. Belnap, A. Porporato, U. Norton, D. A. Ravetta and S. M. Schaeffer, 2004. Water pulses and biogeochemical cycles in arid and semiarid ecosystems, Oecologia, 141, 221-235.

Baldocchi, D.D. 2003. Assessing the eddy covariance technique for evaluating carbon dioxide exchange rates of ecosystems: past, present and future. Global Change Biology, 9, 479–492.

Bartels, J.M., 1996. Methods of Soil Analysis: Chemical Methods. Soil Science Society of America book Series No. 5. Soil Science Society of America. Madison, Wisconsin, USA.

Brierley, J.A., Walker, B.D., Thomas C.J., Smith P.E. and Bock M.D. 2006. Alberta Soil Names File (Generation 3): User's Handbook, Land Resource Unit, Research Branch, Agriculture and Agri-Food Canada.

Bubier, Jill L., Patrick M. Crill, Tim R. Moore, Kathleen Savage, and Ruth K. Varner. 1998. Global Biogeochemical Cycles. Seasonal Patterns and Controls on Net Ecosystem CO2 Exchange in a Boreal Peatland Complex. Volume 12, Issue 4, pages 703–714, December 1998.

CAPP 2008 (Canadian Association of Petroleum Producers) Best Management Practices, Clubroot Disease Management. Available online at: http://www.capp.ca/getdoc.aspx?DocId=139848&DT=PDF.

Carter, M.R., Gregorich, E.G., 2008. Soil Sampling and Methods of Analysis, Second Edition. Canadian Society of Soil Science.

Cerling, T.E. 1984. The stable isotopic composition of modern soil carbonate and its relationship to climate. Earth and Plaentary Science Letters, 11, 229-240.

Cerling, T.E., D. K. Solomon, J. Quade and J. R. Bowman. 1991. On the isotopic composition of carbon in soil carbon dioxide. Geochimica et Cosmochimica Acta, 55(11), 3403-3405.

Chen, J. M., W. Ju, J. Cihlar, D. Price, J. Liu, W. Chen, J. Pan, A. Black and A. Barr. 2003. Spatial distribution of carbon sources and sinks in Canada's forests. Tellus-B, 55(2), 622-641.

Conel, J.E., Green, R.O., Vane, G., Bruegge, C.J., and Alley, R.E. 1987. AIS-2 radiometry and a comparison of methods for the recovery of ground reflectance. In Proceedings of the Third Airborne Imaging Spectrometer Data Analysis Workshop (G. Vane, Ed.), JPL Publ. 87-30, Jet Propulsion Laboratory, Pasadena, CA, pp. 18-47. Available at: http://naca.larc.nasa.gov/search.jsp?R=19880004375&qs=N%3D4294957316%2B4294572792%26Nn%3D4294961259%257CAvailability%2BType%257CAcquire%2Bfrom%2BOther%2BSources Accessed December 2012

Coursolle, C., Margolis, H.A., Barr, A.G., Black, T.A., Amiro, B.D., McCaughey, J.H., Flanagan, L.B., Lafleur, P.M., Roulet, N.T., Bourque, C.P.-A., Arain, M.A., Wofsy, S.C., Dunn, A., Morgenstern, K., Orchansky, A.L., Bernier, P.-Y., Chen, J.M., Kidson, J., Saigusa, N., Hedstrom, N. 2006. Late-summer carbon fluxes

from Canadian forests and peatlands along an east-west continental transect. Can. J. Forest Res. 36, 783–800.

Dunn A.L., Barford C.C., Wofsy S.C., Goulden M.L., Daube B.C. 2006. A long-term record of carbon exchange in a boreal black spruce forest: means, responses to interannual variability, and decadal trends. Global Change Biol., doi:10.1111/j.1365-2486.2006.01221.x.

Ehleringer, J. R., N. Buchmann and L. B. Flanagan. 2000. Carbon isotope ratios in belowground carbon cycle processes, Ecological Applications, 10(2), pp. 412-422.

Flanagan, L. B., Wever, L. A. and P. J. Carlson. 2002. Seasonal and interannual variation in carbon dioxide exchange and carbon balance in a northern temperature grassland, Global Change Biology, 8, 599-615.

Flanagan, L.B., D. S. Kubien and J. R. Ehleringer. 1999. Spatial and temoporal variation in the carbon and oxygen stable isotope ratio of respired CO2 in a boreal forest ecosystem, Tellus-B, 51B, pp. 367-384.

Gaumont-Guay, D., Black, T. A., Giffis, T. J., Barr, A. G., Jassal, R. S. and Z. Nesic. 2006. Interpreting the dependence of soil respiration on soil temperature and water content in a boreal aspen stand, Agricultural and Forest Meteorology, 140, 220-235.

Gilmanov T. G., L. Aires, Z. Barcza, V. S. Baron, L. Belelli, J. Beringer, D. Billesbach, D. Bonal, J. Bradford, E. Ceschia, D. Cook, C. Corradi, A. Frank, D. Gianelle, C. Gimeno, T. Gruenwald, Haiqiang Guo, N. Hanan, L. Haszpra, J. Heilman, A. Jacobs, M. B. Jones, D. A. Johnson, G. Kiely, Shenggong Li, V. Magliulo, E. Moors, Z. Nagy, M. Nasyrov, C. Owensby, K. Pinter, C. Pio, M. Reichstein, M. J. Sanz, R. Scott, J. F. Soussana, P. C. Stoy, T. Svejcar, Z. Tuba, and G. Zhou. 2010. Productivity, Respiration, and Light-Response Parameters of World Grassland and Agroecosystems Derived from Flux-Tower Measurements, Rangeland Ecology & Management, 63(1):16-39.

Gilmanov, T. G., Tieszen, L. L., Wylie, B. K., Flanagan, L. B., Frank, A. B., Haferkamp, M. R., Meyers, T. P. and J. A. Morgan. 2005. Integration of CO2 flux and remotely sensed data for primary production and ecosystem respiration analyses in the North Great Plains: potential for quantitative spatial extrapolation, Global Ecology and Biogeography, 14, 271-292.

Golder Associates Ltd. 2010a. Suggested Operating Procedure: Soil Gas Probe Installation (for internal use only, not available for distribution).

Golder Associates Ltd. 2010b. Suggested Operating Procedure: Soil Gas Sampling (for internal use only, not available for distribution).

Golder Associates Ltd 2010c. Suggested Operating Procedure: Soil Gas Probe Leak Tests (for internal use only, not available for distribution).

Golder Associates Ltd. 2012a. Suggested Operating Procedure: Soil Gas Probe Installation for CCUS Monitoring (for internal use only, not available for distribution).

Golder Associates Ltd. 2012b. Suggested Operating Procedure: CCUS Soil Gas Sampling Using Pre-Evacuated Glass Vials (for internal use only, not available for distribution).

Golder Associates Ltd. 2012c. Suggested Operating Procedure: Leak Testing CCUS Soil Gas Probes (for internal use only, not available for distribution).

Goulden, M. L., P. M. Crill. 1997. Automated measurements of CO2 exchange at the moss surface of a black spruce forest, Tree Physiology, 17(8-9), 537.

Health Canada. 2012. Guidelines for Canadian Drinking Water Quality - Summary Table. Water, Air and Climate Change Bureau, Healthy Environments and Consumer Safety Branch, Health Canada, Ottawa.

Henderson, D. C., B. H. Ellert and M. A. Naeth. 2004. Utility of 13C for ecosystem carbon turnover estimation in grazed mixed grass prairie. Geoderma, 11, 219-231.

Jensen, J.R. 2005. Introductory Digital Image Processing: A Remote Sensing Perspective, 3rd Edition. K.C. Clarke (ed.). Pearson Prentice Hall, Upper Saddle River, NJ. 526 pp.

Jones, D., S. Gordon, B. Mayer, M. Hitz and A. Blyth, 2009. The free gas sampling standard operating procedure for baseline water well testing. Prepared by Alberta Research Council Inc. for Alberta Environment and Sustainable Resource Development, March 31, 2009, 13 p.

Kljun, N., T. A. Black, T. J. Griffis, A. G. Barr, D. Gaumont-Guay, K. Moregenstern, J. H. McCaughey and Z. Nesic. 2007. Response of Net Ecosystem Productivity of Three Boreal Forest Stands to Drought, Ecosystems, 10, 1039-1055.

Klute, A. 1986. Methods of soil analysis: Part I. Agronomy Monographs 9. Soil Science Society of America. Madison, Wisconsin, USA.

Laws, E A. 1997. Mathematical Methods for Oceanographers, John Wiley & Sons, ISBN 0-471-16221-3.

Margolis, H. A., L. B. Flanagan and B. D. Amiro, (2006), The Fluxnet-Canada Research Network: Influence of climate and disturbance on carbon cycling in forests and peatlands, Agricultural and Forest Meteorology 140, 1-5.

McKeague, J.A. 1978. Manual on Soil Sampling and Methods of Analysis, 2nd edition, Canadian Society of Soil Science.

Migliavacca, Micro, Markus Reichstein, Andrew D. Richardson, Roberto Colombo, Mark A. Sutton, Gitta Lasslop, Enrico Tomelleri, Georg Wohlfahrt, Nuno Carvalhais, Alessandro Cescatti, Miguel D. Mahecha, Leonardo Montagnani, Dario Papale, Sonke Zaehle, Altaf Arain, Almut Arneth, T. Andrew Black, Arnaud Carrara, Sabina Dore, Damiano Gianelle, Carole Helfter, David Hollinger, Werner L. Kutsch, Peter M. Lafleur, Yann Nouvellon, Corinna Rebmann, Humberto R. Da Rocha, Mirco Rodeghiero, Olivier Roupsard, Maria-Teresa Sebastia, Guenther Seufert, Jean-Francoise Soussana, And Michiel K. Van Der Molen. 2011. Semiempirical Modeling of Abiotic and Biotic Factors Controlling Ecosystem Respiration across Eddy Covariance Sites. Global Change Biology 17, 390–409, doi: 10.1111/j.1365-2486.2010.02243.x.

Mitchell, P., 2006. Guidelines for Quality Assurance and Quality Control in Surface Water Quality Programs in Alberta, Prepared by Patricia Mitchell Environmental Consulting for Alberta Environment, July 2006, 67 p.

Moisey, D., J. Young, D. Lawrence, C. Stone, M. Willoughby. 2012. Guide to Range Plant Community Types and Carrying Capacity for the Dry and Central Mixedwood Subregions in Alberta. 7th Approximation. Alberta Environment and Sustainable Resource Development: Land Division. Edmonton, AB.

Moss, E.H. 1983. Flora of Alberta, Second Edition. Revised by J.G. Packer. University of Toronto Press, Toronto, Ontario. 687 pp.

National Oceanic & Atmospheric Administoration (NOAA). 2013. Earth System Research Laboratory Global Monitoring Division. About ESRL Global Monitoring Division and NOAA Strategic Plan Elements. Available at: http://www.esrl.noaa.gov/gmd/about/aboutgmd.html.

National Oceanic & Atmospheric Administoration (NOAA). 2013. Earth System Research Laboratory Global Monitoring Division. Environment Canada. Available at: http://www.esrl.noaa.gov/gmd/dv/site/site.php?code=LLB.

NOAA/ESRL. 2012. CCGG Cooperative Air Sampling Network, (http://www.esrl.noaa.gov/gmd/ccgg/flask.html).
Ontario.

Pataki, D. E., J. R. Ehleringer, L. B. Flanagan, D. Yakir, D. R. Bowling, C. J. Still, N. Buchmann, J. O. Kaplan, and J. A. Berry. 2003. The application and interpretation of Keeling plots in terrestrial carbon cycle research, Global Biogeochemical Cycles, 17(1), doi:10.1029/2001GB001850.

Pedocan (Pedocan Land Evaluation Ltd.). 1993. Soil Series Information for Reclamation Planning in Alberta, Vol.1 and 2. Report RRTAC 93-7 Prepared for the Alberta Conservation and Reclamation Council (Reclamation Research Technical Advisory Committee – RRTAC), Edmonton, AB.

Pedocan (Pedocan Land Evaluation Ltd.). 1993. Soil Series Information for Reclamation Planning in Alberta, Vol.1 and 2. Report RRTAC 93-7 Prepared for the Alberta Conservation and Reclamation Council (Reclamation Research Technical Advisory Committee – RRTAC), Edmonton, AB.

Phillips, C. L., Nickerson, N., Risk, D. and B. J. Bond. 2011. Interpreting diel hysteresis between soil respiration and temperature, Global Change Biology, 17, 515-527, doi:10.1111/j.1365-2486.2010.02250.x.

Romanak,K. D., Bennett, P. C., Yang C. and Hovorka,S. D. 2012. Process-based approach to CO2 leakage detection by vadose zone gas monitoring at geological CO2 storage sites. Geophysical Research Letters, 39(L15405), doi: 10.1029/2012GL052426, 2012.

Sala, O. E., Parton, W. J., Joyce, L. A. and W. K. Lauenroth, (1988) Primary production of the central grassland region of the United States, Ecology, 69, 40-45.

Schreader, Cheryl P., Wayne R. Rouse, Timothy J. Griffis, L. Dale Boudreau, and P. D. Blanken. 1998. Global Biogeochemical Cycles. Carbon Dioxide Fluxes in a Northern Fen during a Hot, Dry Summer. Volume 12, Issue 4, pages 729–740, December 1998.

Seinfeld, J. H. and S. N. Pandis. 1998. Atmospheric Chemistry and Physics: From Air Pollution to Climate Change, Wiley Interscience, New York,.

Stewart, R.E. and H.A. Kantrud. 1971. Classification of natural ponds and lakes in the glaciated prairie region. Resource Publication 92. Bureau of Sport Fisheries and Wildlife, U.S. Fish and Wildlife Service. Washington, D.C. 57 pp.

Svejcar, T., Mayeux, H. & Angell, R. 1997. The rangeland carbon dioxide flux project. Rangelands, 19, 16–18.

SCWG (Soil Classification Working Group). 1998. The Canadian System of Soil Classification. Agric. and Agri-Food Can. Publ. 1646 (Revised). NRC Research Press, Ottawa. 187 pp. ISBN: 0660174049. Available at: http://sis.agr.gc.ca/cansis/references/1998sc_a.html

Syed, K. H., L. B. Flanagan, P. J. Carlson, A. J. Glenn and K. E. Van Gaalen. 2006. Environmental control of net ecosystem CO2 exchange in a treed, moderately rich fen in northern Alberta, Agricultural and Forest Meteorology, 140, 97-114.

Trium Environmental Inc. 2011. Site Assessment – SW-30-05-13-W2M Near Weyburn, Saskatchewan, prepared for Cenovus Energy Inc.

6.0 ABBREVIATIONS

%	percent
‰	per mil
°	degrees
°C	degrees Celsius
<	less than
µmol cm^{-2} s^{-1}	micromoles per centimetre squared per second
µmol m^{-2} s^{-1}	micromoles per metre squared per second
µS/cm	microsiemens per centimetre
AER	Alberta Energy Regulator
BCS	Basal Cambrian Sand
CH_4	methane
cm	centimetre
CO	carbon monoxide
CO_2	carbon dioxide
dS/m	decisiemens per metre
e.g.	for example
EC	Electrical Conductivity
EM	electromagnetic
EM38	electromagnetic conductivity
ESRL	Earth System Research Laboratory
et al.	and others
FCRN	Fluxnet-Canada Research Network
g C m^{-2} yr^{-1}	grams of Carbon per meter squared per year
GGA	Greenhouse Gas Analyzer
GIS	Geographic Information System
Golder	Golder Associates Ltd.
GPS	Global Positioning System
H_2	hydrogen
H_2O	water
H_2S	hydrogen sulphide
ha	hectare
HBMP	Hydrosphere and Biosphere Monitoring Program

He	helium
Hg	mercury
Hz	hertz
ID	identification
i.e.	that is
IW	injection well
km^2	square kilometres
kPa	kilopascals
L	litre
L/min	litres per minute
LLB	Lac La Biche
LSD	Legal Subdivision
m	metre
m^2	square metres
masl	metres above sea level
mbgl	metres below ground level
mL	millilitre
mm	millimetre
MMV	Measurement, Monitoring and Verification
mS/m	millisiemens per metre
Mt	million tonnes
N	north
N	Number of samples
N_2	nitrogen
NAD	North American Datum
NEE	Net Ecosystem Exchange
NEP	Net Ecosystem Productivity
nm	nanometres
NOAA	National Oceanic and Atmospheric Administration
O_2	oxygen (gas)
PIFs	Pseudo-Invariant Features
ppbv	parts per billion by volume
ppmv	parts per million by volume
Q	quarter (i.e., three months of a year)

QA/QC	Quality Assurance and Quality Control
QC	Quality Control
RDL	Reported Detection Limit
SAR	Sodium Adsorption Ratio
SCA	Soil Correlation Area
SD	standard deviation
Shell	Shell Canada Limited
spp.	multiple species
StDev	standard deviation
TDS	Total Dissolved Solids
the Project	Quest Carbon Capture and Sequestration Project
TP	vegetation plot
UTM	Universal Transverse Mercator
W	west
W4M	West of the Fourth Meridian

AER Report Signature Page

GOLDER ASSOCIATES LTD.

APEGA PERMIT TO PRACTICE 05122

Prepared by:

Kailli Pigott, B.Sc., BIT,
Terrestrial Ecologist

Lyndon Scholer, BSc.,
Soil Scientist

Davor Gugolj, BA Geog, MGIS,
Remote Sensing/GIS Analyst

Spencer Maxwell, P.Geoph.,
Geophysicist

Cameron S. McNaughton, Ph.D., P.Eng.,
Environmental Engineer

Doreen Chan, M.Sc., P.Geol.,
Hydrogeologist

Christine Ouellet, PMP, P.Eng.,
Associate, Project Manager

Reviewed by:

Ken McCarron, M.Sc., PhD.,
Sr. Vegetation Ecologist

Les Fuller, M.Sc., PhD.,
Sr. Soil Scientist

Carmen Walker B.Sc. (Geog) GISP,
Geomatics Analyst

Mark Bowman, P.Geoph.,
Associate, Sr. Geophysicist

Ian Hers, Ph.D., P.Eng.,
Principal, Sr. Specialist Engineer

Hugh J. Abercrombie, Ph.D., P.Geol.,
Sr. Geochemist

Dan Brown, M.Sc., P.Geol.,
Principal, Project Director

CO/DB/ab

https://capws.golder.com/sites/1213510001shellquesthbmp/project management/11.9 document control/11.9.1 reports/2013/aer report/version 2 (final)/1-master/1213510001_rp013_v2_2013aer_report_final_20140123.docx

As a global, employee-owned organisation with over 50 years of experience, Golder Associates is driven by our purpose to engineer earth's development while preserving earth's integrity. We deliver solutions that help our clients achieve their sustainable development goals by providing a wide range of independent consulting, design and construction services in our specialist areas of earth, environment and energy.

For more information, visit golder.com

Africa	+ 27 11 254 4800
Asia	+ 86 21 6258 5522
Australasia	+ 61 3 8862 3500
Europe	+ 356 21 42 30 20
North America	+ 1 800 275 3281
South America	+ 56 2 2616 2000

solutions@golder.com
www.golder.com

Golder Associates Ltd.
102, 2535 - 3rd Avenue S.E.
Calgary, Alberta, T2A 7W5
Canada
T: +1 (403) 299 5600

Golder Associates

APPENDIX F – MCS CO2 ENTRY PRESSURE RESULTS FOR IW 8-19

Attached is a report of the capillary entry experiment performed on the Quest MCS (primary seal) by Yingxue Wang at the Shell Bellaire Technology Centre (BCT). The experiment illustrates that:

- The capillary entry pressure of the MCS is very high (higher than 999 psi, the top constrained pressure of the experiment) indicating that the MCS is a good seal
- The micro cracks in the core sample which were induced during handling were blocked (partially or fully) by salt precipitation during the experiment which was confirmed by elemental mapping on the SEM images. This is consistent with TOUGHREACT modeling which showed that salt precipitation can plug any natural fractures in the seal. Note that there is no evidence of any natural fractures in the MCS.
- Diffusion of CO2 takes place, leading to mineralogical alteration in the core sample and precipitation of calcite which could further improve sealing capacity

This result indicates that the MCS is a very good seal.

Unrestricted **SR.12.13365**

Capillary Sealing Capacity of Radway Middle Cambrian Shale Core Samples for Quest CCS Project

by

Yingxue Wang (PTU/ADD)

Robert J. Knabe (PTI/RF)

Shell International Exploration and Production Inc., Houston

Further electronic copies can be obtained from the Global Information Centre.

Executive summary

Capillary sealing capacity was assessed via entry pressure measurements on two Radway Middle Cambrian Shale core plug samples, with the aid of imaging and elemental analysis. The Middle Cambrian Shale is one of the main seals for underground CO_2 storage in the Quest Carbon Capture and Storage project. Both core plug samples were from the same well (8-19-59-20w4) at 1958.6 m CD. The pore pressure was 2780 psi, the effective stress was 2950 psi, and the in situ temperature was around 60°C. SEM confirmed that the Middle Cambrian Shale has very tight pores with poor connectivity. From the elemental study, the shale samples consist of quartz, illite, kaolinite, chlorite, pyrite, and feldspar, and have very little organic content. Capillary entry pressure measurements showed no entry for CO_2 pressure less than 999 psi. It also suggested that for CO_2 pressure higher than 999 psi the fluid transport inside the cap rock was not viscous flow, and cannot be described by Darcy's Law. In SEM images on the core sample after the entry pressure test, halite crystals were observed along the edges of micro-cracks close to the inlet side. XRD analysis showed calcite precipitation. In comparison, neither halite nor calcite were observed on samples before the entry pressure measurement. The observation strongly supported that diffusion coupled with CO_2-brine-rock interaction was the dominant mass transfer process inside the cap rock. Recommendation for the future cap rock integrity study include integrated entry pressure measurement, imaging, elemental analysis, formation water analysis, and reactive transport modeling.

Table of contents

List of tables

List of figures

1. Introduction

Among various proposals for Carbon Capture and Storage (CCS), underground geological storage appears to be the most technologically advanced option. Carbon dioxide (CO_2) can be stored in depleted hydrocarbon reservoirs or deep saline aquifers. As one of the largest CCS projects in North America, Quest is a fully integrated project in the oil sands sector involving CO_2 capture, pipeline, and storage. The CO_2 captured at the Scotford Upgrader will be transported via pipeline and stored in a deep (2000 to 2100 m) saline aquifer formation - Basal Cambrian Sand. The project aims to capture and store up to 1.2 million tons of CO_2 per year from 2015 onwards. The Lower Marine Sand (LMS) and Middle Cambrian Sand (MCS) provide the main seal for CO_2 storage. Two of the critical issues for underground CO_2 storage are to demonstrate that CO_2 will remain in a reservoir or aquifer over a long time (hundreds to thousands of years) and that its leak rate is small enough. For Quest, these are considered as critical success factors required to be addressed [1]. The requirement is directly connected to the caprock integrity and seal capacity evaluation. Therefore, it was the objective of this work to perform an experimental study on Quest caprock and evaluate its integrity.

A caprock is usually a fine-grained rock such as shale, mudrock, or siltstone. It is a flow barrier due to the very low permeability. During CO_2 injection and storage, CO_2 may potentially invade the caprock through diffusion, capillarity, and fracturing. Diffusion starts as soon as CO_2 is in contact with the caprock. As CO_2 diffuses into rock saturated with formation water, coupled physical and chemical processes may happen due to the CO_2-rock-brine interaction. Besides, during CO_2 injection into the formation, its pressure builds up. If the pressure exceeds a certain threshold, CO_2 enters pore spaces and displaces the pore fluid. This pressure threshold is the capillary entry pressure. Beyond entry pressure, CO_2 continuously displaces formation fluid and eventually establishes flow paths through the caprock. Finally the caprock could be fractured by the over-pressurized CO_2 or temperature gradient induced in formation during the CO_2 injection. Among those three mechanisms for potential CO_2 leakage, both capillary entry and mechanical failure may happen in a short time scale. Diffusion is generally a much slower process. This work is focused on the capillary sealing capacity study. An overview on caprock integrity and different leak risks can be found in the report by Busch [2]. Readers are also referred to Zhang and Winkler on the geochemical reactive transport modeling of Quest reservoir and caprock [3].

The report is organized as follows. The protocol of capillary entry pressure testing is introduced first in Section 2, followed by the capillary entry pressure measurements on Middle Cambrian Shale (MCS) core plugs under reservoir condition in Section 3. Scanning electron microscope (SEM) images and X-ray Diffraction (XRD) analysis on core samples before and after entry pressure measurement are discussed in Section 4 to study the potential caprock alteration in measurements. At the end, Section 5 summarizes conclusions from this work and provides recommendations for future study.

2. Experimental Protocol

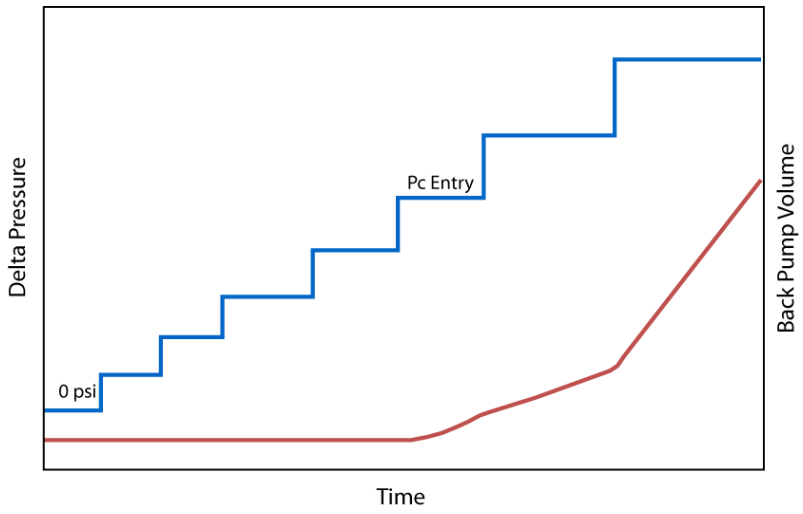

Figure 2.1: Schematic of a capillary entry pressure measurement using a step-wise steady-state method.

Capillary sealing capacity for CO_2 storage purposes has been assessed through either contact angle and interface tension measurement [4] [5], or entry pressure measurement. In core analysis, capillary entry pressure is often deduced from mercury/air capillary pressure measurement. However due to uncertainties in the interfacial tension and the contact angle between CO_2 and rock, various break through measurements have been reported using CO_2 directly and under reservoir condition. For those methods used in the CO_2 break through measurements, they generally split into two main categories: steady state method [6] and pressure transient method [7] [8]. While unsteady state methods could potentially reduce the measurement duration [9], a steady state measurement is straightforward and best represents the in situ CO_2 storage condition.

Capillary entry pressure in this work was measured using a step-wise steady state method. Figure 2.1 demonstrates expected changes in delta pressure across a core sample and pump volume during an entry pressure measurement using this method. A core plug sample is initially saturated with brine at a certain pore pressure. The upstream side of the plug is full of CO_2 initially at the same pressure. The downstream side is filled with brine and connected to a back pump. The pump is used to maintain the pore pressure. At the beginning of measurement, there is no pressure drop across the core. The back pump does not move. CO_2 pressure is then increased in steps to increase the pressure drop. Before the CO_2 pressure reaches the capillary entry pressure of the core plug, no fluid will be displaced from the pore space. The volume of the back pump remains constant. When the CO_2 pressure equals the entry pressure, CO_2 enters pores. Brine is displaced and collected by the back pump. The back pump volume starts increasing in order to maintain the constant pressure. Therefore, the capillary entry pressure can be determined from the volume change in the back pump. When the entry pressure is exceeded and CO_2 breaks through, the pump volume change, ie. flow rate, is proportional to the delta pressure applied.

Mass transfer between CO_2 and brine should be minimized in the above measurement in order to accurately determine the entry under capillarity. In the laboratory, first brine is to be saturated with CO_2 under experimental pressure and temperature before being used to saturate the core sample. Ideally, CO_2 shall be humidified as well. Dry supercritical (SC) CO_2 is often injected instead to better mimic the real injection in fields, and to avoid the potential corrosion on the system from the wet CO_2. Consequently, other processes including dissolution, dry-out, evaporation and precipitation may happen during the SC CO_2 injection. Moreover, depending on the measurement duration, diffusion and other complex CO_2-brine-rock interaction may also play a role. As a result, flow characteristics could be modified substantially from what is shown in Figure 2.1.

The above experimental protocol was established in 2008 in the Rock and Fluid Science Department, where the entry pressure of SC CO_2 into a tight gas core plug was measured. Details of the experiment can be found in the Appendix 1. The tight gas plug was used to mimic a caprock. Its porosity was about 5% and permeability was 0.003 mD. The plug was fully saturated with NaCl brine at 1280 psi and 50 °C. Supercritical CO_2 was injected to the upstream side of the plug. The entry pressure of SC CO_2 into the tight core plug was about 53 psi. The result agreed reasonably well with that calculated from a high pressure mercury injection test (48 psi) using the CO_2-brine interfacial tension and contact angle from literature.

3. Capillary Entry Pressure Measurements

3.1. Core plug samples

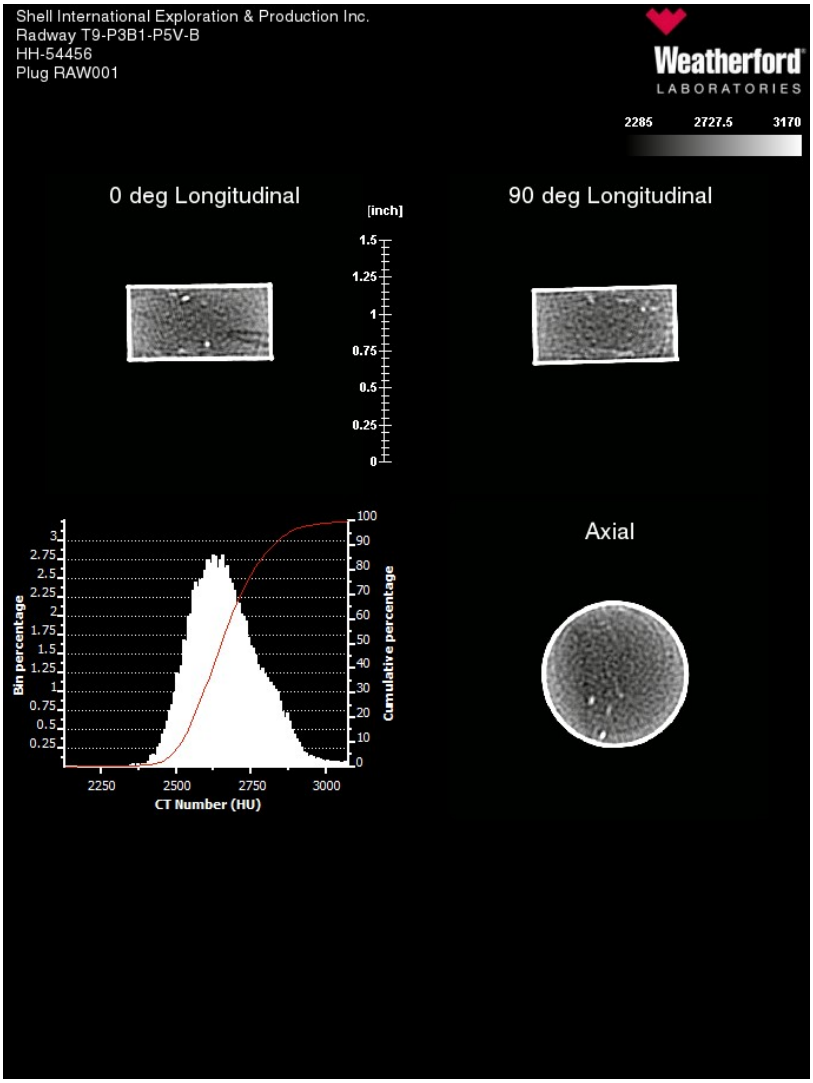

Figure 3.1: CT scan image of RAW001.

Two core plug samples in this study, RAW001 and 004, were from the Radway Middle Cambrian Shale (MCS) at a depth of 1958.65 m. The MCS provides a main seal for Quest CO_2 storage. Both core samples were vertical plugs, drilled by the Rock and Fluid Science Team in Houston. RAW001 was 1.367 cm long and 2.536 in in diameter. RAW004 had the same diameter and was 1.36 cm long. CT images for both plugs are shown in Figure 3.1 and Figure 3.2, where RAW001 was scanned by the Weatherford Laboratories and RAW004 was scanned by Rock and Fluid Science Department. Both images suggest that those shale plugs were very tight and free of vertical fractures. RAW001 was relatively homogeneous. RAW004 contained a layer with relatively lower density in the middle.

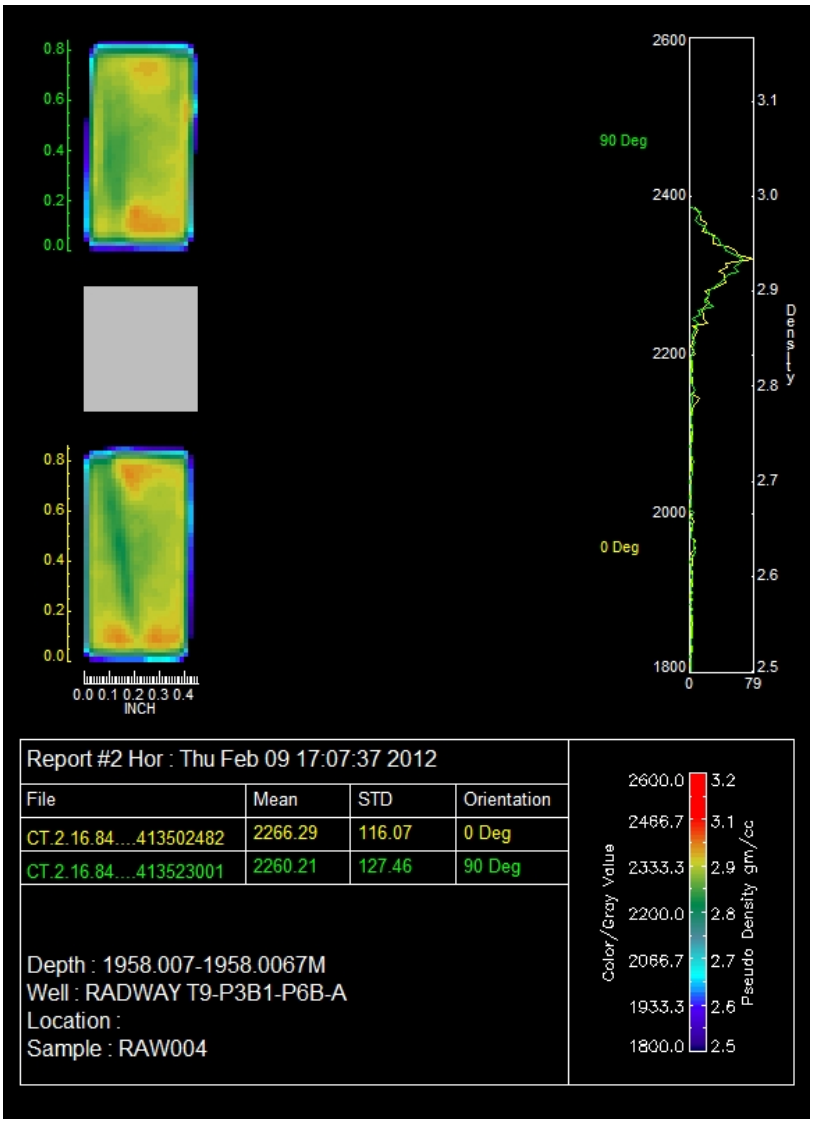

Figure 3.2: CT scan image of RAW004.

An end-trim of RAW004 was used for Scanning electron microscope (SEM) imaging and X-ray Diffraction (XRD) analysis to obtain pore structure and mineralogy information of the MCS before being exposed to CO_2. The SEM image confirmed the very tight pores (< 1 micron) with poor connectivity in the MCS core sample. Horizontal micro-cracks were also observed in the image and was possibly due to the sample nature itself. Elemental analysis indicated that there were Al, Mg, Si, K, Fe, Na, and Cl, etc. in the sample and there is low organic content. XRD analysis suggested that the main minerals in MCS included quartz, illite, kaolinite, chlorite, pyrite, and K-feldspar. The mineralogy information was used to assess the compatibility between core plug and synthetic brine, and will be discussed in the following section. The information also served as a baseline of comparison with that after the CO_2 entry experiment to study the SC CO_2-brine-rock interaction, and will be discussed in Section 4.

Due to the extremely tight nature of MCS plugs, routine core cleaning was skipped and the pore fluid was carefully preserved during core drilling and handling. Mineral oil was used as drilling fluid. Core plugs were subsequently submerged in mineral oil to avoid the evaporation of the pore fluid. With the above procedures, those MCS plugs were saturated with formation brine.

3.2. Brine composition

Table 3.1: Brine Composition

Ion	Concentration (mg/L)	
	Formation Brine	Synthetic Brine
Cl^-	177154	88577
SO_4^{2-}	1840	920
Na^+	111000	55500
K^+	1180	590
Mg^{2+}	905	453
Ca^{2+}	1960	980
TDS (mg/L)	294,039	147,019

Table 3.2: Synthetic Brine Recipe (for 1 liter of solution)

Salt	Mass (g)
$CaSO_4$	1.304
NaCl	141.163
KCl	1.126
$MgCl_2$	1.775
$CaCl_2$	1.652

Composition of formation brine inside MCS was not available. Instead, brine in this work was synthesized based on the composition of Radway BCS brine, the main aquifer for CO_2 storage. The BCS formation water is highly saline with measured total dissolved solid (TDS) around 300,000 mg/L. Major ions in BCS formation water include sodium, potassium, magnesium, calcium, chloride, sulfate, etc. To avoid the potential plugging of tubing due to salt precipitation as water vaporized during dry CO_2 injection, TDS of the synthetic brine was reduced to half of that of the formation water, while the ratio of concentration among the above major ions was maintained. Table 3.1shows the composition for formation brine and synthetic brine, respectively. And Table 3.2

is the recipe for synthetic brine. According to the XRD analysis, the amount of smectite is negligible in MCS. Therefore the decrease in the brine salinity will not cause the clay swelling.

3.3. Experimental system and leak tests

The experimental setup included a coreholder, two piston accumulators, three pumps, and pressure transducers, etc. The coreholder was modified from one used in a resistivity-index test. At the injection side, CO_2 was stored in two piston accumulators. Those two piston accumulators were driven by a ISCO pump, ie. the injection pump. At the downstream side, another ISCO pump (back pump) was filled with the synthetic brine and directly connected to the downstream side of the coreholder. The back pump was used to apply and maintain pore pressure. The brine production due to CO_2 displacement was collected by the back pump and recorded through volume change of the pump. A pair of ISCO500D pumps were used as injection and back pump, respectively for the entry pressure test on RAW001. For the test on RAW004, both pumps were replaced by a pair of ISCO260D pumps for higher pressure rating. A third ISCO pump was used to apply confining stress. Its pressure was controlled so that the difference of absolute confining stress and pore pressure was constant and equal to the (net) effect confining stress during the test. Both accumulators and the coreholder were enclosed in an oven to ensure proper thermal control and stability. During the test, oven temperature was maintained at 60 °C which was estimated as the reservoir temperature.

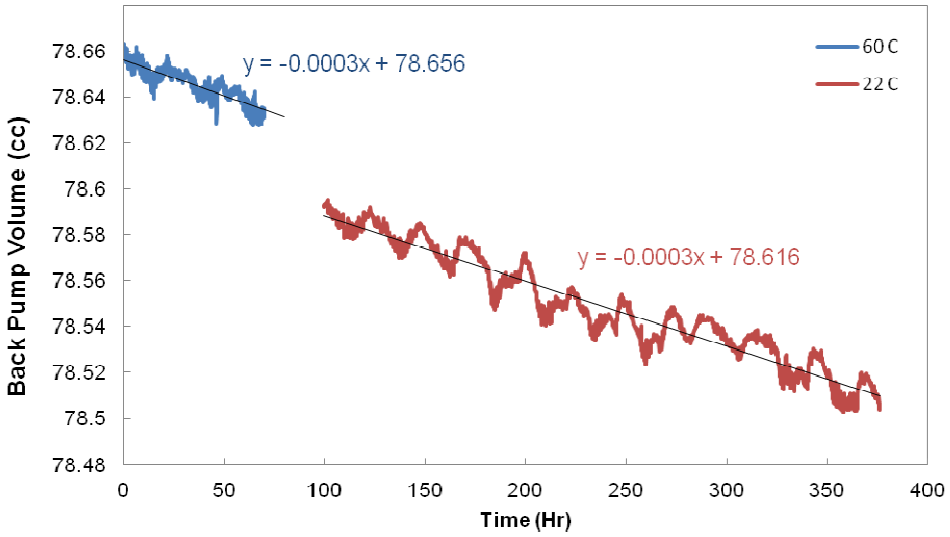

Figure 3.3: Back pump volume change during a system leak test at 60°C (blue) and room temperature around 22°C (red).

Experiments in 2008 and other research work indicated that the measurement duration of the step-wise steady state method could be days or even weeks, depending on the rock permeability. System leaks play an important role in the determination of entry pressure from the pump volume change in those long-duration measurements. Before the test on RAW001, a leak test was performed on the system with a steel billet loaded into the coreholder. Figure 3. shows the volume change of the back pump as a function of time at reservoir temperature of 60 °C and room temperature around 22 °C, while the back pump was maintained at 2914.7 psi. When at room temperature, the back pump volume change was recorded for about 275 hours. Overall the same leak rate of 0.0003 cc/hr were observed for both sets of data. Small fluctuations in both sets of data were due to pump control and temperature variation. Before the test on RAW004, another leak test was performed as both injection and back pump were replaced. The back pump was maintained at 2774.7 psi, and the leak rate on the back side was about 0.04 cc/hr.

3.4. Experimental procedure

Experimental procedure was similar to the protocol in Section 2 and that used in 2008, except that special precaution was taken to preserve the formation water during system preparation. After the core assembly was loaded into the coreholder with an initial confining stress of 500 psi applied, the confining pressure was increased slowly to 800 psi and maintained overnight for leak test. In the following, the tubing of the core outlet was saturated with synthetic brine under vacuum and connected to the back pump. As the core plug was saturated with the formation brine, to prevent

the formation brine from being sucked out, a flash-vacuum was used. Similarly at the injection side, to fill the injection tubing with CO_2 gas, the flash-vacuum was used to remove air in the inlet tubing. With the entire system connected and properly saturated, the oven was turned on with temperature set at 60 °C. The confining stress was slowly increased to the test stress in about 20 hours and subsequently stabilized for 3 to 7 days.

During the stabilization of confining stress, pore pressure was carefully increased. Due to the fact that the inlet of the core plug was filled with SC CO_2, and the outlet was filled with brine, both injection pressure and back pressure had to be increased at the same time and the same rate so that the pore pressure in the plug was increased uniformly. More importantly the difference between CO_2 pressure and back pressure was small enough that neither CO_2 would enter the pore space nor the synthetic brine would displace the formation brine from the downstream side. The system was left for both thermal and pressure stabilization for about 12 hours after the test pressures were reached. Based on in situ reservoir condition and geomechanics measurements, pore pressure (P_0) and effective confining stress of those MCS plugs were 2780 psi and 2950 psi, respectively.

Injection of SC CO_2 was started after system stabilization. The injection pressure (ie. CO_2 pressure, or P_{in}) was increased by a certain pressure step (ΔP_{step}) while the back pressure was still maintained at 2780 psi, ie. pore pressure (P_0) was 2780 psi. The pressure difference was then maintained for certain amount of time while volume of the back pump was monitored and recorded. An increase in the back pump volume meant that extra fluid was collected into the pump, which indicated CO_2 entry. Otherwise, CO_2 pressure was not high enough to overcome the capillarity. CO_2 pressure was subsequently increased by another pressure step and maintained to look for the capillary entry. The above process was repeated until a capillary entry was measured or the equipment pressure limit was reached.

3.5. Results and discussion

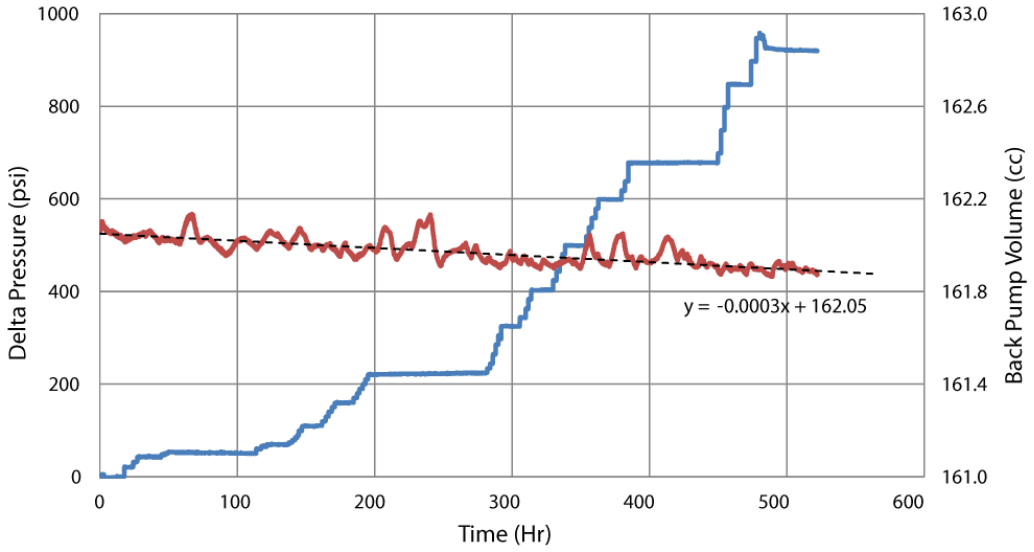

$P_{in} - P_0$	0 - 99	100 - 244	245 - 699	700 - 958
ΔP_{step}	5	10	20	50

Figure 3.4: Top: Delta pressure (blue) and back pump volume change (red) during SC CO_2 entry pressure measurement on RAW001. Bottom: Step size used in the measurement.

Figure 3. shows the pressure drop (ie. $\Delta P = P_{in}-P_0$) across RAW001 and the back pump volume as a function of time. The table at the bottom of Figure 3. summarizes sizes of pressure steps used in the measurement. The stabilization time at each step was at least 2 hours for $\Delta P_{step} \leq 20$ psi, and about 4 hours for $\Delta P_{step} = 50$ psi. The sizes were chosen as a result of balancing test duration and measurement precision. With the step sizes shown in the table, the uncertainty in the measured entry pressure was around 5 - 10% of the pressure drop. From the figure, the pressure drop was built up to 920 psi. During 522 hours of the test, volume of the back pump overall decreased at a rate of 0.0003 cc/hr, which was probably due to the very small leakage in the downstream side as discussed in the previous section. There were small fluctuations about ±0.1 cc in the back pump volume during the measurement, possibly due to unoptimized pump control parameters to maintain a constant pressure. Those parameters such as proportional gain, integrator, and differentiator (PID) were built into the ISCO pump controller and could not be adjusted. Nonetheless, The above measurement on RAW001 showed that there was either no fluid production or the production rate was much smaller than 0.0003 cc/hr at the end of injection. As mentioned in the Introduction and in Figure 2.1, the expected change in the back pump volume due to CO_2 entry was opposite to that caused by leak. As a result, if CO_2 entered sample RAW001, the rate of decrease in the back pump volume would be slowed. Depending on core sample's permeability and the pressure drop, the back pump volume may start increasing eventually as more and more CO_2 enters the pore space and its flow path is established. No such transition was observed in Figure 3.. Therefore the test on RAW001 suggested no CO_2 entry for capillary pressure less than 900 psi. Those micro-cracks observed in SEM images were sealed under reservoir stress and not conductive.

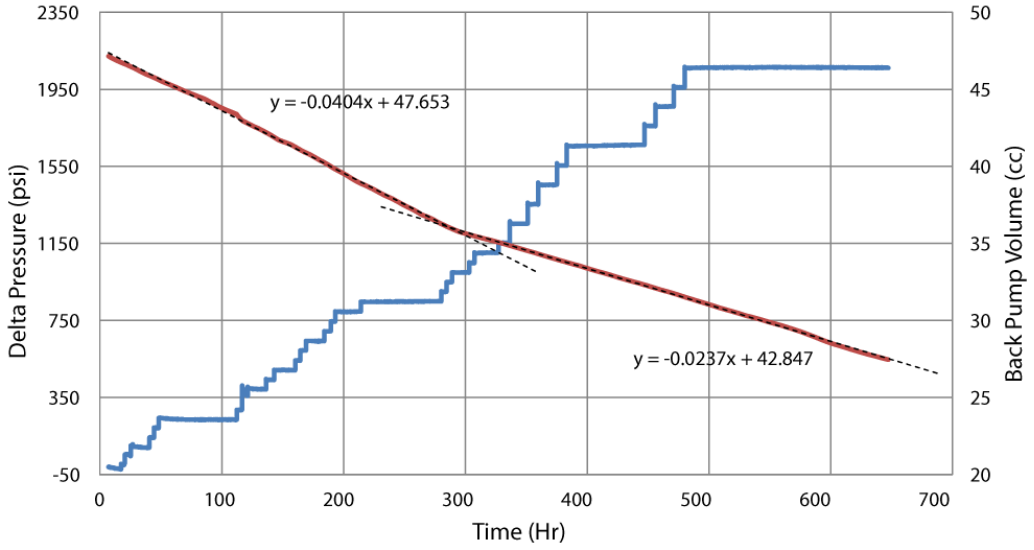

$P_{in} - P_0$	0 - 1153	1154 - 2063
ΔP_{step}	50	100

Figure 3.5: Top: Delta pressure (blue) and back pump volume change (red) during SC CO_2 entry pressure measurement on RAW004. Bottom: Step size used in the measurement.

The test on RAW001 was stopped when the injection pressure was increased to 3740 psi or $\Delta P \approx$ 960 psi, as the injection pump had reached its pressure limit. In the next test, both injection and back pumps were replaced by ones with higher pressure ratings. Entry pressure test was repeated on RAW004. Figure 3. shows the measured pressure drop (ΔP) across RAW004 and the back pump volume as a function of time. From the measurement on RAW001, an entry pressure possibly higher than 900 psi was expected. The SC CO_2 injection scheme was modified accordingly to shorten the measurement duration and is shown in the table at the bottom of Figure 3.. Potential uncertainty in the entry pressure was around 5\%. At each pressure step, the stabilization time was chosen to be at least 4 hours for ΔP_{step} = 50 psi and 8 hours or longer for ΔP_{step} = 100 psi. The duration of the test on RAW004 was 673 hours and the pressure drop was built up to 2063 psi. The back pump volume decreased at 0.040 cc/hr during the first 295 hours, and slowed to 0.024 cc/hr afterwards.

In Figure 3., during the first 295 hours, the pressure of SC CO_2 was built up from pore pressure 2780 psi to 3779 psi so that $P_c = P_{in} - P_0 \leq 999$ psi. The volume change of the back pump was linear, probably due to the leakage at the downstream side as the rate was the same as that from the leak test (0.04 cc/hr). SC CO_2 did not seem to enter the core sample when its pressure was less than 999 psi. At P_c = 999 psi and $t_{exp} \sim$ 295 hr, the rate of decrease in back pump volume slowed to 0.024 cc/hr. Based on the above discussion, this rate range in the back pump may be due to the SC CO_2 entry and displacing the formation water. Figure 3. shows the back pump rate versus the delta pressure across the core plug at each injection step during the measurement on RAW004. The back flow rate was averaged to be 0.040 cc/hr with fluctuations about $\pm$ 0.01 cc/hr for the delta pressure less than 999 psi. An increase in back flow rate was observed at the delta pressure around 999 psi.

The change in flow rate in the individual injection steps (Figure 3.) was consistent with the observation from Figure 3..

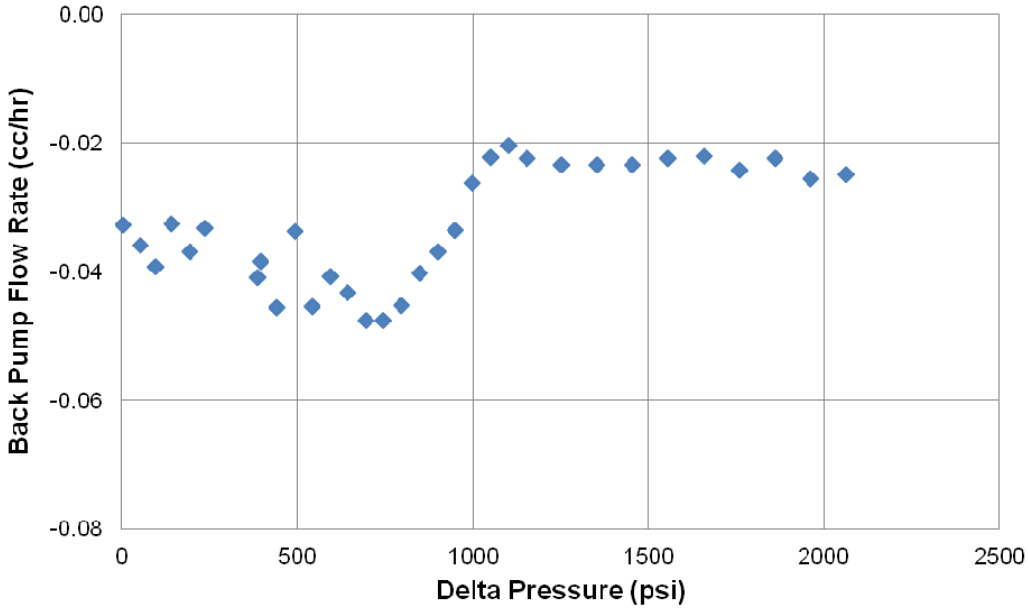

Figure 3.6: Back flow rate at each individual pressure step during SC CO_2 entry pressure measurement on RAW004

In Figure 3. from t_{exp} = 295 hr to 673 hr, the CO_2 pressure was increased at 100 psi per step until the pressure drop across the core plug was 2063 psi. During 378 hours of injection, however, the back pump volume change remained linearly at the same rate of 0.024 cc/hr no matter what the pressure drop was. Figure 3. confirms that the flow rate after the "entry" seemed to be independent of delta pressure. As shown in the thought experiment of Figure 2.1, the back pump starts moving at the capillary entry. The volume may change nonlinearly before CO_2 breakthrough. After the breakthrough, the volume change is expected to become linear with a rate proportional to the pressure drop as described by Darcy's Law for viscous flow. The entry pressure measurement on a tight gas core plug sample in 2008 showed this behavior (Figure A1.1 and Figure A1.2). By comparison, the relation between volume change and pressure drop in the RAW004 test indicates that other processes may have modified the flow characteristics greatly.

During the above entry pressure measurements, the pore pressure was maintained through the back pump at 2780 psi. Before CO_2 entry, the pore pressure was constant along the plug. The effective stress was defined as the absolute confining stress minus the pore pressure. Therefore before CO_2 entry, the effective stress was 2950 psi and was constant along the plug as well. When the SC CO_2 entered the core plug, the pore pressure close to the inlet side increased. Correspondingly the plug experienced a decreased effective stress at the inlet side and deformed with some bulging towards the outlet side. As the pressure drop increased from 999 psi to 2063 psi during the CO_2 injection, at the inlet side, the pore pressure increased from 2780 psi to 3844 psi, and the effective stress

decreased from 2950 psi to 1886 psi. Decrease in the effective stress could potentially cause pore volume expansion. As a result, some fluid injected could be "stored" in the pore space close to the inlet side and did not flow to the downstream. The flow rate at the outlet would not change greatly. As an order-of-magnitude estimation, a relative bulk volume change around 0.04% is expected with an average effective confining stress decrease by 532 psi. A bulk modulus of 1.5×10^6 psi was assumed in the above estimation. Higher bulk modulus will yield less volume change. From the plug dimensions given above, 0.04% porosity change was about 0.003 cc. This volume change was too small to explain the measured constant rate (0.024 cc/hr) over 378 hours.

Other processes may have changed the flow characteristics. As mentioned in the Introduction, three main processes may happen during the SC CO_2 injection and storage, including diffusion, capillarity, and fracturing. The core plug sample may fracture as CO_2 pressure builds up. However, the flow in fractures is expected to be sensitive to the pressure drop as well as the applied stress and, which was not the case shown in Figure 3. and Figure 3.. Moreover no induced fracture was found on the core plug after the entry pressure measurement when un-loaded from the core holder. The above observations suggested that mass transfer (diffusion and dissolution) and interaction among SC CO_2, brine, and rock minerals may have played an important role and changed the flow characteristics. SEM imaging and XRD analysis were performed on the samples after the entry pressure measurement to aid the assessment.

4. Imaging Study and Mineral Alteration

Scanning electron microscope (SEM) imaging combined with Energy Dispersive X-Ray Spectroscopy (EDS) and X-Ray Diffraction (XRD) analysis were performed on RAW004 before and after SC CO_2 entry pressure measurement. Where samples for imaging were prepared by argon ion beam milling to enable a better view of grains and pore structure.

4.1. Core samples before CO_2 exposure

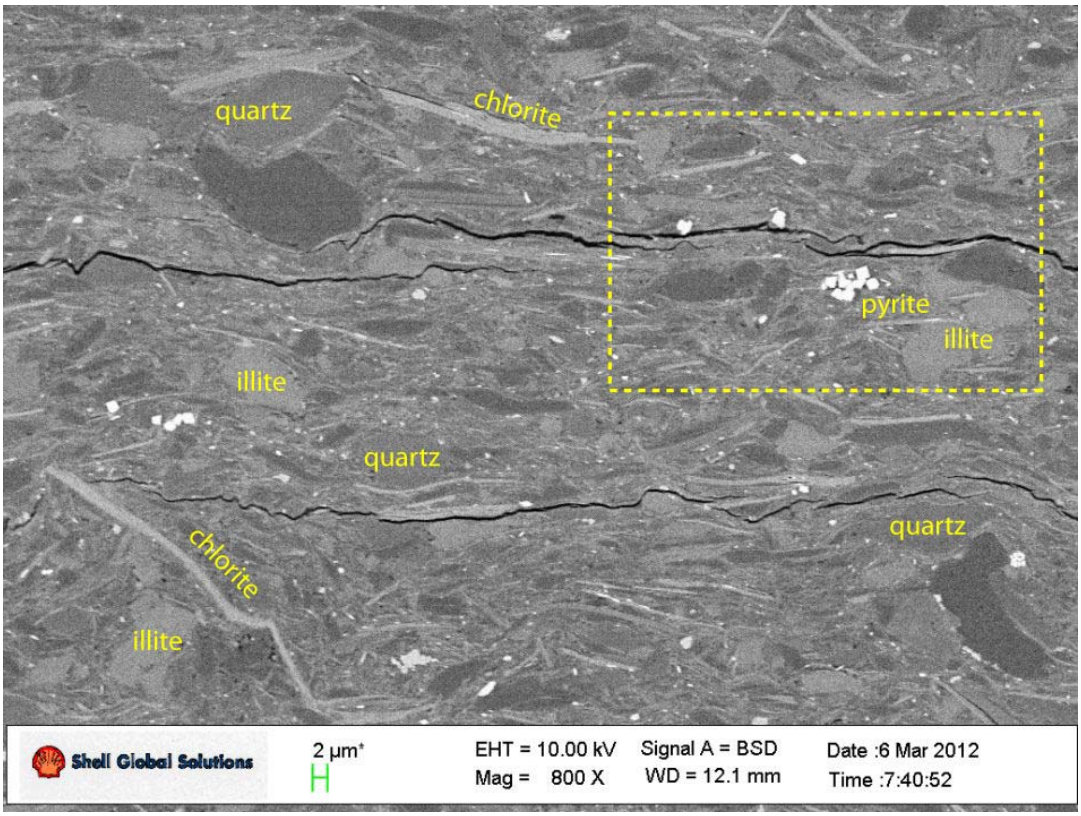

Figure 4.1: SEM image on the end-trim of RAW004 before the SC CO2 entry pressure measurement.

Figure 4.1 is the SEM image on the end-trim of RAW004 before the SC CO_2 entry pressure measurement, with some main minerals marked. Micro-cracks were observed in the image, possibly occurring naturally. As indicated from the entry pressure measurements, the micro-cracks were not conductive under reservoir stress. The area highlighted by the dashed box was magnified and is shown in Figure 4.2. Elemental mapping in Figure 4.3, combined with XRD analysis, suggested that the core sample contained quartz, illite, kaolinite, chlorite, pyrite, and K-feldspar, and had relatively lower organic contents. Where in Figure 4.1, some quartz was relatively big and appeared like distorted diamond, chlorite had the elongated shape, and illite was more rounded. Both were widely distributed in the core. Pyrite was more squared and localized. Figure 4.1 and Figure 4.2 also indicated that pores were very tight (< 1 µm) and appeared to be poorly connected.

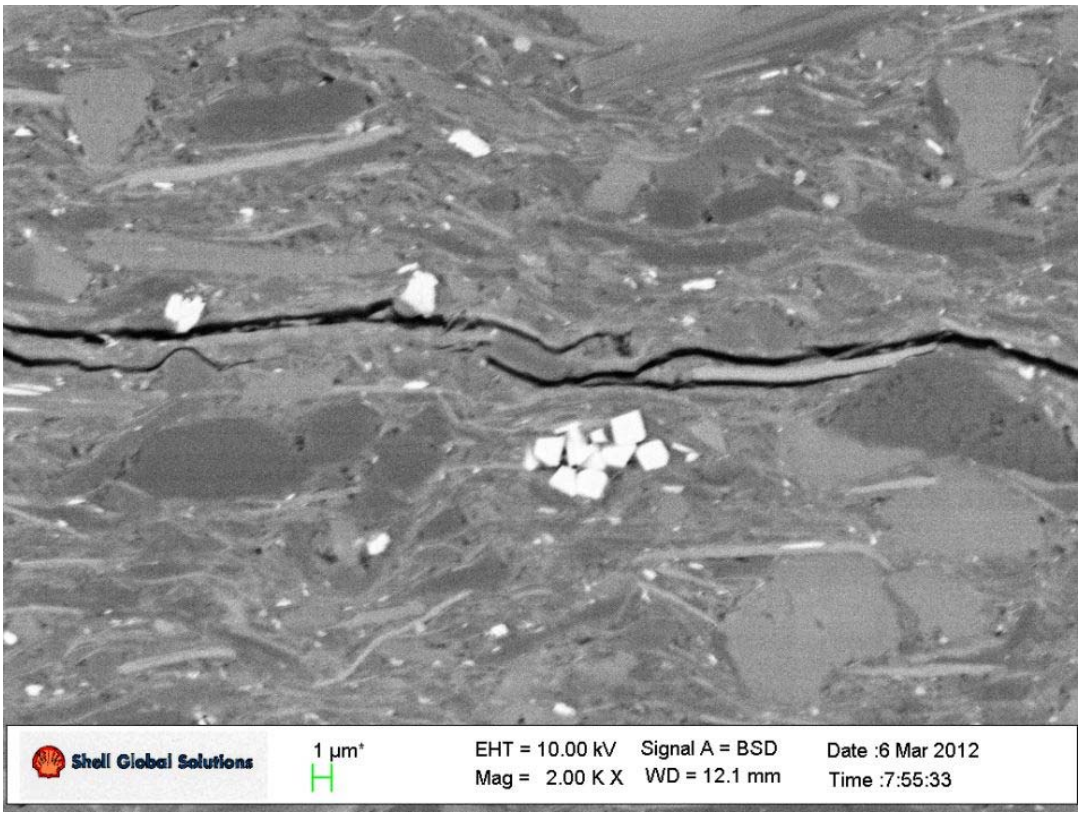

Figure 4.2: Magnified image on the area highlighted by dashed box in Figure 4.1.

Table 4.1: Elemental Analysis on the Image in Figure 4.1

Element	Atom	Mass	Error
	at.%	wt.%	wt.%
Carbon (‘C)	3.35	2.02	0.7
Oxygen (O)	67.34	54.11	11.0
Sodium (Na)	0.65	0.75	0.1
Magnesium (Mg)	0.99	1.21	0.1
Aluminum (Al)	7.8	10.56	0.6
Silicon (Si)	16.6	23.42	1.2
Chlorine (Cl)	0.09	0.15	0.0
Potassium (K)	1.34	2.63	0.1
Titanium (Ti)	0.16	0.39	0.0
Iron (Fe)	1.69	4.75	0.3

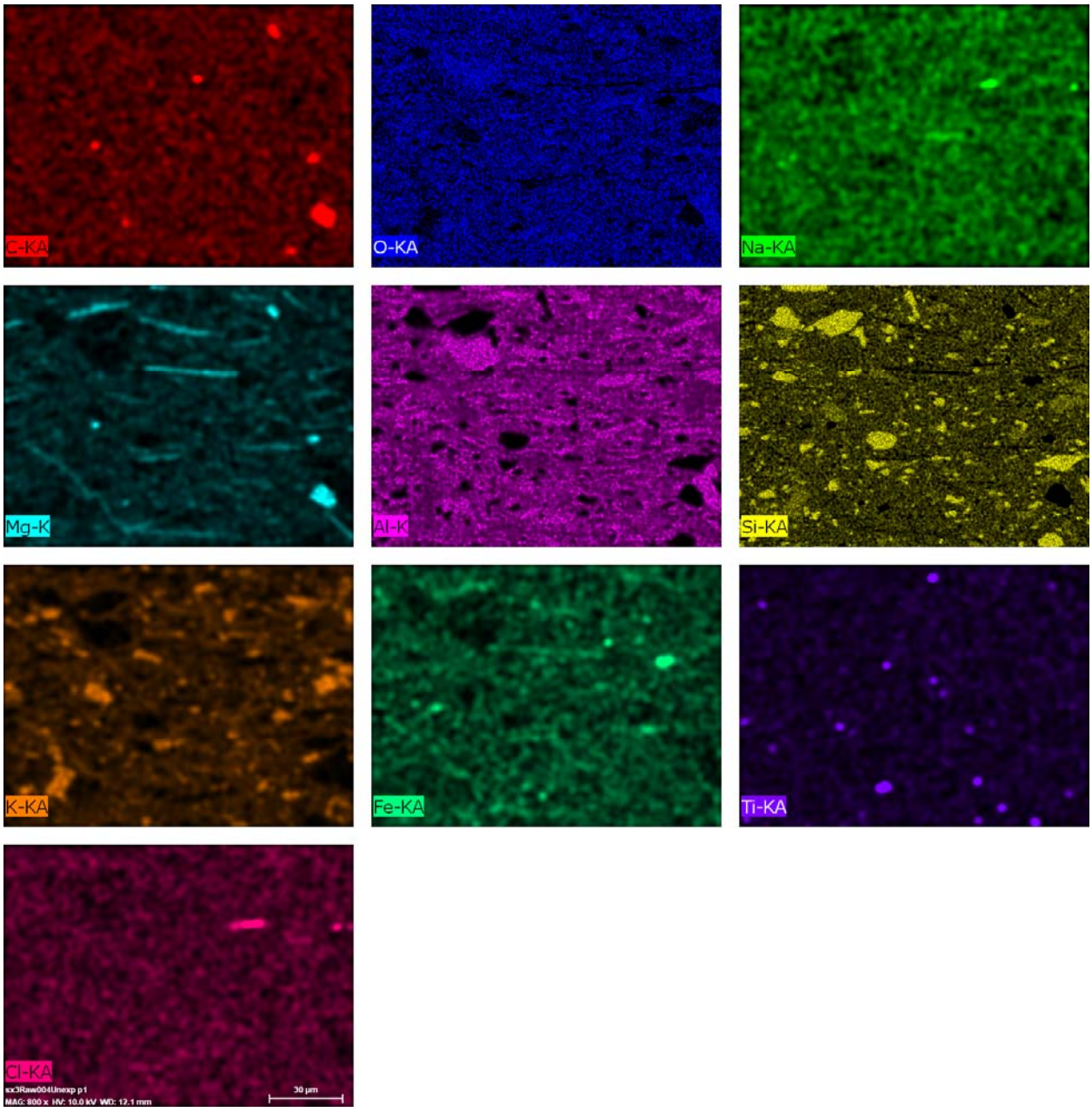

Figure 4.3: Elemental maps on the end-trim of RAW004 before SC CO_2 entry pressure measurements.

4.2. Core samples after CO_2 exposure

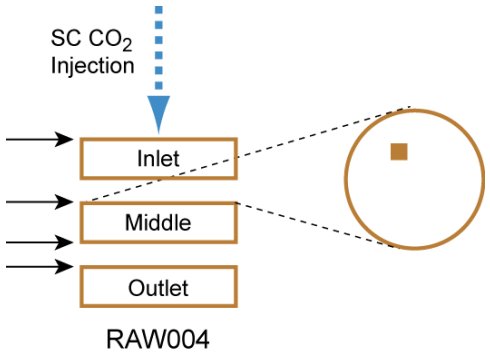

Figure 4.4: Schematic cross sections of RAW004 where the SEM and elemental analysis were performed after the entry pressure measurement. See text for explanation.

After the entry pressure measurement RAW004 was divided into three disks (Figure 4.4). Black arrows in the figure indicate those surfaces where small core chips were taken for milling and imaging, including the top surface of the inlet disk, top and bottom surfaces of the middle disk, and top surface of the bottom disk, respectively. The approximate location of the core chip on each surface was shown on the right hand side. SEM images were taken on three to four spots on each core chip.

Four spots were scanned on the sample from the inlet disk of RAW004, where two spots were near micro-cracks. Figure 4.5 - Figure 4.8 show the SEM images and the corresponding elemental analysis. Images still show tight and poorly connected pores, micro-cracks, and minerals with different shapes, very similar to those on the end-trim of RAW004 before the entry pressure measurement. More importantly, Figure 4.5 and Figure 4.7 clearly indicate the presence of sodium chlorine (NaCl) along the edges of cracks. The halite crystals appeared as if they had oozed out from cracks. In comparison, no halite crystals were observed near cracks on the sample before exposure to CO_2.

On the middle disk of RAW004, three spots on the sample from the top surface and three spots on the sample from the bottom surface were scanned. Figure 4.9 and Figure 4.10 show an SEM image and the corresponding elemental mapping from the top surface. Figure 4.11 and Figure 4.12 show an SEM image and the corresponding elemental mapping from the bottom surface. On both surfaces of the middle disk, micro-cracks were still observed. No halite crystals were found along those cracks in either of those SEM images. Results from the elemental analysis on the top surface as shown in Table 4.2 also indicated negligible amounts of sodium and chlorine.

Four spots on samples from the outlet disk of RAW004 were scanned. One of the SEM images and the corresponding elemental mapping are shown in Figure 4.13 and Figure 4.14. Similar to those images on the middle disk, no halite was found along micro-cracks.

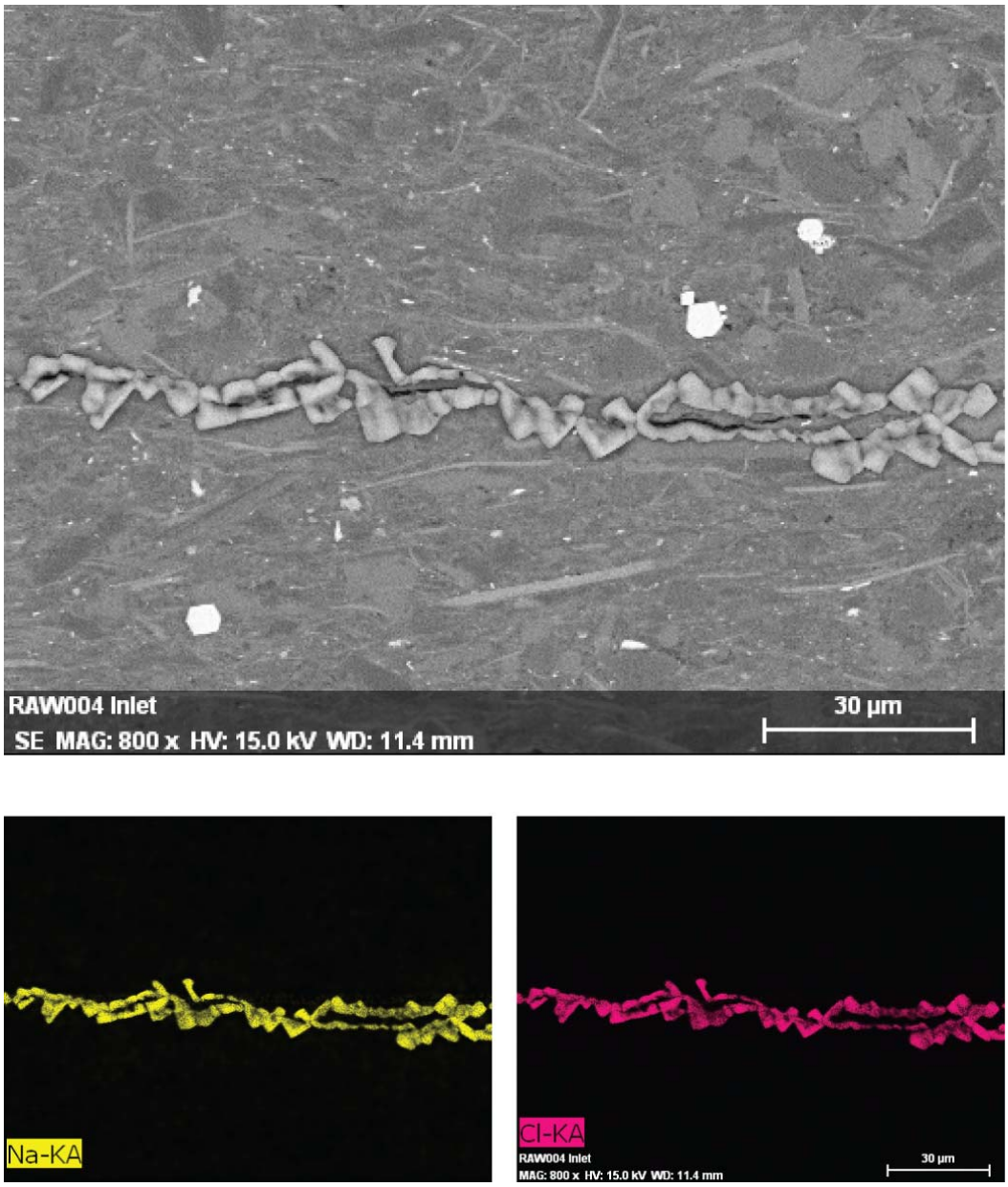

Figure 4.5: **Top: SEM image taken on the top surface of RAW004 inlet disk after SC CO_2 entry pressure measurements. Bottom: elemental mapping on the above image for Na and Cl.**

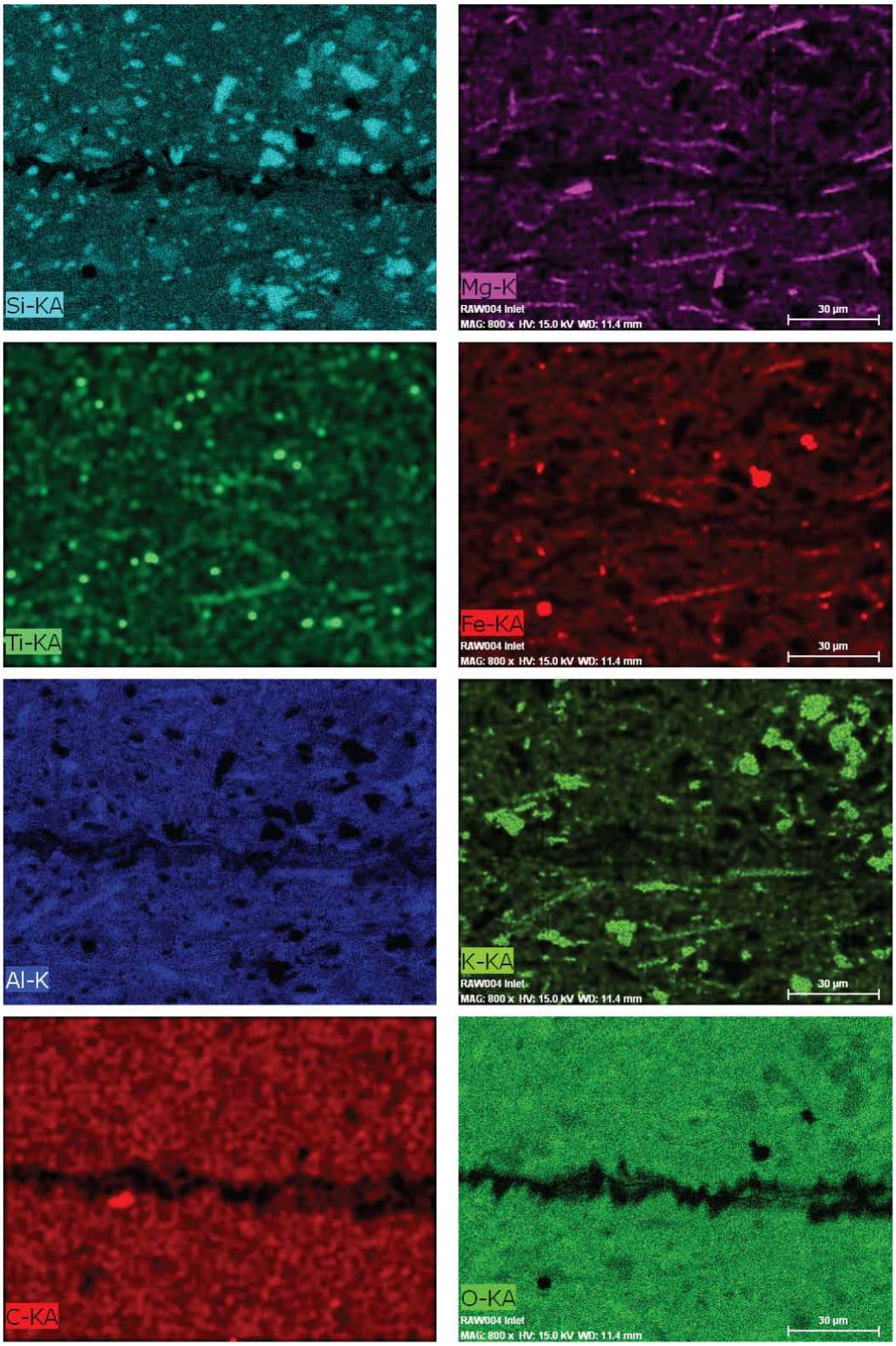

Figure 4.6: Elemental mapping on the SEM image in Figure 4.5 for other major elements.